ON THE MODEL FOR U GEMINORUM

by

John Harwood B.A.(Hons.)

Submitted to the Department of Astronomy, University of Cape Town, in partial fulfilment of the requirements for the M.Sc. degree in Astronomy.

May 1973

CONTENTS

ACKNOWLEDGEMENTS

It is a pleasure for me to thank Prof. B. Warner for his help and encouragement at all stages of this work. The photometric data and the tracings of Dr. R. Kraft's spectra, reduced by Mr. W. Peters, were made available for study by Prof. Warner. I wish to thank Dr. R. E. Nather for helpful discussion and advice. I am grateful for the financial support of a Research Associateship from U.C.T. .

CHAPTER ONE

Introduction

The term cataclysmic variable comprises several types of variable star --- novae, recurrent novae, dwarf novae; and to these we add the nova-like variables, stars which exhibit many of the characteristics of the novae but which have not been observed to erupt. U Geminorum, discovered by Hinds in 1855, is the nomotype of the dwarf novae. These stars are characterised by large, abrupt, temporary increases in brightness that occur erratically at intervals of ten days to a year or more.

The dwarf novae are faint objects, few reaching 11th magnitude at maximum, whereas at minimum light most are fainter than 16th magnitude. Thus they are spectroscopically inaccessible to all but the largest telescopes. Conventional photometric techniques applied to these objects gave no information indicating their physical nature. The time-scale of the observations was so long that only the gross variations in brightness were detected. Much of the observing was undertaken by amateurs (Fig. 1), and from this work several of the basic features of this group have emerged.

Although the outbursts occur erratically, in U Gem at intervals from 60 to 200 days; there is a mean interval between outbursts and a mean range in magnitude for a particular star. U Gem outbursts roughly every 102 days, with a range in magnitude of 5.1 (14.0 to 8.9). It was also found that the 'shape' of maxima vary; some being 'narrow' where the star was at maximum for only a few days, others being 'wide' where maximum light was maintained for up to two weeks.

It was also apparent that all dwarf novae do not behave in the same fashion. Some did not always return to minimum light following an outburst, but paused at an intermediate level for long periods. This characteristic, first noted in Z Chamelopardis, caused the dwarf novae to be subdivided into categories --- the U Gem or SS Cyg type, and the Z Cam type. There is a tendency, although there is much overlap, for the Z Cam stars to have smaller ranges and rather more frequent outbursts.

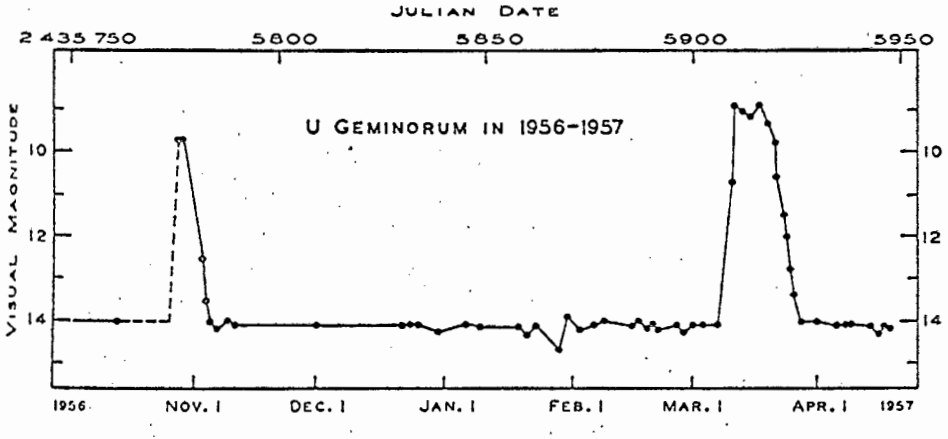

Figure 1. U Gem. From observations of the AAVSO.

The first move towards understanding these objects was made at Mt. Wilson by Humason(1938) who took spectra of nova remnants, and this was followed by a survey of the spectra of dwarf novae (Elvey & Babcock, 1943). Both investigations found a continuous spectrum with few or no absorption features, but showing CaII and Balmer emission. In some objects HeI and HeII were present, also in emission.

Photometry, permitting higher time resolution, showed unexpected features. In 1953 Walker observed the blue variable MacRAE $+43^{\circ}1$ (= MV Lyr) and found it to be "rapidly and continuously variable.

The periods of the fluctuations range from 1 to 30 minutes." (Walker, 1954a). He found similar variations in Nova Per 1901, T CrB, Q Cyg, DQ Her and UX UMa.

However it was the discovery that both UX UMa (Walker & Herbig, 1954) and DQ Her, or Nova Her 1934, (Walker, 1954b) are eclipsing binaries of very short period that provided the clue to the interpretation of these variables. Joy(1954) showed that the nova-like variable AE Aqr is a spectroscopic binary, also of very short period. In 1960 Kraft made a spectroscopic test for binary motion among the U Gem stars (Kraft, 1962), and advanced the hypothesis that all cataclysmic variables are short period binaries. The present evidence for this hypothesis is summarised in Table 1. (Warner, unpublished). In addition to these stars, EY Cyg (Kraft, 1962) and V1017 Sgr (Kraft, 1964a) both show composite spectra, and are assumed to be pole-on. There is no well studied cataclysmic which has failed to show evidence of duplicity.

We note from Table 1 that there is no correlation between type of outburst and the binary period. This suggests that it may be possible to develop a 'unified model' to fit all cataclysmic variables. The only correlation apparent in Table 1 is that the secondary spectrum is visible only in those systems with $P \geqslant 6\frac{1}{2}$hr. Also, with the exception of T CrB, there is a strong preference for short periods. However there are indubitably selection effects operating in this table, due to the difficulty of detecting small radial velocity changes in faint objects.

Having established that we are dealing with binary systems, we look

TABLE 1.

	Type	V	P	Spect(2^y).	Ref.
T Cr B	RN	10.5	$227^d.6$	gM3	1
GK Per	N	13.0	$16^h\ 26^m$	K2IVp	2,3,9
V Sge	NL	12.2	12 21	dG:	4
AE Aqr	NL		9 53	dKO	5,6
RU Peg	UG	12.8	8 54	G8IVn	7
EM Cyg	NL	12.9	7 00	G or K	8,9
Z Cam	UG	13.6	6 56	dG1	10
SS Cyg	UG	11.4	6 38	dG5	7,11
TT Ari	NL	10.6	6 23	---	12
RW Tri	NL	12.9	5 34	---	13
RX And	UG	12.6	5 05	---	7,9
T Aur	N	14.9	4 54	---	14,15,9
UX UMa	NL	12.3	4 43	---	16
DQ Her	N	14.2	4 39	---	2,17,18
SS Aur	UG	14.7	4 20	---	19
U Gem	UG	14.5	4 10	---	7,20,21
WW Cet	UG	13.6	3 50	---	22,9
BV Cen	UG	12.9	3 47	---	23
RR Pic	N	12.0	3 29		23,24
VZ Scl	NL	15.6	3 28		25
V 603 Aql	N	11.5	3 19	---	2,9
MV Lyr	NL	13.3	2:	---	26
Z Cha	UG	15.2	1 47	---	23
VV Pup	NL	14.5	1 40	---	27,28
EX Hya	UG	13.7	1 39	---	29
WZ Sge	RN	15.2	1 22	---	2,30
AM CVn	NL	14.2	18	---	31.32

References to Table 1.

1. Kraft 1958
2. Kraft 1964a
3. Paczynski 1965a
4. Herbig et al 1965
5. Joy 1954
6. G. Chincarini, unpublished
7. Kraft 1962
8. Mumford & Krzeminski 1969
9. Kraft, unpublished
10. Kraft et al 1969
11. Walker & Chincarini 1968
12. Smak & Stepien 1968
13. Walker 1963a
14. Walker 1963b
15. Mumford 1967a
16. Walker & Herbig 1954
17. Greestein & Kraft 1959
18. Walker 1961
19. Kraft & Luyten 1965
20. Krzeminski 1965
21. Warner & Nather 1971
22. Kraft 1964b
23. Mumford 1971
24. van Houten 1966
25. Krzeminski 1966
26. Walker 1966
27. Herbig 1960b
28. Warner & Nather 1972a
29. Mumford 1967b
30. Krzeminski & Smak 1971
31. Smak 1967
32. Warner & Robinson 1972

Note: A dash indicates definitely no secondary spectrum present.

. Otherwise not known.

to the spectra to provide the identity of the components. In those systems which show a secondary spectrum, narrow absorption lines of a cool star, a G or K dwarf, are seen superimposed on the high energy spectrum.

In the spectrum of WZ Sge the absorption features of a DA white dwarf are present (Greenstein 1957); and broad shallow hydrogen absorption is observed in DI Lac (Kraft 1964a) and UX UMa (Walker & Herbig 1954). This, together with the indication that these are intrinsically faint objects with M_v +5 to +10 (Kraft & Luyten 1965), suggests that the primary component of such systems is a white dwarf.

It is the emission spectrum that is characteristic of these objects. There is a clear correlation between the type of outburst (or the time scale of the outbursts) and the emission spectrum, in the sense that only the novae and the recurrent novae show the λ4650 lines of CIII - NIII and the forbidden nebular lines. The region producing these lines is identified with the nova shell, and will not concern us further. The emission lines --- the Balmer series, CaII, and sometimes HeI and HeII --- are very wide or doubled. Kraft (1963) found that the HeII velocity curve for DQ Her showed a classical rotational disturbance before and after mid-eclipse (Fig. 2). Furthermore the radial velocity changes for the emission lines are in antiphase to those of the secondary spectrum, where visible. See Fig. 3 .

We conclude that the emission spectrum originates in a flattened,

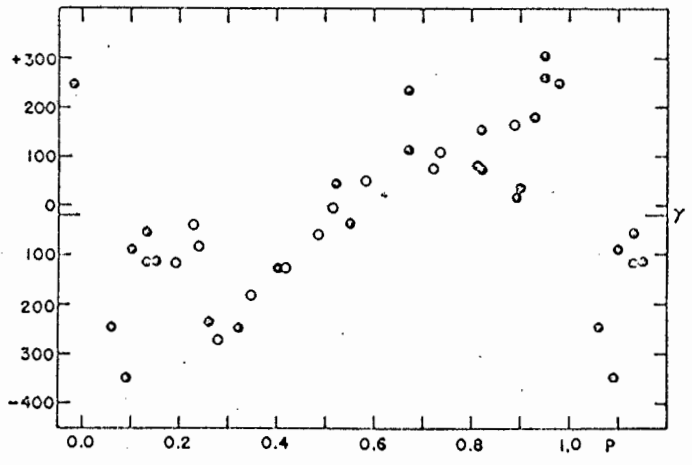

Figure 2 . Radial velocities (km sec^{-1}) of HeII (λ4686) for DQ Her.

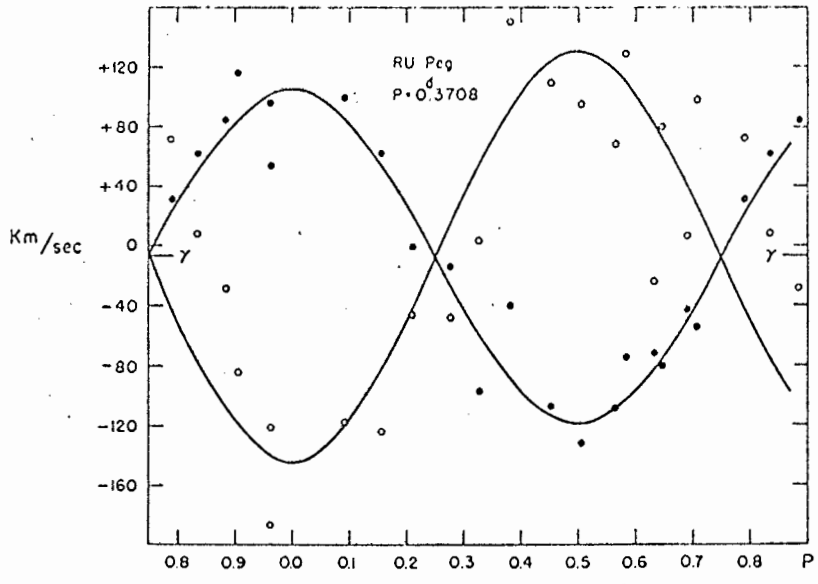

Figure 3 . Radial velocities for RU Peg. Open circles refer to the bright lines, solid circles to the dark lines.

rapidly rotating region surrounding the primary; which we call the 'ring' or 'disc'. The line-width, or line separation, corresponds to a projected velocity of rotation of 200 to 1500 km sec^{-1}.

The photometry indicates that we are to identify the strong continuum with a fourth light source located assymmetrically in

the plane of the orbit. In U Gem there is a conspicuous hump in the light curve, and shortly after the maximum of this hump it is cut into by a deep eclipse (Fig. 4).

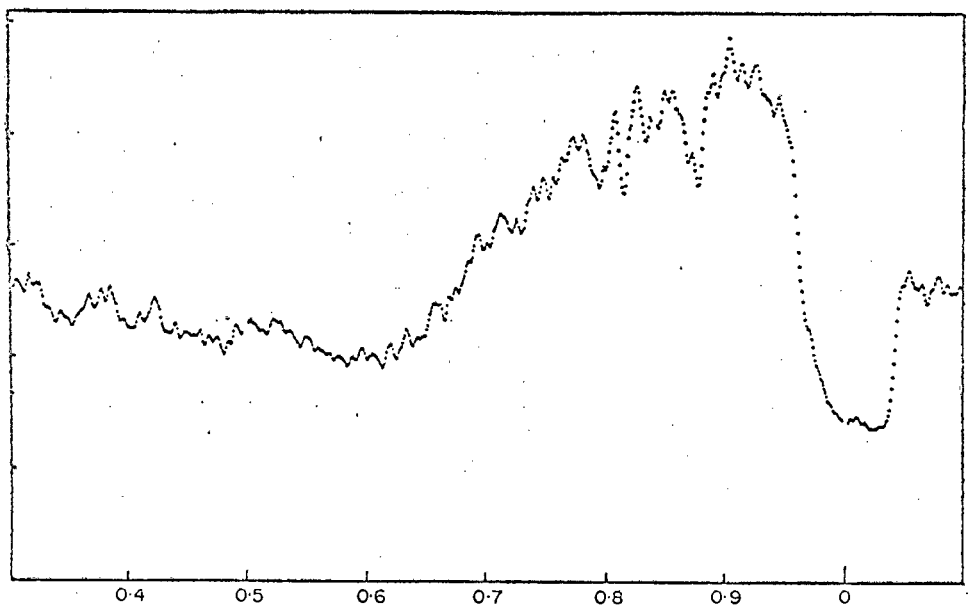

Figure 4 . U Gem. Vertical axis is intensity (counts sec^{-1}).

Time resolved spectra have shown that changes in line intensity are insufficient to account for the hump (e.g. SS Cyg, Walker & Chincarini 1968), and that emission persists during eclipse. Although the colours of cataclysmic variables cannot be determined with great accuracy due to the flickering present, changes in colour around the orbit are of great interpretive value. We note that in U Gem the hump is bluer in (B-V) and redder in (U-B) than the rest of the orbital cycle. The colour change in eclipse is the reverse of this (Fig. 5). We note also that the flickering activity is greatest at the maximum of the hump, and that it disappears during eclipse. These observations indicate that the object producing the hump is the object eclipsed. The (U-B) excess in eclipse suggests that the continuum has been reduced, and that the

residual light is largely due to the emission lines (Krzeminski 1965). We conclude that the 'hot spot' responsible for the hump is the origin of the strong continuum, and that it is totally eclipsed in the case of U Gem (the eclipse is essentially flat bottomed).

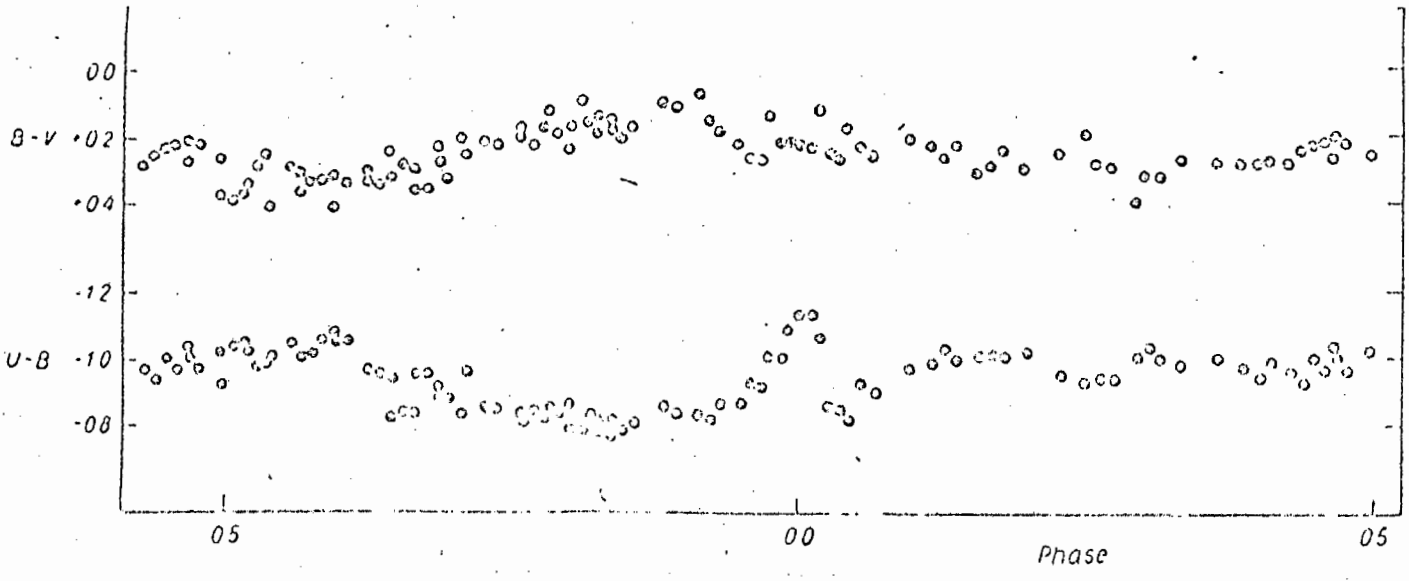

Figure 5 . Colour for U Gem.

It was Kraft's interpretation of DQ Her (Kraft 1963) which provided the mechanism for the production of such a 'hot spot'. He observed that in the widely differing systems --- T CrB, DQ Her, SS Cyg --- an invariant emerged, and it is that the inferred radius of the secondary is of the same order as the characteristic dimension of the system, defined as $\frac{1}{2}\left\{(a_1 + a_2) \text{ Sin } i\right\}$. In other words the secondary fills one lobe of the inner Lagrangian surface, and under such conditions will lose mass through the inner Lagrangian point. This material will stream towards the following hemisphere of the primary, and may form a ring or disc around it (e.g. Gould 1957). Such a ring will have a limited lifetime, decaying as the particles fall to the surface of the primary (Gorbatsky 1969).

Since these rings are observed to be persistent features we may deduce that the mass transfer is continuous.

There is some observational evidence to support the theory that the secondaries fill their Roche lobe. RU Peg has a secondary spectrum roughly constant at G8. The MK luminosity class, however, varies from III at conjunction with the secondary behind; to V at elongations. A dwarf star would imitate a giant by a reduction of its effective surface gravity. The inferred change is in the direction we would expect if the star were filling its Roche lobe (Kraft 1962).

When the stream of material from the secondary encounters the ring encircling the primary a portion of the kinetic energy of the particles will be converted into radiation. This will produce a bright spot, whose size will be determined primarily by the cross section of the gas stream, and will generally be small (Warner & Peters 1972). The rapid flickering observed is then due to the inhomogeneities in the gas stream. We note that in eclipsing systems (i.e. those with high orbital inclinations only) the spot is visible for only half the orbital period (Fig. 4) so the ring must be optically dense (e.g. UX UMa, Walker & Herbig 1954) --- in fact disc would be a better term for this structure. There is a pronounced variation in the V/R ratio of the emission lines around the orbit, indicating that the disc is most luminous along the line of sight at phase 0.75~0.85, that is in the region of the spot.

This model of a binary system containing an emission ring and a

bright spot (Fig. 6) had been proposed for several systems such as UX UMa (Walker & Herbig 1954), VV Pup (Herbig 1960b), DQ Her (Kraft 1959), RW Tri (Walker 1963a), and U Gem (Krzeminski 1965).

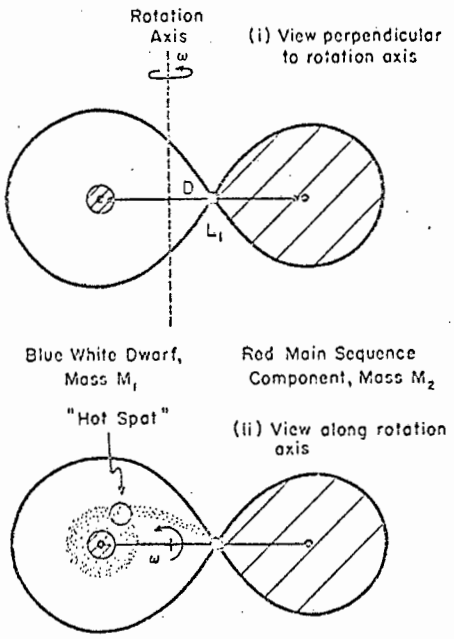

Figure 6 . The model for a cataclysmic variable.

The difficulties encountered by most of the early models were due to the siting of the hot spot on the surface of the primary, and the assumption that it was the primary that was being eclipsed. The reasons for siting the spot in the ring may be summarised:-

1. The spot cannot extend far in longitude, or the hump would extend for more than half the orbital cycle. The duration of ingress is, in U Gem, observed to be about 100 seconds. If the (small) spot were located on the surface of the primary, ingress would occupy only a few seconds.
2. The spot extends only a few degrees in longitude, and it is not plausible that the small cross-section of the gas stream could be maintained passing through an extended and fairly dense medium (as indicated by the emission lines) before impingeing on the spot.

That it is the spot that is eclipsed rather than the primary is evidenced by;-

1. The flickering, which we associate with the spot, disappears during eclipse.
2. It is difficult to explain the marked assymmetry of the eclipse as the obscuration of the central star.
3. The phase, shape, and duration of the eclipses are somewhat variable, and this is simply explained as being due to changes in the radius vector of the spot, and the distribution of light in the disc.

A further difficulty of the model proposed by Krzeminski for U Gem was that it required that it was the secondary which was responsible for the outbursts. It is more probable, indeed certain, that it is the primary which outbursts because it is currently thought that the outbursts of cataclysmic variables are due to non-radial pulsations of the white dwarfs. These pulsations are excited by the thermal runaway caused when the hydrogen-rich material accreted on the surface of the white dwarf is ignited (Warner 1972a). The observational evidence is as follows:-

1. Spectra of U Gem taken just before maximum show the characteristics of a B subdwarf. (Elvey & Babcock 1943, Krzeminski 1965)
2. The 71 sec oscillations observed in DQ Her, attributed to the non-radial pulsations of the white dwarf, are not present during primary minimum. (Walker 1961, Warner & Nather 1969)
3. In Z Cha the eclipses are total at minimum light. During outburts, however, they become only partial eclipses, and as the star returns to normal light the flat-bottomed eclipse reappears. (Warner, unpublished)

CHAPTER TWO

The Observations of U Gem

A1 Spectroscopic Observations at Minimum Light

Elvey & Babcock (1943) obtained two low dispersion plates of U Gem. Their observations were extended by a series of plates taken by Kraft (1962) at a somewhat higher dispersion (~ 180 Å mm^{-1}).

No absorption spectrum is visible. The emission lines of hydrogen and CaII are strong and clearly doubled. There are weak emission lines of HeII (λ 4686), HeI ($\lambda\lambda$ 4471,4026) and FeII ($\lambda\lambda$ 4584, 4522, 4508, 4303, 4233, 4173). The V/R ratio of the strong lines is reversed at opposite elongations.

Kraft published radial velocity measures for the emission lines, (Kraft 1962) and the radial velocity curve is shown in figure 7 . The fitted curve is for the elements:

$P = 0^d.17690591$ $\qquad \gamma = +42$ km sec^{-1}

$K_1 = 265$ km sec^{-1} $\qquad a_1 = 6.46 \times 10^{10}$ cm

Spectroscopic conjunction is at photometric phase 0.04 .

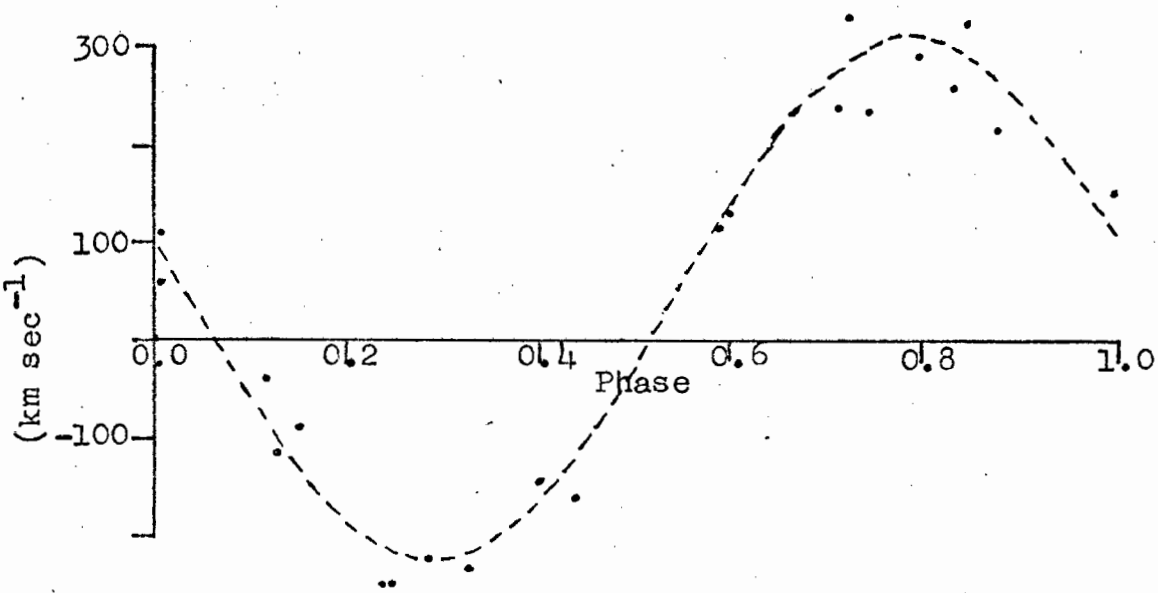

Figure 7 . The radial velocity curve for U Gem.

Microdensitometer tracings of Kraft's spectra, reduced to intensity, were measured in order to determine the line separations and total line widths. The relevant sections of these tracings are reproduced in the Appendix. The scale of the tracings, determined from a calibration plate of β Ari, was found to be

$$1 \text{ mm} = 2.04 \pm 0.02 \text{ Å}$$

Measures of the peak-to-peak line separation are presented in Table 2 . We note that, within the experimental error, all lines show the same separation between the components. The average for all lines gives

$$2v \sin i = 990 \pm 10 \text{ km sec}^{-1}$$

However if we plot the mean line separation for each exposure against phase (Fig. 8), we see that there are disturbances of the rotational velocity at phases 0.7 and 0.2 .

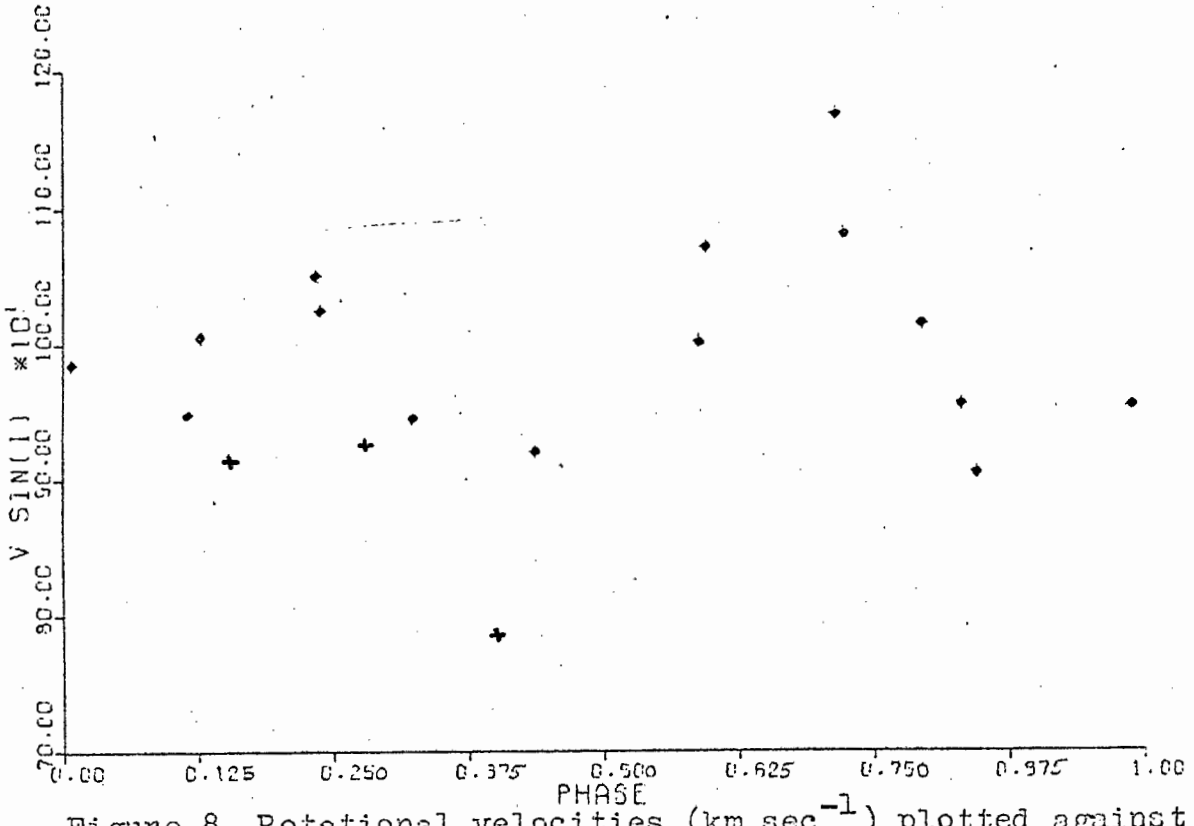

Figure 8. Rotational velocities (km sec^{-1}) plotted against binary phase. Measures from Plate 1277 are plotted as crosses.

TABLE 2.

Line Separations (km sec^{-1}).

Plate	Phase	H_β	H_γ	H_δ	H_ε	K	H_ς	H_η	Mean H_β to H_δ	Mean H_ε to H_η	Mean
1277a	0.153	932	917	970	---	808	945	---	940	877	914
b	0.279	920	917	940	894	933	930	958	926	929	927
c	0.400	880	845	---	725	685	---	800	863	737	787
1323a	0.795	---	973	---	1018	1058	---	---	973	1038	1016
b	0.322	969	902	1000	925	934	---	---	957	930	946
c	0.435	831	---	955	---	---	976	---	893	976	921
1324a	0.587	1007	987	1030	956	934	1102	---	1008	997	1003
b	0.722	---	987	1164	1079	---	1102	---	1076	1091	1083
c	0.844	---	---	865	---	887	944	926	865	919	906
1325a	0.987	919	1043	1015	864	934	---	---	992	899	955
b	0.115	856	1015	1015	864	934	---	1006	962	935	948
c	0.234	1058	987	1089	987	1136	---	---	1045	1062	1051
1326a	0.594	1133	1010	1089	1049	965	1133	1133	1077	1070	1073
b	0.714	1259	1128	1134	1203	1075	1196	1197	1174	1168	1170
c	0.831	---	987	895	---	965	976	---	941	971	956
1327a	0.008	1007	987	985	---	965	---	---	993	965	986
b	0.126	907	1015	940	1049	1120	---	---	954	1085	1006
c	0.238	969	959	985	1079	1136	---	---	971	1108	1026
Means:	All Plates	975	979	1004	976	967	1034	1003	986	988	987

At these positions, near the elongations of the spot, the contribution of the spot will greatly enhance one of the disc components, moving the core of the line from its true position. Thus, from figure 8 , we estimate the rotational velocity of the disc as measured by the line separation to be

$$v_d' \text{ Sin } i = 480 \pm 10 \text{ km sec}^{-1}$$

Measures of the total width of the line pairs at half-height are presented in Table 3 . The measures were made by estimating the level of the underlying continuum by eye, and the average level of the two line peaks; the width was then measured to the nearest millimeter.

TABLE 3

Total Line-widths at Half-height

Width (mm)	Number of measures for: H_β	H_γ	H_δ	H_ε	K	H_ς	H_η
8							1*
9					1*	1*	1
10				2*	7**	1	3*
11				6 **	8	3	-
12			3	6	1	2	1
13			4*	3			
14		10***	7*				
15	2*	5	1				
16	10**	2					
17	1						
18	2						
½ Width km/sec	1020	1036	1007	894	817	858	782

Asterisks refer to measures from Plate 1277

We note that the apparent line width decreases as we move to shorter

wavelengths. This effect is probably due to uncertainty in the true continuum level as the Balmer jump is approached --- causing the widths to be measured too 'high' on the profiles. We note that the measures for plate 1277 are not very different to those for the other plates. In what follows we shall take the mean line width to refer to the lines H_β to H_δ only. Furthermore, at this dispersion, there is apparently no correlation between the total line width and the binary phase. We find:

$$v' \text{ Sin } i = 1020 \pm 10 \text{ km sec}^{-1}$$

We can correct this measure for the instrumental broadening in a rather crude manner. The half width of each line will be approximately (1020 - 480) km sec^{-1}. We have no measure of the instrumental width, but estimate it by rule-of-thumb, i.e. that the line width in km sec^{-1} is equal to the dispersion in Å mm^{-1}. The correction to be applied is thus; $v \text{ Sin } i = (540^2 - 90^2)^{\frac{1}{2}} + 480 \text{ km sec}^{-1}$

$= 1012 \text{ km sec}^{-1}$

The correction is small, and we will not be too far out due to our crude model. Further broadening due to the exposure time will be discussed in Chapter 4 .

Here we encounter a problem of interpretation --- are we to adopt the line separations, or the line widths, as a measure of the rotational velocity of the disc? Smak (1969) has found that generally the mean rotational velocity of the disc is larger than that determined from the measures of radial velocities of the emission lines. Figure 9 (from Smak 1969) shows a set of calculated line profiles where:

r_1: is the inner radius of the ring in terms of its outer radius

Case 1 ; density distribution within the ring is uniform

Case 2 ; density decreases linearly with radius

and the dotted line represents the true mean velocity of rotation given by:

$$v = \left(\frac{G M_1}{r}\right)^{\frac{1}{2}} \qquad \ldots\ldots\ldots\ldots\ldots\ldots\ldots\ldots\ldots\ldots (1)$$

where M_1 is the mass of the primary, and r the radius of the ring.

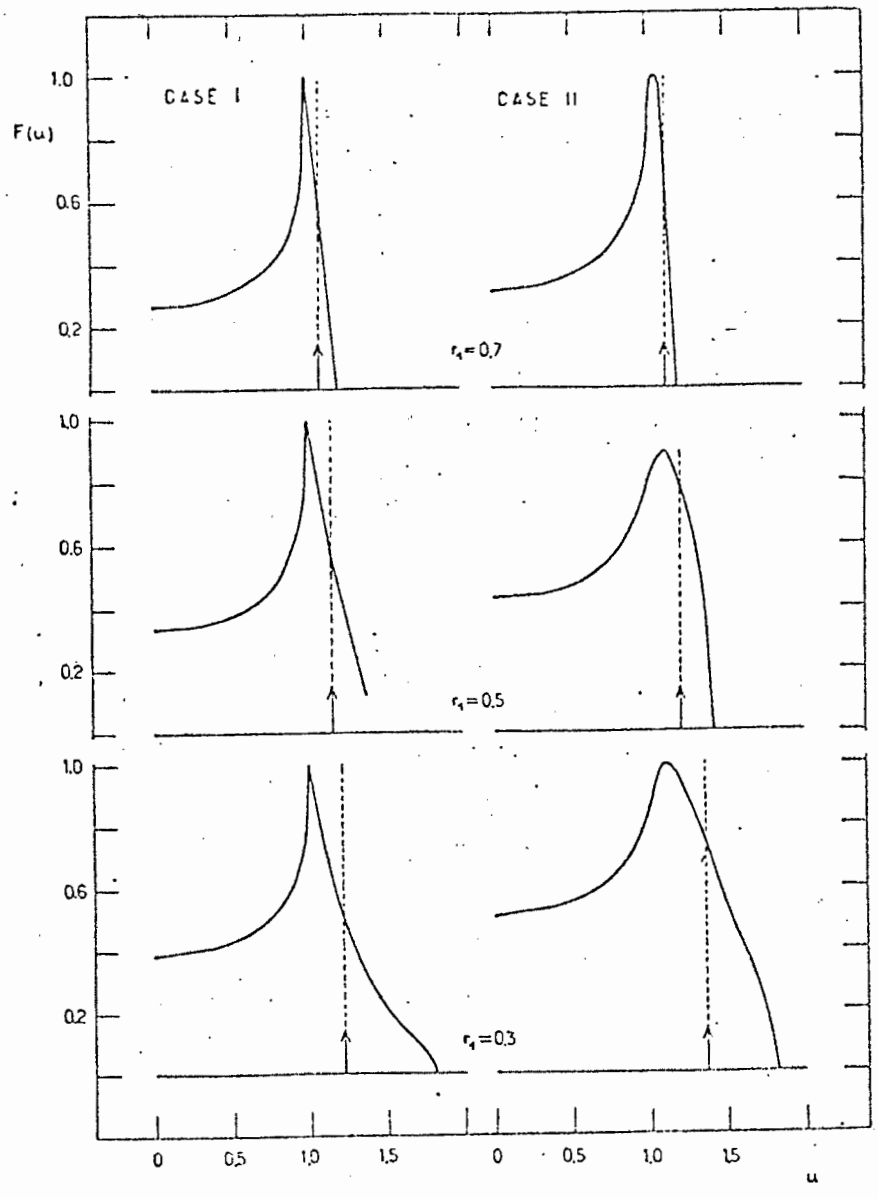

Figure 9 . Theoretical profiles (see text).

Clearly the total line width will be a more reliable estimate of v Sin i, and we note in passing that for $M_1 \sim 0.7\ M_\odot$ and

$r = 0.12 \times 10^{11}$ cm ; we obtain $v \doteq 900$ Sin i km sec^{-1}, which is in good agreement with our observations.

Smak (1970) has discussed the effects of the blending of the emission lines on the radial velocity curves, and finds that it will in general lead to an underestimate of the radial velocity amplitude. In the case of U Gem this analysis would appear to be unreliable, and will be discussed further in Chapter 4 . Spurious eccentricities and phase shifts of conjunction will not concern us here, as we shall assume that e=0 (Kruszewski 1966) and determine the moment of true conjunction from the photometric model.

A2 Spectroscopic Observations at Maximum

Spectra of U Gem during outburst have been obtained by Joy (1940), Elvey & Babcock (1943), and Krzeminski (1965) . At maximum the spectrum is continuous, with very faint HeII (λ 4686) and H_β in emission. However on the rise to maximum there are very wide, shallow hydrogen absorption features, reminiscent of a white dwarf; with faint absorption of HeI at $\lambda\lambda$4471 and 4026 .

B1 Photometric Observations at Minimum Light

In 1961 Krzeminski discovered that U Gem is an eclipsing binary (Krzeminski 1965), and all further published eclipse photometry has been collected in Table 4 . (Paczynski 1965, Mumford 1964, Mumford 1970, Warner & Nather 1971). In addition there are eleven eclipses observed by Warner at McDonald Observatory, and one (N = 22824) observed by Warner and the author at the South African Astronomical Observatory at Sutherland; using the equip-

ment described by Nather & Warner (1971). The unpublished eclipses are reproduced in the Appendix. All data have been reduced according to the method described by Krzeminski (1965) and the (O-C) values refer to the elements:

$$\text{Min} = 2437638.82704 + 0.17690591 \times N$$

The depth of eclipse is expressed in magnitudes, the width and the duration of egress in terms of the orbital period.

The light curve varies from one cycle to another, but several basic features are well repeated. (See Fig. 4) There is a large hump which appears at phase (0.605 ± 0.005)P and lasts for half the period. Maximum of this hump occurs at 0.85P, and it is symmetrical about the maximum. There is a deep flat-bottomed eclipse centred on phase 0.0P (by definition). The eclipse width at half depth is 0.056P, and egress lasts about 0.006P . The shape of ingress is somewhat variable, but the duration of ingress is about 0.012P . The colours (See Fig. 5) have been discussed in the introduction.

B2 Photometric Observations at Maximum

We have no further observations to add, and quote the summary given by Smak (1971).

> (*a*) Initial rise, at $T = -2$; examples: JD 2437732·76 (Krzemiński 1965), JD 2438001·84 and 002·02 (Mumford 1964). While the shape of eclipse begins already to change, its central phase remains close to $\varphi = 0$, and the second and the third contacts are still quite well defined. The colours of the body eclipsed are not much different from those observed before the outburst (see Figs. 6 and 7 of Paczyński (1965)).
>
> (*b*) Final rise, at $T = -1$ and 0; examples: JD 2438002·90, 003·07, 003·78, and 003·96 (Krzemiński 1965, Fig. 5). The central phase of eclipse shifts to about $\varphi = 0{\cdot}985P$ at $T = 0$ (Krzemiński 1965, Fig. 9). No second and third contacts can be distinguished as the eclipse becomes progressively shallower. The colours at the bottom of eclipse (JD 2438003·96, $T = 0$) become different.

TABLE 4.

AVAILABLE ECLIPSE PHOTOMETRY FOR U GEMINORUM

ISS	COL	N	WT.	OBSERVED	(O-C)	DAY O/B	DEPTH	WIDTH	EGRESS
K	V		0	2437637.9000		61	.66		.0061
K	V		2	2437638.8269	-.0001	62	.74	.0571	.0071
K	V	1	2	2437639.0038	-.0001	62	.60	.0560	
K	B	6	2	2437639.8883	-.0002	63	.73	.0588	.0068
K	B	209	0	2437675.6000		8	.02		
K	B	215	2	2437676.8617	-.0001	9	.03	.1040	
K	B	299	2	2437691.7221	.0002	24	.54	.0752	.0111
K	V	327	2	2437696.6754	.0001	29	.69	.0701	.0083
K	B	491	2	2437725.6678	-.0000	58	.61	.0565	
K	B	492	2	2437725.8649	.0002	58	.57	.0577	
K	V	531	2	2437732.7640	-.0001	65	.56	.0690	
K	B	531	2	2437732.7641	.0000	65	.65	.0690	
K	B	531	2	2437732.7641	.0000	65	.63	.0695	
K	V	621	2	2437748.6858	.0002	14	.70	.0820	.0109
K	V	672	2	2437757.7084	.0006	23	.81	.0690	
K	U	785	1	2437777.6979	-.0003	43	.69	.0639	
K	B	819	2	2437783.7129	-.0001	49	.73	.0616	.0083
P	V	1646	2	2437930.0140	-.0002	18	.71	.0746	
K	V	1691	2	2437937.9750	.0001	26	.62	.0741	.0093
P	V	1691	2	2437937.9749	-.0000	26	.61	.0746	
P	B	1691	2	2437937.9754	.0005	26	.61	.0774	
P	U	1691	2	2437937.9758	.0009	26	.41	.0786	
P	V	1725	2	2437943.9897	-.0000	32	.65	.0695	
P	B	1725	2	2437943.9898	.0001	32	.74	.0746	
P	U	1725	2	2437943.9892	-.0005	32	.56	.0752	
P	V	1938	2	2437963.9796	-.0005	52	.59	.0627	
P	B	1938	2	2437963.9800	-.0001	52	.71	.0538	
P	U	1638	2	2437963.9796	-.0005	52	.53	.0633	
K	V	2030	0	2437997.9000		86	.76	.0492	
K	B	2030	0	2437997.9000		86	.80	.0537	
K	U	2030	0	2437997.9000		86	.58	.0582	
M	V	2052	0	2438001.8000		-2	.65	.0503	
M	B	2052	0	2438001.8000		-2	.68	.0543	
M	U	2052	0	2438001.8000		-2	.50	.0531	
M	V	2053	0	2438002.0000		-2	.58	.0520	.0114
M	B	2053	0	2438002.0000		-2	.72	.0543	.0100
M	U	2053	0	2438002.0000		-2	.49	.0560	.0113
K	V	2058	1	2438002.8979	-.0015	-1	.27		
K	V	2059	2	2438003.0742	-.0021	-1	.29	.0724	
K	V	2063	1	2438003.7812	-.0027	0	.06		
K	V	2064	2	2438003.9580	-.0028	0	.04	.0865	
K	B	2064	2	2438003.9574	-.0034	0	.04	.0707	
K	U	2064	1	2438003.9591	-.0017	0	.02	.0893	
K	V	2081	2	2438006.9689	.0007	3	.05	.1029	
K	B	2081	2	2438006.9680	-.0002	3	.04	.1057	
K	U	2081	2	2438006.9688	.0006	3	.04	.1204	
K	V	2086	2	2438007.8525	-.0003	4	.07	.1051	
K	B	2086	1	2438007.8514	-.0014	4	.06	.1080	
K	U	2086	1	2438007.8520	-.0008	4	.06	.1102	
K	V	2087	2	2438008.0295	-.0002	4	.07	.1040	
K	B	2087	2	2438008.0301	.0004	4	.06	.1080	
K	U	2087	2	2438008.0289	-.0008	4	.06	.1198	
K	V	2091	2	2438008.7381	.0008	5	.12	.0978	

TABLE 4 (continued)

AVAILABLE ECLIPSE PHOTOMETRY FOR U GEMINORUM

...SS	COL	...	...T.	OBSERVED	(O-C)	DAY O/B	DEPTH	WIDTH	EGRESS
C	V	2092	2	2438008.9143	.0001	5	.09	.0961	
K	B	2092	1	2438008.9150	.0008	5	.07	.0972	
K	U	2092	U	2438008.9000		5	.05		
P	V	2142	2	2438017.7595	.0000	14	.70	.0803	
K	V	2193	2	2438025.0124	-.0002	21	.71	.0735	.0100
K	V	2204	1	2438028.7280	.0003	25	.67	.0695	
K	B	2204	1	2438028.7280	.0003	25	.76	.0695	
K	U	2204	1	2438028.7277	.0000	25	.42	.0712	
K	V	2216	2	2438030.8506	.0001	27	.83	.0695	.0101
K	V	2217	2	2438031.0275	.0001	27	.78	.0684	.0103
P	V	2300	2	2438045.7103	-.0003	42	.77	.0667	
P	V	2363	2	2438056.8558	.0001	53	.84	.0571	
P	B	2363	2	2438056.8556	-.0001	53	.90	.0588	
P	U	2363	2	2438056.8554	-.0003	53	.61	.0616	
P	V	2364	2	2438057.0323	-.0003	53	.86	.0639	
P	V	2464	2	2438074.7231	-.0001	71	.73	.0554	
P	V	2538	2	2438087.8143	.0001	84	.80	.0464	
P	B	2538	2	2438087.8138	-.0004	84	.84	.0520	
P	U	2538	2	2438087.8139	-.0003	84	.78	.0509	
P	V	2707	2	2438117.7118	.0005	12	.23	.1051	
P	B	2707	2	2438117.7116	.0003	12	.22	.1046	
P	U	2707	2	2438117.7116	.0003	12	.13	.1074	
M	[illegible]	3997	2	2438345.9198	-.0002	239			
M	[illegible]	4359	2	2438409.9601	.0002	49			
M	[illegible]	4364	2	2438410.8443	-.0001	50			
M	[illegible]	4370	2	2438411.9059	.0000	51			
P	U	4477	2	2438430.6348	.0000	70	.50	.0588	
M	[illegible]	4832	2	2438493.6367	.0003	27			
M	[illegible]	4849	2	2438496.6440	.0002	30			
M	[illegible]	5857	2	2438674.9658	.0008	208			
M	[illegible]	7014	2	2438879.6464	.0013	97			
M	[illegible]	7999	2	2439053.8987	.0013	66			
M	[illegible]	8005	2	2439054.9596	.0008	67			
M	[illegible]	9004	2	2439231.6897	.0018	19			
M	[illegible]	10677	2	2439527.6533	.0019	60			
M	[illegible]	10678	2	2439527.8300	.0017	60			
M	[illegible]	12860	2	2439913.8392	.0022	18			
M	[illegible]	12894	2	2439919.8548	.0030	24			
M	[illegible]	16704	2	2440593.8666	.0032	15			
M	[illegible]	16710	2	2440594.9279	.0031	16			
M	[illegible]	16727	2	2440597.9360	.0038	19			
M	[illegible]	17189	2	2440679.6662	.0035	23	.56	.0769	.0096
M	[illegible]	17195	2	2440680.7279	.0037	24	.64	.0746	.0097
M	[illegible]	18869	2	2440976.8680	.0033	123	.51	.0543	.0054
M	[illegible]	20559	U	2441275.8400		35	.46		.0118
M	[illegible]	20593	2	2441281.8543	.0039	40	.53	.0735	.0102
M	[illegible]	20670	2	2441296.8915	.0041	56	.52	.0667	.0066
M	[illegible]	20683	2	2441297.7760	.0040	57	.58	.0678	.0060
M	[illegible]	21016	2	2441356.6862	.0046	116	.46	.0543	.0082
M	[illegible]	21045	2	2441361.8161	.0042	121	.40	.0560	.0056
M	[illegible]	21067	2	2441365.7083	.0045	125	.40	.0543	.0080
M	[illegible]	21084	2	2441368.7153	.0041	128	.41	.0537	.0041
M	[illegible]	22824	2	2441676.5322	.0047		.59	.0599	.0065

(c) Maximum, roughly from $T = 0$ to $T = 3$ or longer, when the eclipses (if any) are practically undetectable among the fluctuations (see Fig. 6 of Krzemiński (1965)).

(d) Decline, roughly from $T = 3$ or later; examples: JD 2438006·97 — — 008·91 (Krzemiński 1965) with $T = 3 - 5$, and other observations at larger T's. As the eclipse reappears, its central phase is again at $\varphi = 0$. And once the minimum becomes deep enough, so that its shape can be discussed, the second and the third contacts become visible again. The colours of the eclipsed body are practically identical with those between the outbursts although the colours at the bottom of eclipse are initially similar to those reached at maximum (see Figs. 6 and 7 of Paczyński (1965)).

C1 The Photometric behaviour between outbursts

In figures 10, 11, 12 the eclipse parameters are plotted against time from outburst, all colours having been plotted together. The changes in the eclipse are fairly well defined. An important observation is that the brightness of the spot --- interpreted as the relative brightness of the shoulder -- is practically constant throughout the outburst cycle (cf. Table 4 of Smak (1971)).

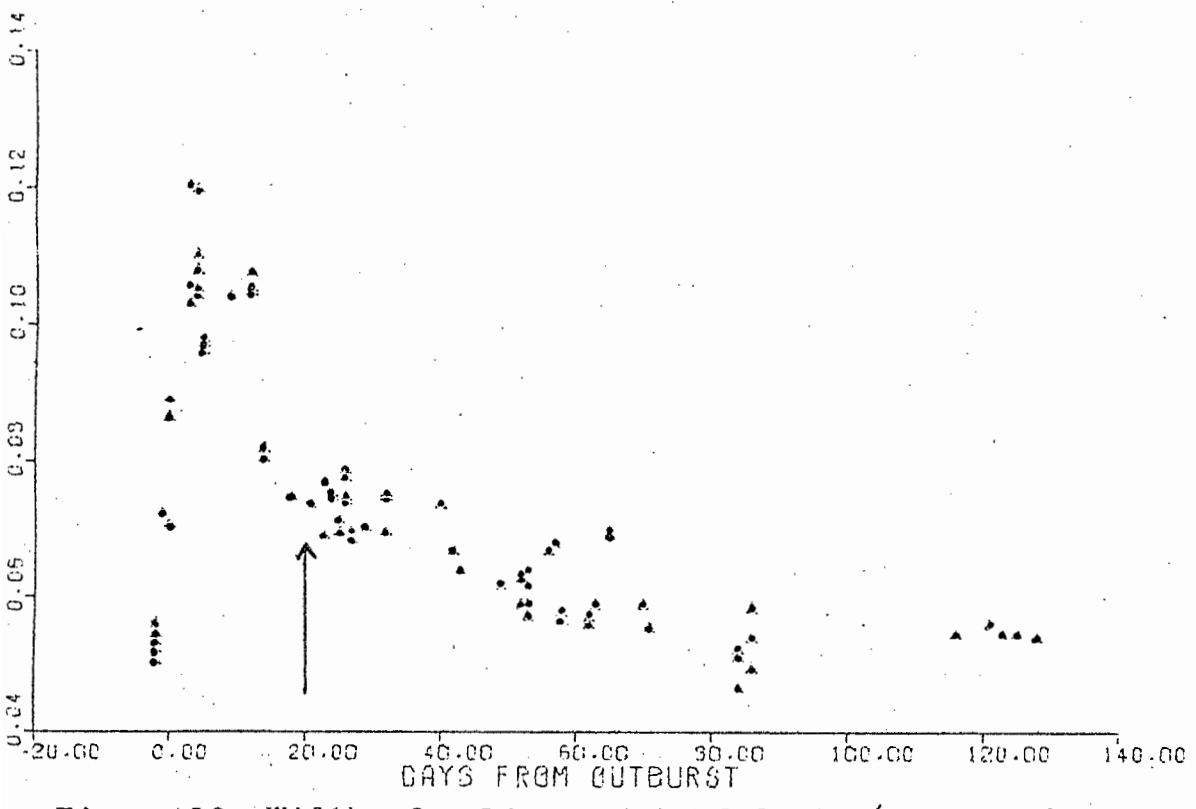

Figure 10. Width of eclipse at half depth (expressed in terms of the orbital period) against time from outburst.

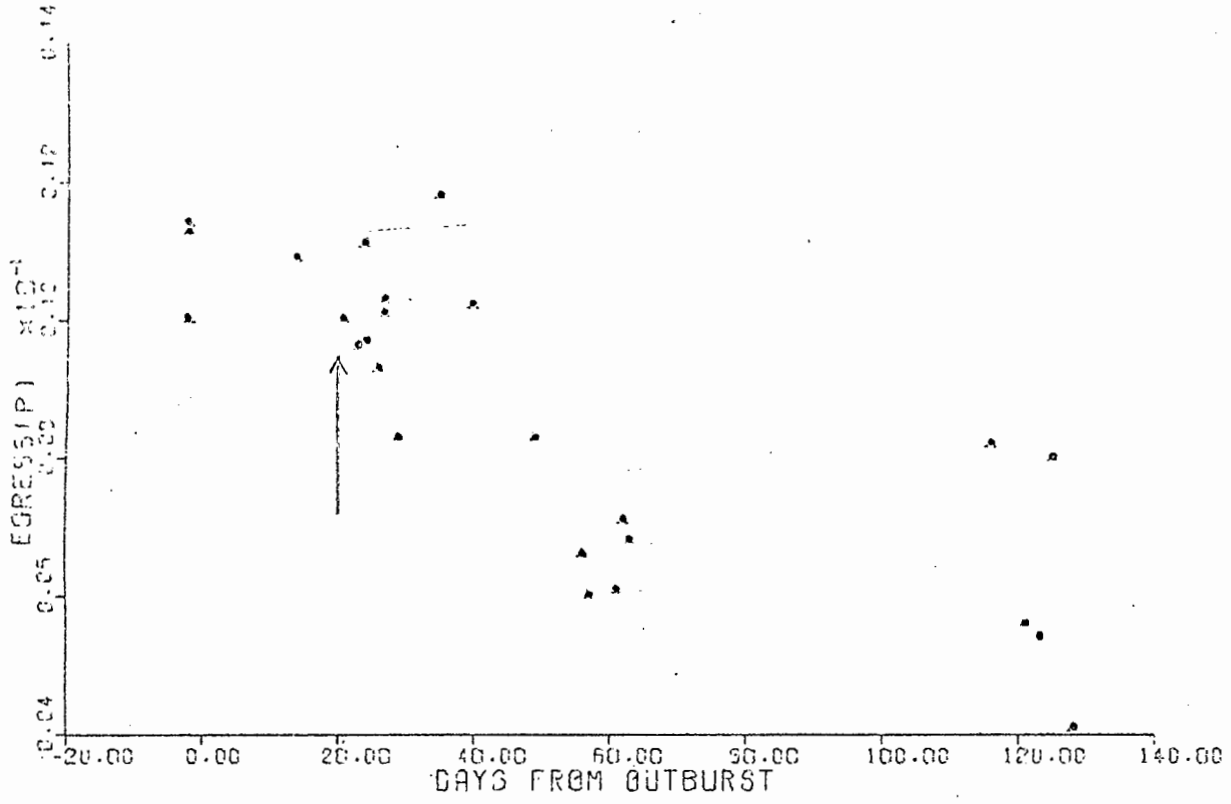

Figure 11. Duration of egress (expressed in terms of the orbital period) against time from outburst.

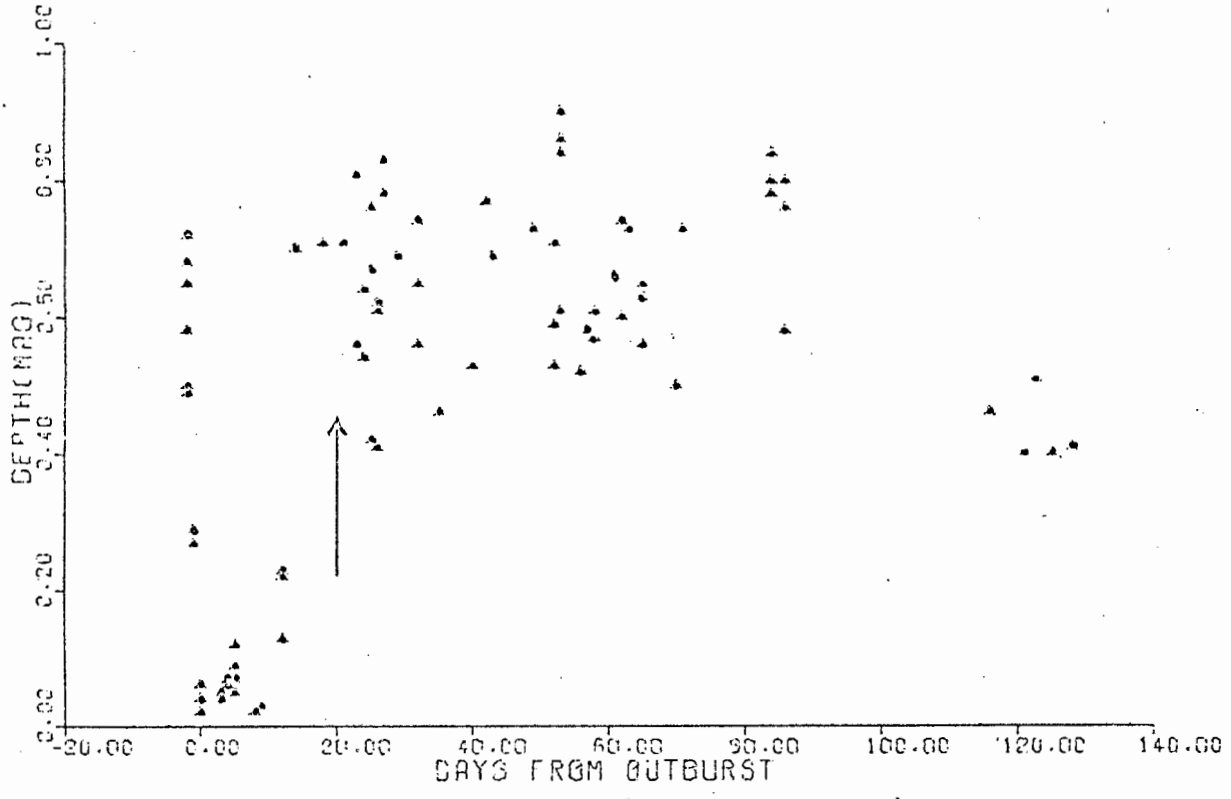

Figure 12. Depth of eclipse (in magnitudes) against time from outburst.

We may also examine the phase of the eclipse as a function of the time from outburst. Smak (1972) has examined this (O-C) versus T relationship in order to reduce the scatter in the (O-C) versus N relationship. Smak found

$$(O-C) = 3 \times 10^{-4} - 7 \times 10^{-6} \times T$$

If we invert the process, removing the trend in Figure 13 by fitting a curve to it, and then examine the (O-C) versus T relationship (Fig. 14) we obtain

$$(O-C) = 1.7 \times 10^{-4} - 4.4 \times 10^{-6} \times T \quad \ldots\ldots\ldots \quad (2)$$

in the range $2 < T < 100$, where only observations of weight /2/ have been included.

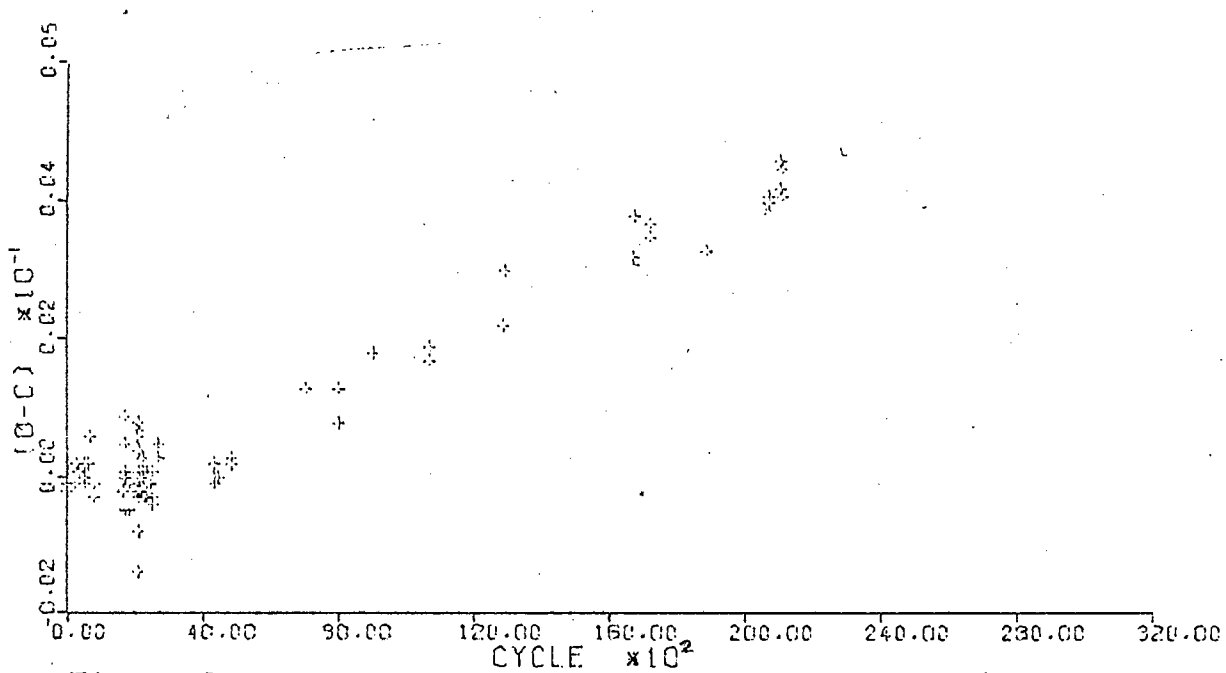

Figure 13. Residuals calculated from Krzeminski's elements against cycle number.

The numerical values in equation (2) are very sensitive to the weighting of the observations, however we may say that eclipses tend to be shifted earlier than predicted as the time from the last outburst increases. Over a 100 day period this shift amounts to about 0.0025P .

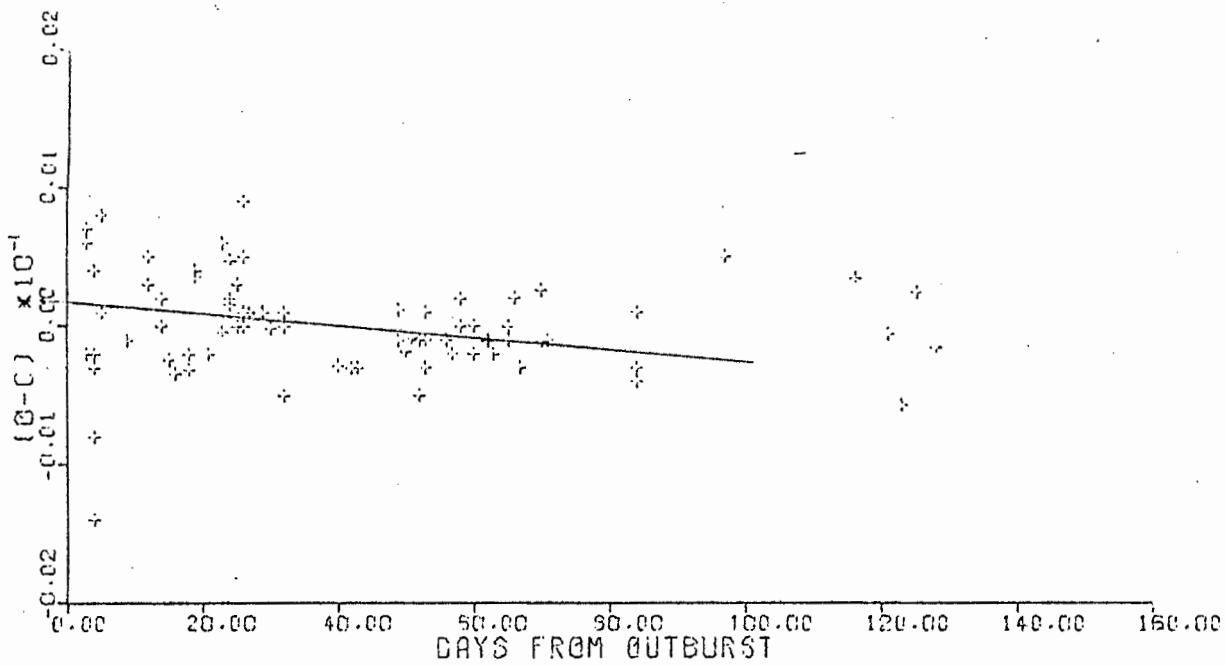

Figure 14. Residuals, corrected for the trend in Fig.13, plotted against time from outburst.

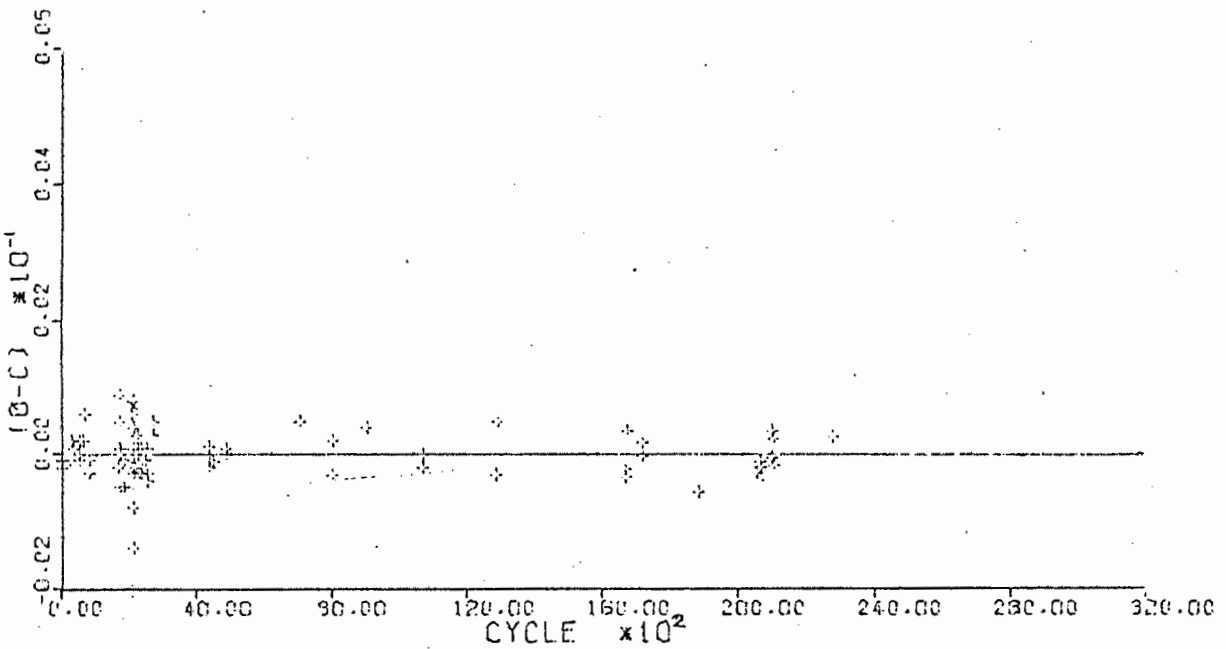

Figure 15. Corrected residuals of Fig.14 plotted against cycle number.

C2 The Spectroscopic behaviour between outbursts

Unfortunately all but one (No. 1277) of Kraft's plates that were available for study were taken at the same epoch, 85 days from outburst. Plate 1277 was taken 12 days from outburst.

We see (Fig. 8) that the line separation on plate 1277 is about 80 km sec^{-1} smaller than that on the other plates. The line widths cannot be measured with the same certainty as the separations, but those from plate 1277 are generally smaller than the average. However we note that a variation of the radius vector of the spot does not necessarily imply a change in the size of the disc, as measured from the line width (Krzeminski & Smak 1971). The changes in the radius vector of the spot will be due largely to the changes in the density of the disc along the particle trajectory.

The large change in the rotational velocity of the disc found by Paczynski (1965) was due to the oversight of the variation in the line separation around the orbital cycle.

CHAPTER THREE

Geometry, and choice of the model

One of the main difficulties in dealing with the cataclysmic variables is that no physical dimension or parameter of the system is directly measureable. Two measurements we can make directly are i) the position of the hump relative to the eclipse, and ii) the width of the eclipse. We shall use some basic equations relating these observables to the geometric parameters of the system, based on the simple geometric model developed by Smak (1971). We shall assume that:

i) the hot spot is a point source located in the orbital plane

ii) the secondary is spherical, its radius being the average of the three principal radii of the Roche surface, R_2

iii) the orbit is circular.

We define two systems of coordinates (Fig. 16):

i) Oxyz . The frame of the stars. The primary is located at the origin, the secondary at (1,0,0), and the spot position is described by the vector (r,α) . The xy plane is the orbital plane.

ii) OXYZ . The frame of the observer. The X axis is located in the orbital plane, and the observer views along the Z axis.

These two frames are rotating relative to one another, and the transforming matrix is:

$$\begin{pmatrix} X \\ Y \\ Z \end{pmatrix} = \begin{pmatrix} \sin\psi & \cos\psi & 0 \\ -\cos\psi\cos i & \sin\psi\cos i & \sin i \\ \cos\psi\sin i & -\sin\psi\sin i & \cos i \end{pmatrix} \begin{pmatrix} x \\ y \\ z \end{pmatrix}$$

We define two systems of phase --- the true phase from conjunction, ψ ; and the photometric phase, or phase from mid-eclipse, ϕ . We see from figure 16 that if ψ_o is the phase at mid-eclipse:

$$\text{Tan } \psi_o = \frac{r \text{ Sin}\alpha}{1 - r \text{ Cos}\alpha} \qquad \ldots\ldots\ldots\ldots\ldots\ldots \quad (3)$$

and we have that $\phi = \psi - \psi_o$ $\qquad \ldots\ldots\ldots\ldots\ldots\ldots \quad (4)$

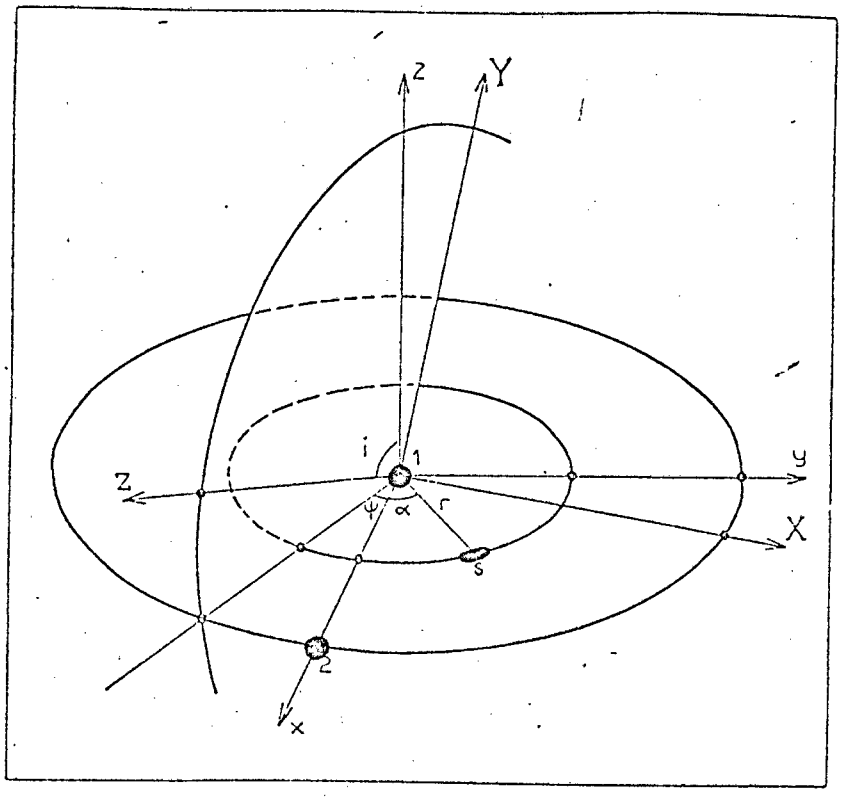

Figure 16 . The coordinate systems.

Smak (op. cit.) has derived the following equation for the half width of eclipse, $\Delta\psi$:

$$\text{Cos } \Delta\psi = \left\{ 1 - R_2^{\,2} \left(\frac{\text{Cos } \psi_o}{1 - r \text{ Cos}\alpha} \right)^2 \right\}^{\frac{1}{2}} \text{Cosec i} \quad .. \quad (5)$$

We note that if the spot is extended, provided that the eclipse is total and that the width is measured at half depth, equation (5) will still be valid.

Plavec (1968) has given the following expression for the radius of the Roche surface, which we identify with the radius of the

secondary: $$\frac{R_2}{(a_1 + a_2)} = 0.38 + 0.20 \log_{10}(q) \quad \ldots\ldots\ldots (6)$$

where $q = M_2/M_1$ and

$$(a_1 + a_2) = \left(1 + \frac{1}{q}\right) \frac{a_1 \text{Sin } i}{\text{Sin } i} \quad \ldots\ldots\ldots\ldots (7)$$

The maximum of the hump will occur at

$$\phi_{max} = -(\psi_o + \alpha) \quad \ldots\ldots\ldots\ldots (8)$$

Thus from (5), (6) and (8) we can construct tables relating the observables ϕ_{max} and $\Delta\psi$, with the parameters (q, R_2, r, α, i). This was done using program Eclpar (see Appendix) in the ranges $0.06 \leqslant r \leqslant 0.19$; $42^\circ \leqslant \alpha \leqslant 56^\circ$; $0.34 \leqslant R_2 \leqslant 0.42$; $63^\circ \leqslant i \leqslant 70^\circ$; where the angles were incremented a degree at a time, and the distances (in units of $(a_1 + a_2)$) by 0.01 at a time.

In order to single out the physically plausible solutions we make use of the particle trajectory calculations of Warner & Peters (1972). We note that the spot positions calculated are essentially independent of the angle and velocity of ejection from the secondary, and thus assume nothing of the physical scale of the system.

Fortunately the shape of the equations is such that there are a limited number of solutions, since $r \uparrow$ as $\alpha \uparrow$; $\Delta\psi \uparrow$ as $r \uparrow$ or $\alpha \downarrow$; and $|\phi_{max}| \uparrow$ as $r \uparrow$ or $\alpha \uparrow$. Table 5 lists the possible models for $\phi_{max} = -0.15P$ and $2\Delta\psi = 0.056P$.

We see that the problem is effectively reduced to that of determining the mass ratio of the system. From Table 1 of Warner & Peters (op. cit.) we find that $1.0 < q < 4.0$ from the position of the spot. We shall see that the most important arguments concerning

TABLE 5.

U Gem Models

Inclination i	Radius / R_2	Mass Ratio q	Spot Position α	r
64°	0.43	1.8	48°	0.12
65°	0.42	1.6	48°	0.11
66°	0.41	1.4	48°	0.10
67°	0.39	1.1	48°	0.12
68°	0.38	1.0	48°	0.11
69°	0.36	0.8	49°	0.14
70°	0.35	0.7	49°	0.13

the mass ratio relate to the photometry following an eruption. However at this point we may attempt to determine the mass ratio on theoretical grounds. Warner (1973) has derived an expression between the mass ratio, q, and the ratio K_1/v Sin i . We emphasise that this relationship assumes only that the secondaries have captured rotation and that after leaving the inner Lagrangian point the particle conserves its angular momentum about the primary, about which it takes up a circular orbit. This relation is well defined observationally (Fig. 1 of Warner 1973). Other relationships which could be used to determine the mass ratio --- for example the period / mass ratio relation --- embody several additional assumptions; and in the case of U Gem, where these methods differ, we prefer to use the former. This rather uncertain approach will be discussed further in the next chapter.

From figure 1 of Warner (op. cit.), for K_1/v Sin i = 0.26 , we find $q \sim 1.1$.

Table 6 shows the table in the region of the selected model.

TABLE 6.

Width of eclipse (W) and phase of the hump maximum (H) for the model : $i = 67^{\circ}$ and $R_2 = 0.39$

	Angle of Spot. 46°	47°	48°	49°	50°	
0.10	0.051	0.051	0.050	0.050	0.049	W
	-0.140	-0.143	-0.146	-0.149	-0.152	H
0.11	0.054	0.054	0.053	0.052	0.052	W
	-0.141	-0.144	-0.147	-0.150	-0.153	H
0.12	0.057	0.056	0.055	0.055	0.054	W
	-0.143	-0.146	-0.149	-0.152	-0.155	H
0.13	0.059	0.059	0.058	0.057	0.056	W
	-0.144	-0.147	-0.150	-0.153	-0.156	H
0.14	0.062	0.061	0.060	0.060	0.059	W
	-0.145	-0.148	-0.152	-0.155	-0.158	H

CHAPTER FOUR

Discussion and Analysis of the Light Curve

By examination of the gross features of the light curve we have determined the basic geometrical parameters of our model for the U Gem system: $i = 67^{\circ}$ $R_2 = 0.39$ $\alpha = 48^{\circ}$ $r = 0.12$ and we will now discuss the observations in more detail to examine the consistency of this tentative solution.

Due to the presence of extensive and variable nebulosity in the system (e.g. WZ Sge, Krzeminski & Smak 1971) it is not possible, and indeed it would not be plausible, to construct a detailed photometric model to include such effects as the Roche geometry of the secondary. We will use the simple model outlined in Chapter 3 . A straightforward analogue computer program was written to generate light curves for these variables, and is presented in Appendix 3 .

The Size of the Spot . We can infer something of the physical size of the spot from the duration of egress, which we take to be 0.006P (from Fig. 11). By calculating the moments of contact we find that the spot extends about 10° in longitude; which implies, using equation (7), a physical size of 2.7×10^9 cm (diameter) .

Several other arguments have been used to estimate the size of the spot. Warner & Nather (1971), by consideration of the flickering timescales, find that the largest 'elements' in the gas stream are of the order of 2.5×10^9 cm in size, and this we identify with the size of the spot.

Warner & Nather (op. cit.) also suggest that the spot cannot extend more than 5^{o} in longitude because the hump extends over $\lesssim 0.515P$. However we have already shown that the ring must be optically thick, as has been done for UX Uma (Walker & Herbig 1954), VV Pup (Warner & Nather 1972a), RW Tri (Walker 1963a); and it is probable that the spot is not on the outer surface of the ring, but located some distance within the ring (e.g. WZ Sge, Krzeminski & Smak 1971). Hence this argument will provide only a lower limit for the dimension of the spot. We note that the trajectory calculations of Warner & Peters(1972) suggest that the spot extends only 5^{o}. However this value is based on the two most widely separated trajectories, and any encounter between the gas stream,and gas within the system (e.g. the outer extremities of the ring) will remove any strong constraint on the spot size as deduced from these calculations. The arguments concerning the energy radiated by the spot (Warner & Nather 1971, Sect.9) are not altered due to fortuitously compensating changes, and are in agreement with those outlined above.

The Light Curve . The light from the system must be comprised of four components, viz.

i) The light from the primary, masked by optically thick nebulosity.

ii) The light from the secondary.

iii) The light from the hot spot.

iv) The emission from the disc.

Since we see no trace of the secondary spectrum, ii) is presumably small, and any variation with phase will be negligible. The contribution of the primary we will assume to be independent of phase,

so that the observed changes in light level are due to the phase dependence of iii) and iv) , eclipse excluded.
With the exception of the hump the light curve shows no large scale variations. Since we associate the hump with the spot, as a first approximation we assume iv) to be phase independent as well. This is a reasonably good approximation as it would appear that integrated light from the emission of the disc is very much less than the contribution of the spot in the continuum.

The amplitude of the flickering is clearly correlated with the brightness of the system, and persists over the entire cycle except during eclipse. Hence, by examining the RMS of the flickering (which we take to be a measure of the contribution of the spot) about the orbital cycle we can estimate the contribution of the spot to the total light. A computer program (Program RMS) was written to perform such an analysis on the two runs 1098 and 1100 of Warner & Nather (1971) which cover the entire orbit.
The program takes 60 data points at a time (which is equivalent to 120 seconds, or about four times the timescale of the flickering) and calculates the mean level and the RMS of the flickering of that section. The process is repeated at increments of 30 data points, so that the sections are overlapped. If the contributions of the disc, primary and secondary are indeed constant, we expect the quantity (amp - bkg)/rms to be constant; where amp = mean level or amplitude, bkg = constant level or background , and rms = the RMS value of the flickering.

The analysis was repeated several times using different values of the background, and the results were plotted to examine the solution. (See Figs. 17, 18)

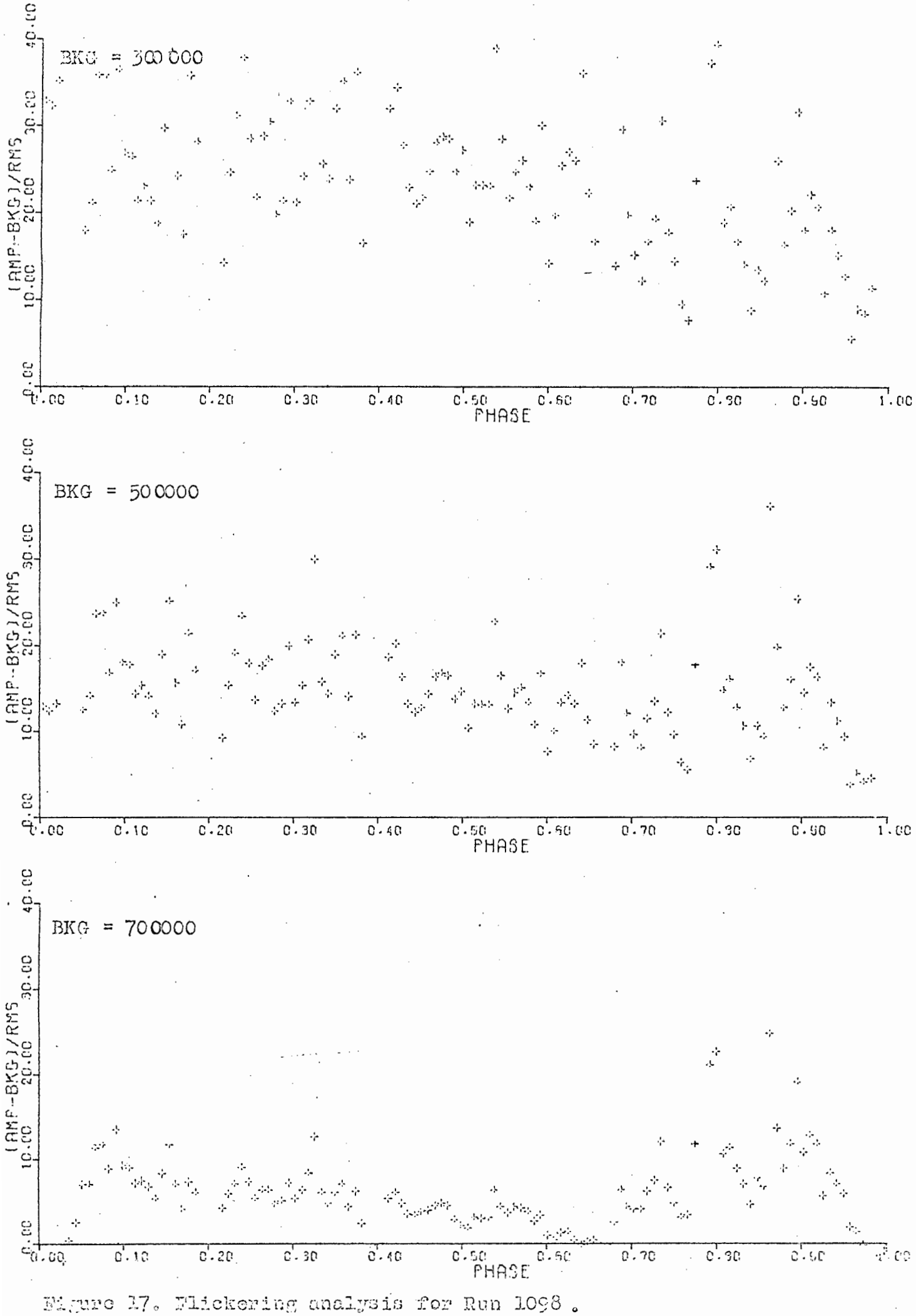

Figure 17. Flickering analysis for Run 1098 .

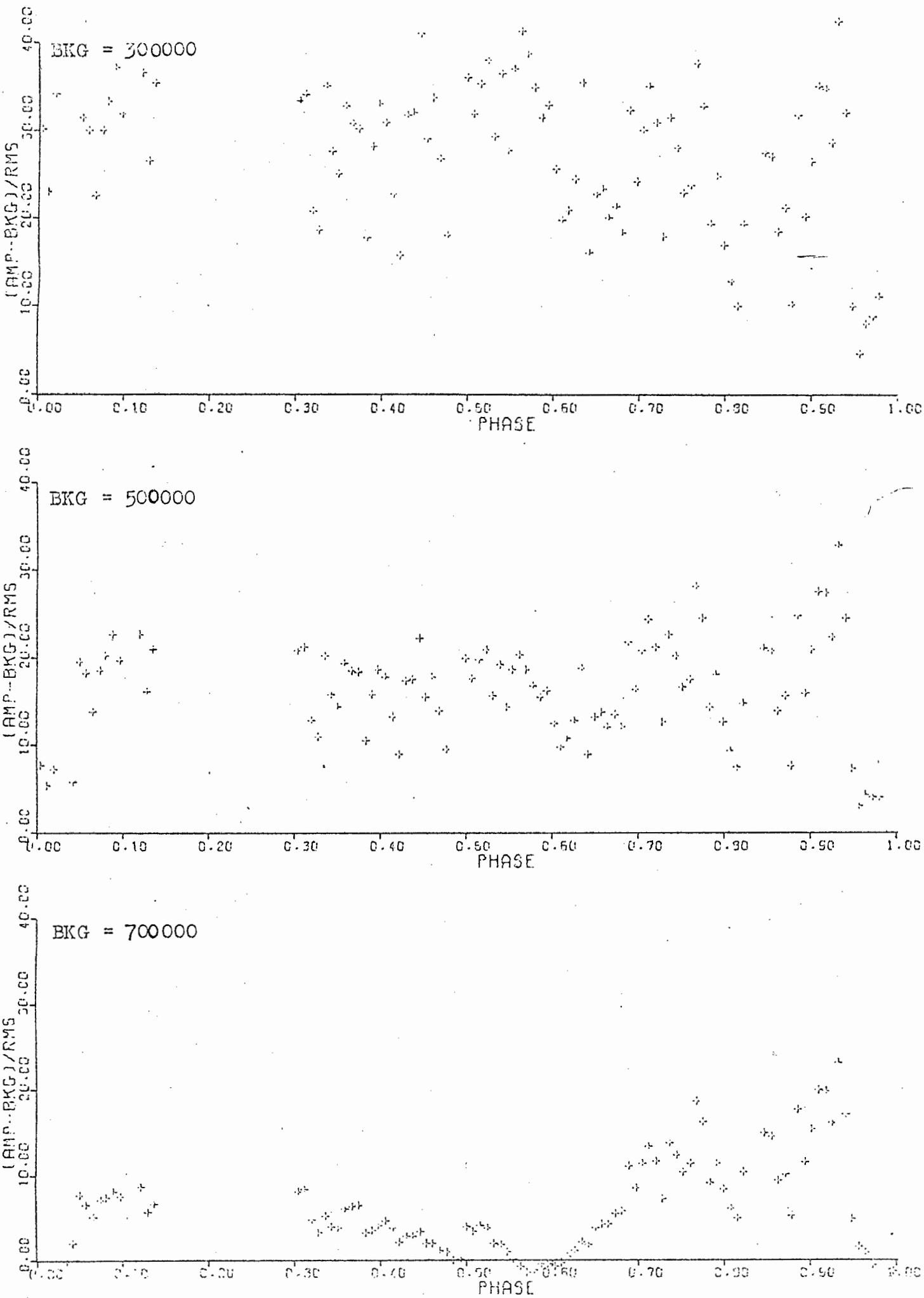

Figure 18. Flickering analysis for Run 1100 .

There is a unique solution to this analysis, albeit rather poorly defined. We see that with a background level of approximately 500000 counts $\frac{\text{sec}}{\text{min}}^{-1}$ the discriminating function is nearly flat. Thus the spot contributes about 600000 counts $\frac{\text{sec}}{\text{min}}^{-1}$, or just over half the total light from the system. The background level is, within the error of its determination, the same as the level at mid-eclipse. Thus the spot is totally eclipsed --- a conclusion we had reached by observing that the flickering disappears in eclipse. Furthermore the (U-B) excess in eclipse implies that the residual light is mostly in the emission lines (Krzeminski 1965).

On the eclipse of the disc . The irregular shape of ingress, and of the eclipse, suggests that there is obscuration of variable, nebular material (e.g. in DQ Her, Kraft 1963). That it is not only the spot that is eclipsed can be deduced from the changes in the eclipse following an outburst.

During the rise to maximum the eclipse becomes shallower, since the brightness of the spot remains constant; but remains at phase 0.0 . The gaseous envelope surrounding the primary is expanding, and is now highly luminous. During the final rise an eclipse appears at phase 0.985 which we interpret as a partial eclipse of the bright envelope encircling the primary. Our model predicts the phase of this eclipse, $-\psi_o$, to be 0.9846 . We note that this interpretation predicts that during the early decline from maximum eclipses would again be visible first at phase 0.985 . However the eclipse is very shallow, and the system very active, so it could easily be missed or obscured by the extensive luminous gas present following an eruption. This agrees closely with the orbital inclination

derived by consideration of the eclipse width and the mass ratio; since we find that Sin(90 - i) = 0.391 , and the primary is only just not eclipsed.

The outburst of a dwarf nova occupies typically two to three weeks before the system has returned to normal light. Paczynski (1965) noted that 12 days from maximum U Gem was still $1^{m}.5$ above minimum, whereas in the period 25 to 85 days from outburst the brightness of the system remained constant. We see in Figs. 10 to 12 that there is a fairly abrupt change in the behaviour of the parameters of the eclipse in the region of 20 days from outburst. We suggest that, during the first 20 days from outburst, some of the enlarged, bright central 'nucleus' surrounding the primary is eclipsed. By about 20 days from the eruption this 'nucleus' has faded and contracted to its equilibrium state.

It is clear that at inclinations where the primary is on the point of being eclipsed, that some of the disc must be eclipsed. Moreover we have to explain the observations that between 20 and 100 days from outburst the width of the eclipse decreases from 0.08 to 0.06P, and the duration of egress from 0.01 to 0.006P; accompanied by a phase shift of roughly 0.002P .

It is possible to explain this as being due to a change in the spot position alone. During an eruption the only change experienced by the secondary would be a heating of the surface facing the white dwarf --- and we expect the particle trajectory to be unchanged as it is only weakly dependent on the velocity of ejection. An increase in the radius vector of the spot thus results in a decrease in the angle of the spot, which is what we require to reconcile a

small phase shift with a large change in the eclipse width. If r is increased to 0.16 , we find $\alpha \sim 38^{\circ}$, and this leads to the correct changes in phase and width; and together with a contraction of the spot, will explain the changes of egress.

We favour an alternative interpretation where the trends apparent in Figures 10 and 11 are due partly to changes in the eclipse of the disc. Firstly the radial velocity data shows that between 12 and 85 days from outburst the rotational velocity of the disc decreased by 10% at most, and since $v^2 r$ = constant we find a change in r of not more than 20% . Furthermore if our interpretation of the photometric behaviour in the first 20 days is correct, we expect the spot vector to have 'stabilised' in 20 days or so, and predict that there is no change in the radial velocities in the period following 25 days from outburst.

We see that in run 1098, 22 days from maximum, there is what appears to be an 'overshoot' of the eclipse. Similar features are sometimes present in the eclipses of VV Pup (Warner & Nather 1972a), another cataclysmic with a high orbital inclination. We suggest that this is due to the eclipse and reappearance of a portion of the bright, central nucleus of the disc. The eclipse on the night following, run 1100, shows an interesting 'standstill' during ingress. A hint of this standstill is apparent in all the other runs, and it occurs at the point where the slope of ingress changes. We suggest that the 'core' of the spot is eclipsed first, and that where the slope of ingress changes the bright region downstream from the spot is eclipsed. Some weight is added to this argument by noting that the ratio of the intensities of the first portion

of ingress to that of the linear portion of egress is roughly constant, and equal to the ratio of the projection factors at the two phases, 1 : 1.25 .

Paczynski (1965) found that the brightness in U of the eclipsed body increases with time, whereas the opposite is true of the brightness in eclipse. We therefore suggest the following explanation. Following an eruption the disc is relatively dense and bright, and the spot is diffuse and extended due to scattering of the energy from its centre. Between the outbursts the density of the disc decreases as the material falls to the surface of the white dwarf, and the spot shrinks and becomes more compact. We are dealing with a total eclipse of the spot and the bright disc downstream from the spot, plus a partial eclipse of the disc.

Smak's Analysis . We have used the simple model advanced by Smak (1971). The solution found by Smak is untenable due to the siting of the spot at $\alpha \sim 10^{\circ}$. Smak's approach to the problem --- to set up a system of equations and to solve them simultaneously using data from two epochs, interpreted as two spot positions --- would appear to be unreliable, although it has the great advantage of being essentially independent.

Our qualitative interpretation of the light curve agrees essentially with Smak's completely independent approach. He finds that the disc immediately adjacent to the spot is brighter than elsewhere, and that the inferred brightness of the spot will include this bright region of the disc. This brightened region about the spot we identify with the second portion of ingress, and represents

about 30% of the calculated intensity of the spot. Smak found that the proportion of the light from the disc that was eclipsed increased with time from outburst, and that it could be as much as 40% . He concludes that the radius vector of the spot is less than the radius of the disc, which is extended in the z coordinate. The brightness distribution of the disc is not uniform. (Sect. 4.2 of Smak op.cit.). In the course of our discussion we have assembled the same picture of the eclipse of the disc.

CHAPTER FIVE

Physical Properties and Conclusion

Up to this point we have used no absolute dimension. It is in the determination of this 'scale factor' that the difficulties and the curiosity of U Gem become apparent. The one datum which separates U Gem from the other cataclysmic variables is its exceptionally large K_1 of 265 km sec^{-1}. This would imply either a very high mass ratio for the system; or that the total mass is rather smaller than that of the other cataclysmics.

There is no evidence, theoretical or observational, to suggest that lobe-filling secondaries will depart from the mass / radius for normal main sequence stars. The mass / radius relationship we shall be using is that computed by Bodenheimer (Faulkner et al 1971), taken from Warner (1973).

With q known we can determine M_2 directly from Kepler's third law and K_1. We obtain $M_2 = 1.6\ M_\odot$, and from equation (6) $R_2 = 0.78\ R_\odot$. This is an impossible situation, since from the spectrum of the disc we know that the composition of the secondary cannot be too unusual --- in particular it is not a helium star --- and so cannot fall below the mass / radius relationship for the main sequence.

This situation casts doubt on the assumed value of q we have been using --- but in the range $0.7 \leqslant q \leqslant 4.0$ there is no value of q for which M_2 (from Kepler) and R_2 (from Roche geometry) are compatible with the mass / radius ralation. We know that the period is correct, and this would suggest that the published value of K_1

is misleading. Smak(1971 Sect 5.2) reached the same conclusion.

The published radial velocities of U Gem are the average of the measures for the two component lines (Kraft 1962). If the phase dependence of the motions of the two components are different due to the additional spot component, the radial velocities taken from the averages will be erroneous. We see (Fig. 8) that this is indeed the case. At phases 0.6 to 0.8 , when the spot plus the bright region downstream of the spot is approaching, v Sin i is increased by about 160 km sec^{-1} relative to that at phase 0.5 . At phases 0.1 to 0.3 , when the spot is receding, there is a somewhat smaller disturbance of 100 km sec^{-1}. These disturbances at the peaks of the radial velocity curve are sufficient to increase the true radial velocity from 200 km sec^{-1} to the observed value of 265 km sec^{-1}. Smak (1970) has examined the effects of the blending of the emission lines. This analysis fails in the case of U Gem because it is assumed that the intensity of the emission line from the spot is a symmetric function of ϕ. Furthermore the line intensity from the spot is presumably large, and it is questionable whether such a crude treatment of the blending, or the variation of intensity with velocity, will give useful results.

The above discussion makes the validity of our mass ratio --- derived from the measured K_1/ v Sin i --- highly questionable. Whereas we have shown that the value of K_1 is an overestimate, so too is that of v Sin i . Firstly it is difficult to define what we are to measure to evaluate v Sin i . In all other cataclysmic variables it is taken to be half the total width of the line (single or doubled) measured from the plates. If the same procedure is followed

in each case, the good correlation between K_1 / v Sin i (observed) and mass ratio found by Warner (1973) is due to a number of compensating factors present in most or all cataclysmic variables.

However this rather dubious situation may be redeemed by noting the constraints placed on the mass ratio by the photometry. Firstly, from Table 5 , if $q < 1.1$ the primary will be eclipsed at minimum light, and this is not the case. Secondly, Kepler's third law, together with the Roche geometry and the mass / radius relationship for the secondary, will define a simple (K_1 , q , M_2) surface for a given system. For true K_1 = 200 km sec^{-1} we obtain q = 1.1 and $M_2 = 0.68\ M_\odot$.

Thus we have that $M_1 = 0.62\ M_\odot$. We can make an independent estimate of M_1 from equation (1) . Our measurement of v Sin i was 1000 km sec^{-1}, but during the exposure of 30 minutes the line profile will have moved on average 100 km sec^{-1}, and the true v Sin i is 900 km sec^{-1}. With $r = 1.2 \times 10^{10}$ cm we find $M_1 = 0.62\ M_\odot$.

The value we obtain for M_1 is roughly half that found for the primary mass of other dwarf novae. This is to be expected since we know that U Gem does not obey the period / mass ratio relationship found for other cataclysmic variables. It is easy to show that this relation requires that the primary mass is constant for the group (Warner 1973).

The period / luminosity relationship of Kraft(1964a) gives $M_v(2^y)$ of about (9.0 ± 1.5) . We note in passing that this relationship explains why the secondary spectrum is visible only in those

systems with $P \gtrsim 6\frac{1}{2}$ hours (See Table 1). With $M_2 = 0.68\ M_\odot$ we find that the secondary is of spectral type K2 or K3 , and that $M_v \sim 8$, which agrees satisfactorily with our first estimate.

We know that the secondary does not contribute more than about 25% of the light of the system (or we would detect its spectrum) , and adopting $M_v(2^y) \sim 8.5$ we find that the absolute magnitude of U Gem is about 7.0 . This estimate is highly uncertain, but agrees adequately with Kraft & Luyten's (1965) mean absolute magnitude for the U Gem stars.

The Result

The mass we have derived for the primary of U Gem is slightly uncertain due to the uncertainty in true K_1. However one result is clear, and that is that the primary mass in U Gem is considerably less than the value found by Warner(1973) for the primaries of all other cataclysmic variables for which a mass could be derived. Warner found that, with the exception of U Gem, the masses of the primaries were in the range $(1.2 \pm 0.2)M_\odot$, which we note is just short of the Chandrasekhar limit, whereas the mass of a typical field white dwarf is of the order of $0.4\ M_\odot$.

The low mass found for the primary may be of considerable evolutionary significance, for it gives credence to the suggestion that the primaries start out as ordinary white dwarfs, and retain all the accreted material until they approach the Chandrasekhar limit, at which point the outbursts become sufficiently energetic to cause mass loss from the system.

Conclusion

We have found that the following set of parameters provides a consistent solution for U Gem :

$i = 67^{o}$ $\qquad$ $r = 0.12$

$q = 1.1$ $\qquad$ $\alpha = 48^{o}$

$(a_1 + a_2) = 10^{11}$ cm $\qquad$ $M_2 = 0.68\ M_{\odot}$

While the primary is presumed to be a white dwarf, the secondary is a main sequence dwarf of spectral class ~K2 (Allen 1955). It is the primary component that is responsible for the eruptions.

Further work on U Gem must await both theoretical and observational advances:

i) Observations at minimum light are required over a wider range of wavelength --- particularly the ultraviolet --- in order to evaluate the total flux of the system.

ii) High time resolution photometry through the outburst is required to establish the behaviour of the hump relative to the eclipse.

iii) Further radial velocity data at several epochs from outburst is urgently required. It is essential to measure the velocities of the line components separately in order to evaluate K_1 , and hence q , more accurately.

iv) We require theoretical work on the structure of the disc to interpret our observations of the disc --- in particular v Sin i --- more realistically. Several authors (e.g. Warner & Nather 1971, Krzeminski & Smak 1971) have examined the energetics of the spot. However, due to the difficulties of interpretation, we feel that there is little to be gained by repeating these analyses at this stage.

REFERENCES

Allen, C.W., 1955 . 'Astrophysical Quantities', Athlone Press, London

Elvey, C.T. & Babcock, H.W., 1943 . Ap. J. 97, 412

Faulkner, J., Flannery, B.P. & Warner, B., 1972 . Ap. J. (Lett.) 175,L79

Gorbatsky, V.G., 1969 . 'Non-periodic Phenomena in Variable Stars', ed. Detre, Academic Press, Budapest

Gould, N.L., 1957 . P.A.S.P. 69, 541

Greenstein, J.L., 1957 . Ap. J. 126, 23

Greenstein, J.L. & Kraft, R.P., 1959 . Ap. J. 130, 99

Herbig, G.H., 1960a . Ap. J. 131, 632

Herbig, G.H., 1960b . Ap. J. 132, 76

Herbig, G.H., Preston, G.W., Smak, J. & Paczynski, B., 1965 . Ap. J. 141, 617

Humason, M.L., 1938 . Ap. J. 88, 237

Joy, A.H., 1940 . P.A.S.P. 52, 324

Joy, A.H., 1954 . Ap. J. 120, 377

Kraft, R.P., 1958 . Ap. J. 127, 625

1959 . ibid 130, 110

1962 . ibid 135, 408

1963 . Adv. Astr. Astrophys., Vol 2, p. 41, ed. Kopal, Academic Press, New York.

1964a. Ap. J. 139, 457

1964b. 'First Conference on Faint Blue Stars', ed. W.J. Luyten, University of Minnesota.

Kraft, R.P. & Luyten, W.J., 1965 . Ap. J. 142, 1041

Kraft, R.P., Krzeminski, W. & Mumford, G.S., 1969 . Ap. J. 158, 589

Krzeminski, W., 1965 . Ap.J. 142, 1051

1966 . IAU Inf. Bull. Var. Star, 160

Krzeminski, W. & Smak, J., 1971 . Acta Astr. 21, 133

Kruszewski, A., 1966 . Adv. Astr. Astrophys., Vol 4, p. 233, ed. Kopal
Academic Press, New York

Mayal, M., 1962 - 1972 . J.R.A.S. Canada, 56, 133; 57, 125; 58, 143;
59, 147; 60, 153; 61, 155; 62, 141; 63, 173;
64, 205; 65, 141; 65, 247; 66, 179

Mumford, G.S., 1964 . Ap. J. 139, 476
1967a. IAU Inf. Bull. Var. Star, 197
1967b. Ap. J. Suppl. 15, 1
1970 . Ap. J. 162, 363
1971 . Ap. J. 165, 369

Mumford, G.S. & Krzeminski, W., 1969 . Ap. J. Suppl. 18, 429

Nather, R.E. & Warner, B., 1969 . M.N.R.A.S. 143, 145

Paczynski, B., 1965a . Acta Astr. 15, 197
1965b . Acta Astr. 15, 307

Plavec, M., 1968 . Adv. Astr. Astrophys., Vol 6, p. 202, ed. Kopal
Academic Press, New York

Smak, J., 1967 . Acta Astr. 17, 255
1969 . Acta Astr. 19, 155
1970 . Acta Astr. 20, 311
1971 . Acta Astr. 21, 15
1972 . Acra Astr. 22, 1

Smak, J. & Stepień, K., 1968 . 'Non-periodic Phenomena in Variable
Stars', ed. Detre, Academic Press, Budapest

van Houten, C.J., 1966 . Bull. Astr. Inst. Netherlands, 18, 439

Walker, M.F., 1954a . P.A.S.P. 66, 71
1954b . P.A.S.P. 66, 230
1961 . Ap. J. 134, 171
1963a . Ap. J. 137, 485

Walker, M.F., 1963b . Ap. J. 138, 313

1966 . Adv. Electronics, Vol 22B, p. 761

Walker, M.F. & Chincarini, G., 1968 . Ap.J. 154, 157

Walker, M.F. & Herbig, G.H., 1954 . Ap.J. 120, 278

Warner, B., 1972a . M.N.R.A.S. 160, 35P

1973 . M.N.R.A.S. in press

Warner, B. & Nather, R.E., 1971 . M.N.R.A.S. 152, 219

1972a. M.N.R.A.S. 156, 305

Warner, B. & Peters, W.L., 1972 . M.N.R.A.S. 160, 15

Warner, B. & Robinson, E.L., 1972 . M.N.R.A.S. 159, 101

APPENDIX 1

Photometric Data

This section contains reproductions of the eclipse photometry. The vertical axis is intensity (detected photon rate in counts sec^{-1} corrected to outside the atmosphere) on the instrumental system. For Runs 1098 & 1100 the units are counts min^{-1}, and Runs 1231 & 1245 were made under poor conditions of transparency. The horizontal axis is the heliocentric Julian date in the sense

$$\text{Time} = JD_{\odot} - 2440\ 000.$$

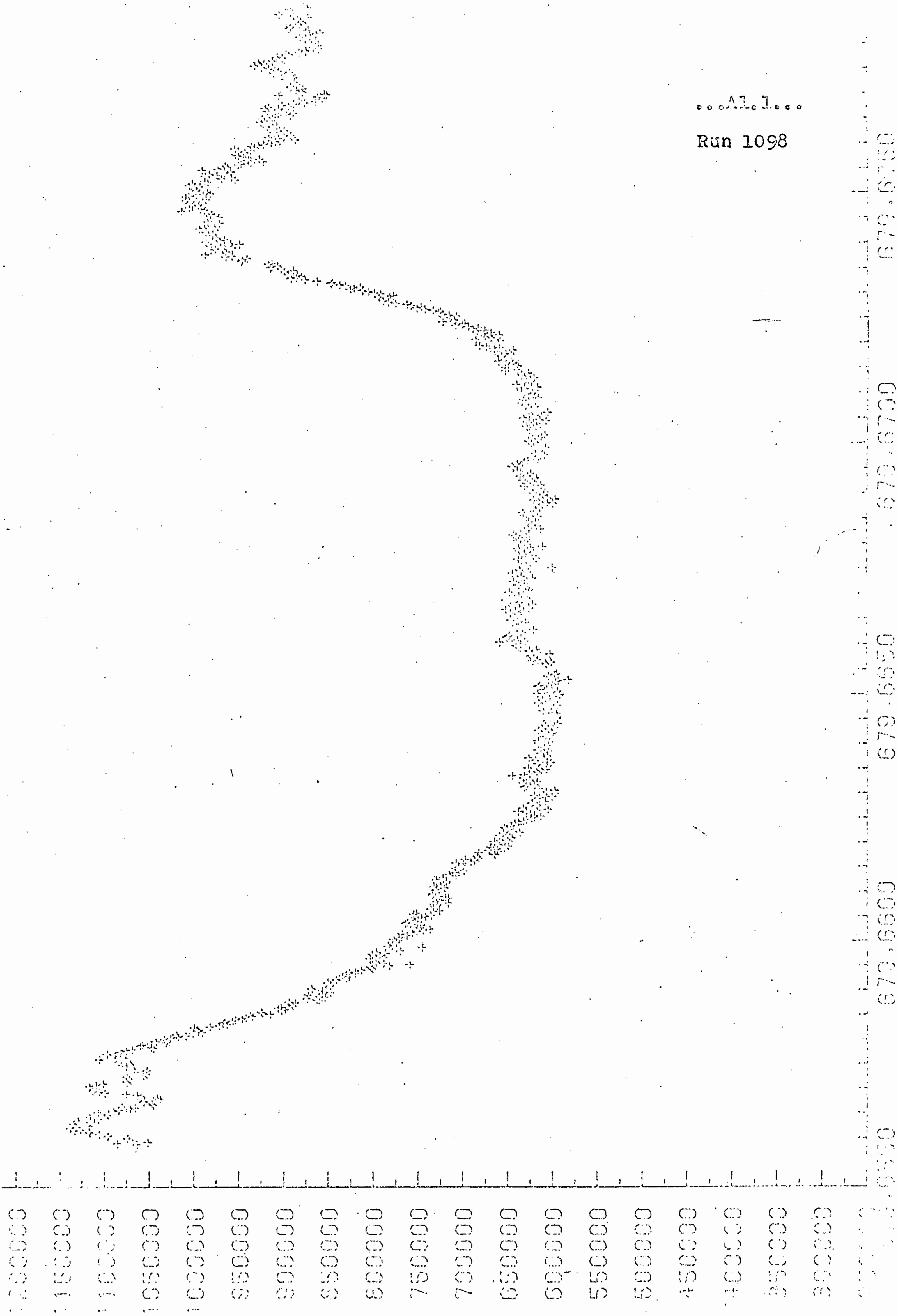

Run 1098
679.6750
679.6700
679.6650
679.6600
1150000
1100000
1050000
1000000
950000
900000
850000
800000
750000
700000
650000
600000
550000
500000
450000
400000
350000
300000

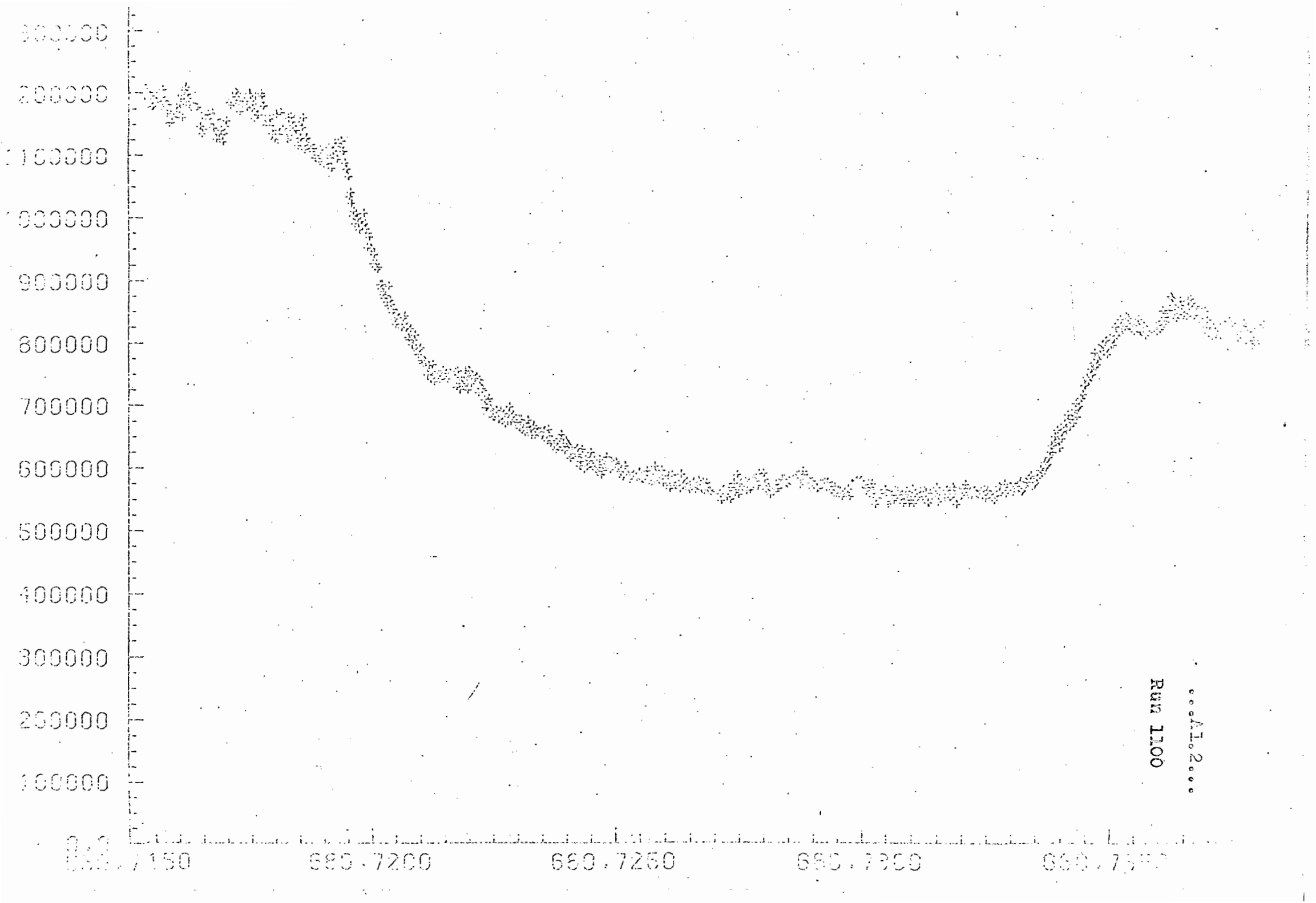
1100000
1000000
900000
800000
700000
600000
500000
400000
300000
200000
100000
680.7150
680.7200
680.7250
680.7300
Run 1100

Run 1150

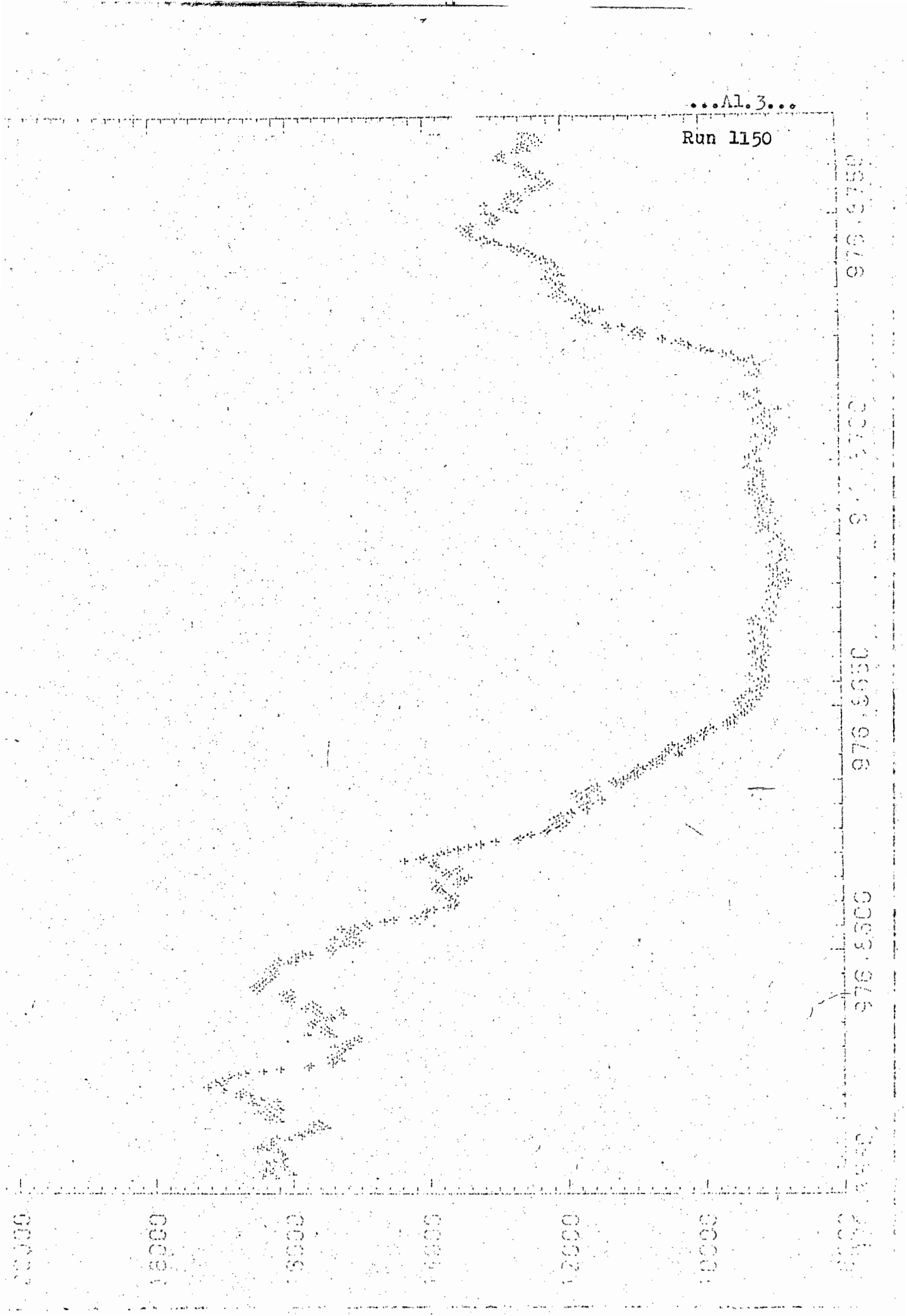

Run 1231

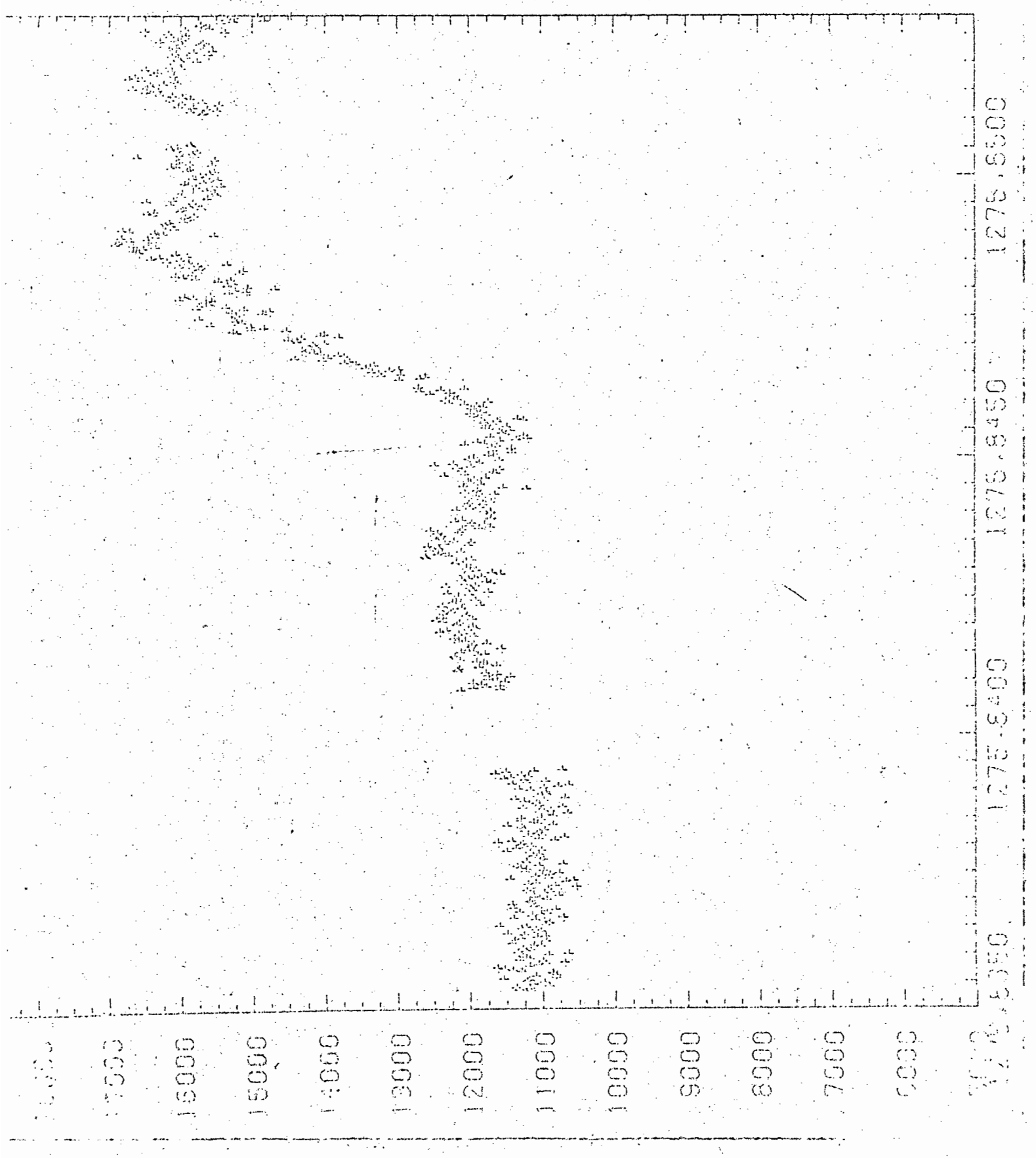
0033.3721
0038.3721
0043.3721
0048.3721
0053.3721
16000
15000
14000
13000
12000
11000
10000
9000
8000
7000
6000

Run 1239

Run 1243

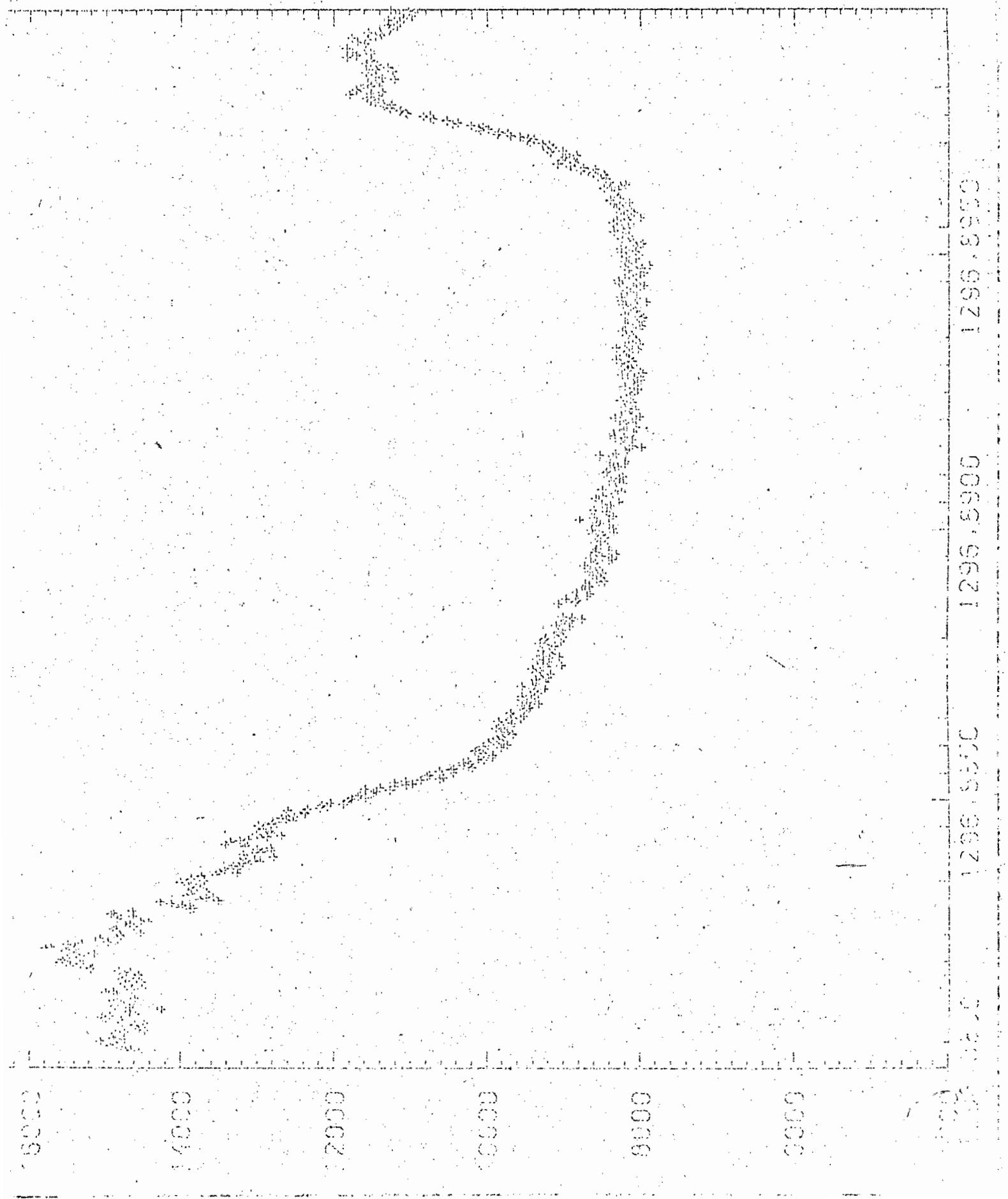

Run.1245

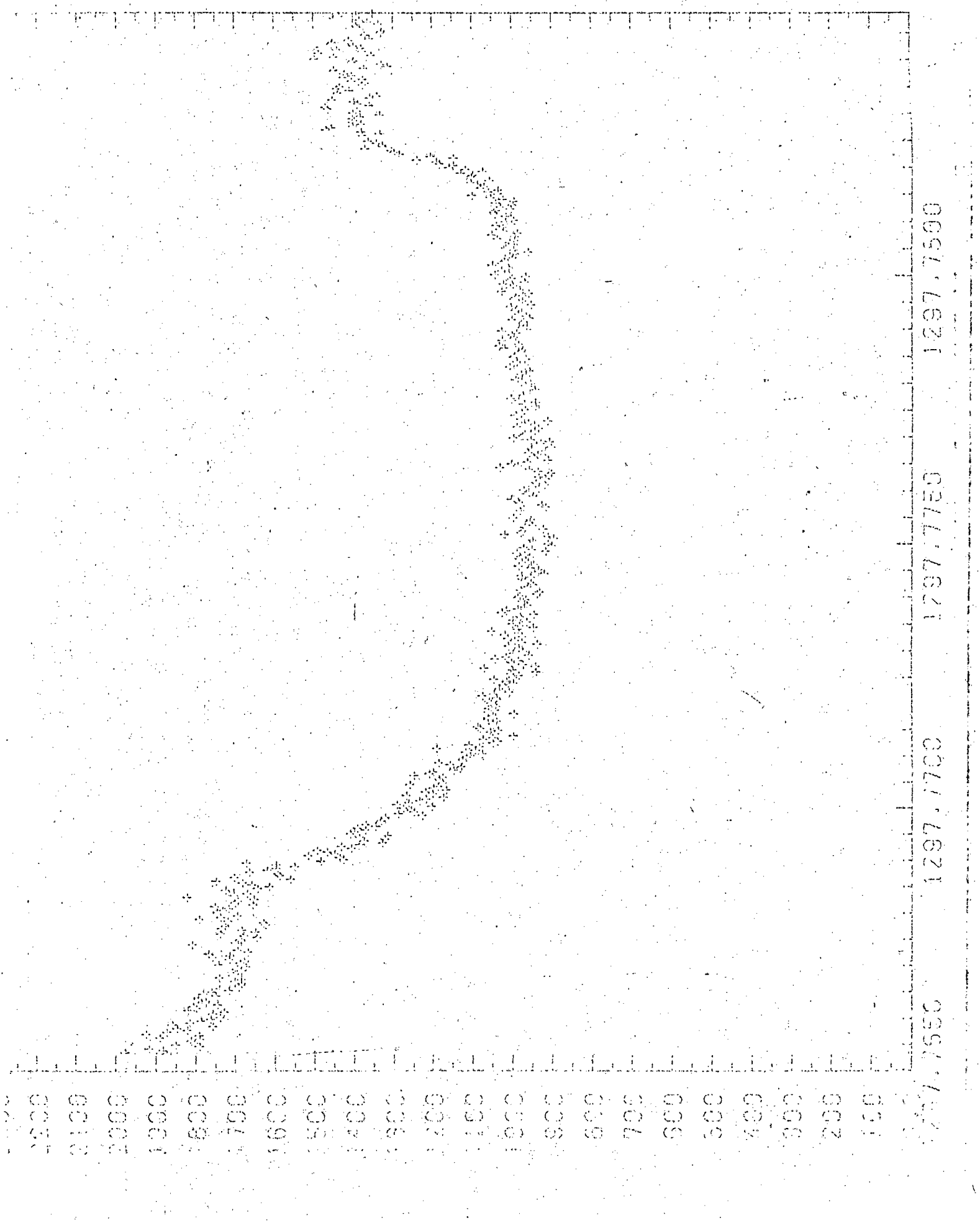

Run 124?
...A1.8...
1356.9950
1356.9960
1356.9970
1356.9980
1356.9990
0.0000
0.0002
0.0004
0.0006
0.0008
0.0010

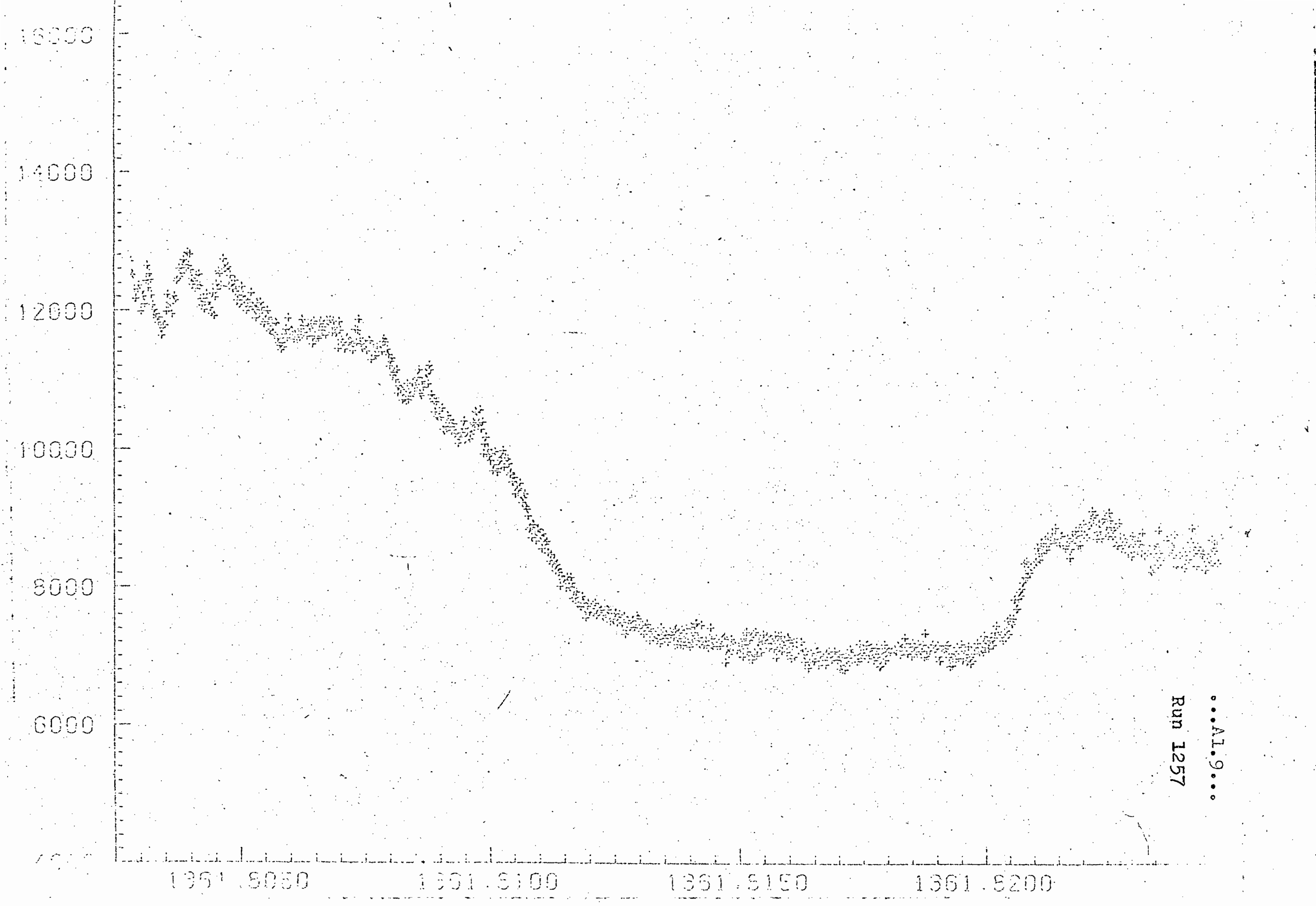
16000
14000
12000
10000
8000
6000
1361.5050
1361.5100
1361.5150
1361.5200
...A1.9...
Run 1257

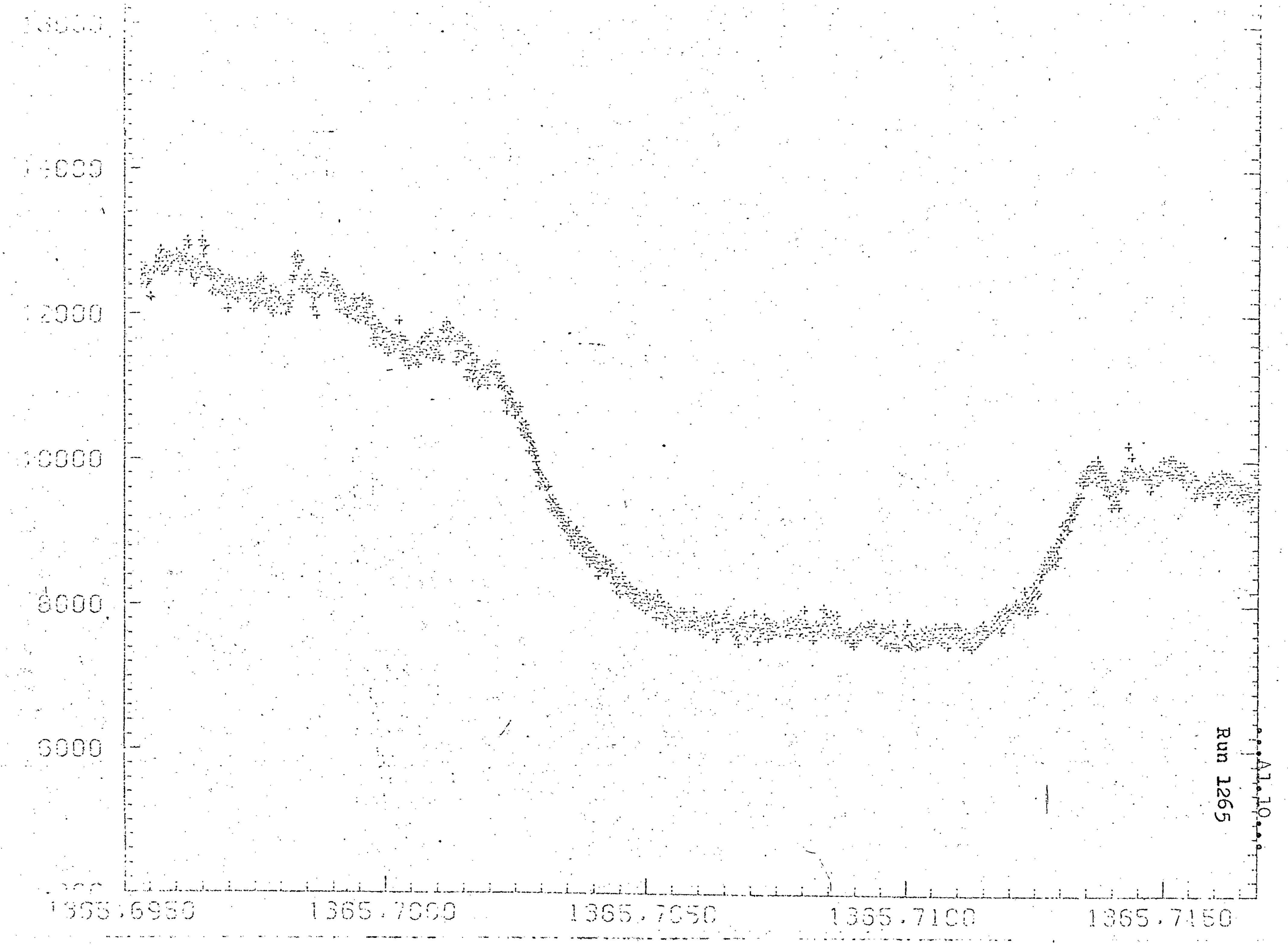
Run 1265
A1.10
14000
12000
10000
8000
6000
1365.6950
1365.7000
1365.7050
1365.7100
1365.7150

Run 1273
A1-11
1366.7200
1366.7150
1366.7100
1366.7050
0.0000
0.0005
0.0010
0.0015
0.0020
0.0025

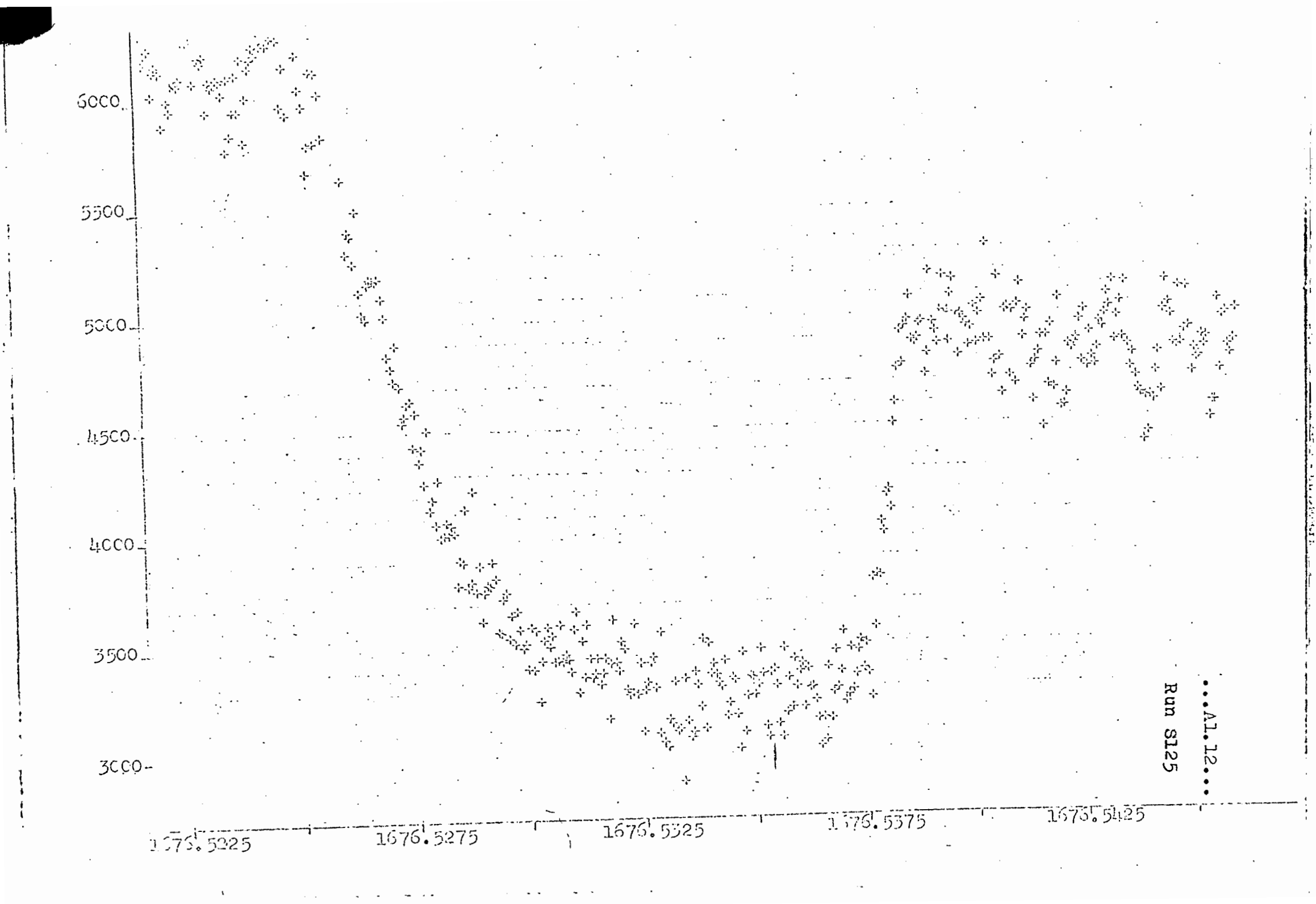
6000
5500
5000
4500
4000
3500
3000
1676.5225
1676.5275
1676.5325
1676.5375
1676.5425
Run S125
...A1.12...

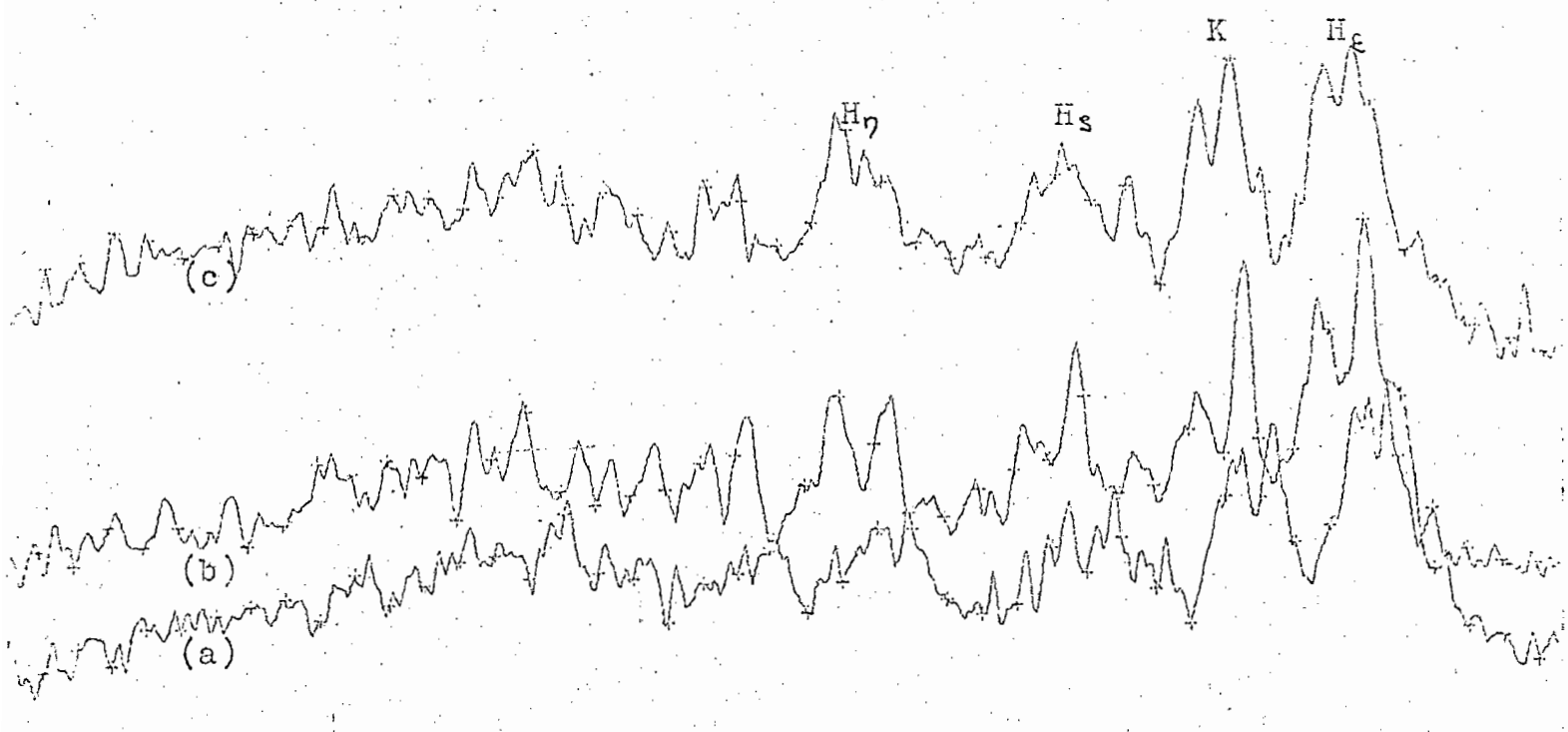

Plate 1277

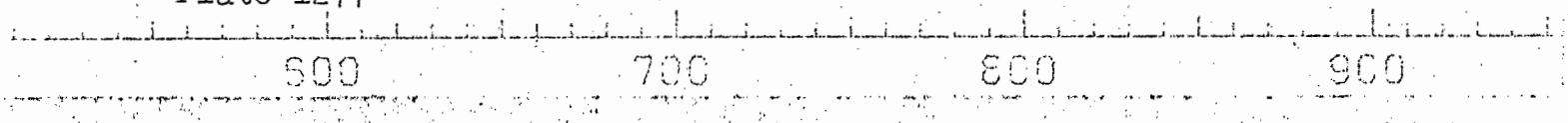

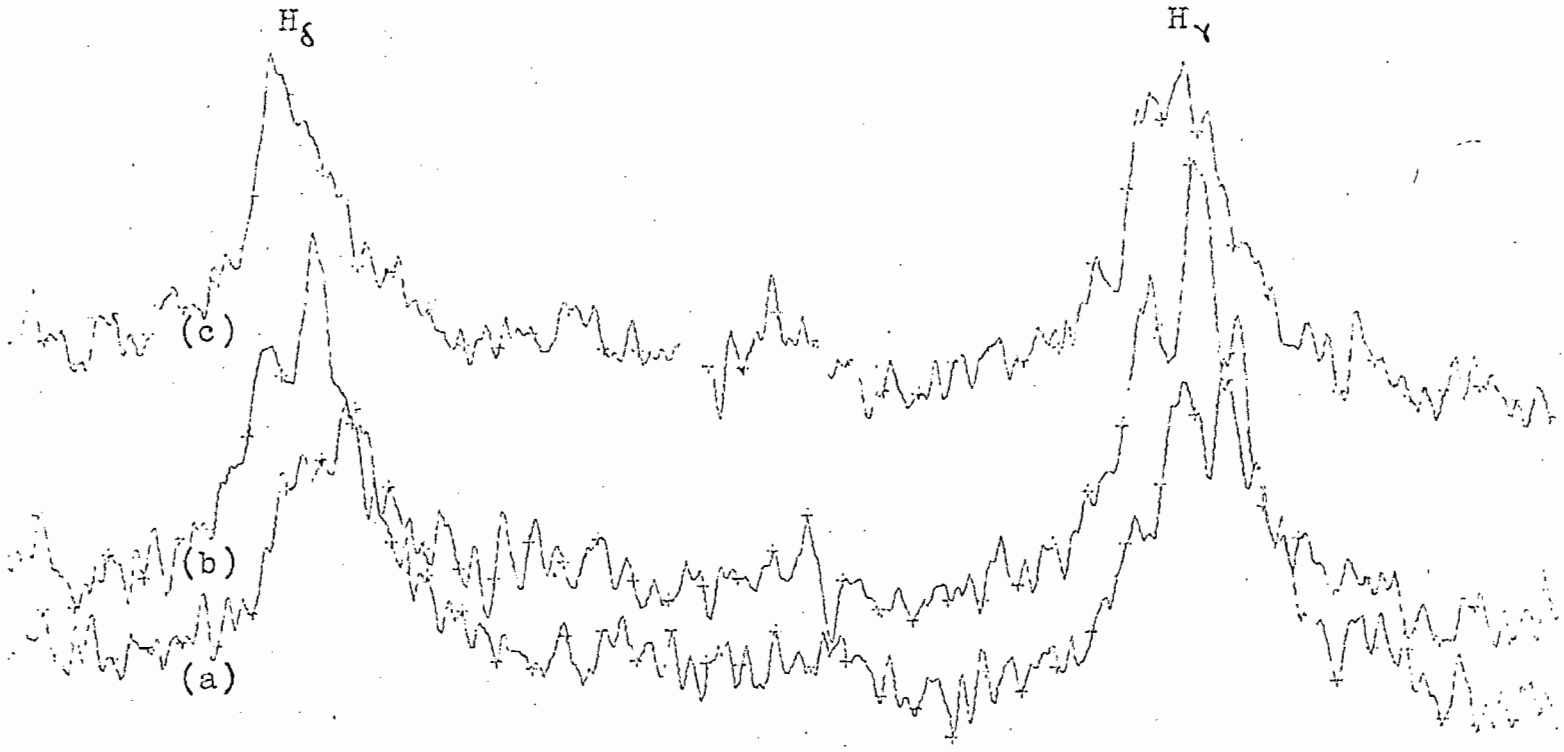

Plate 1277

1000 1100 1200 1300

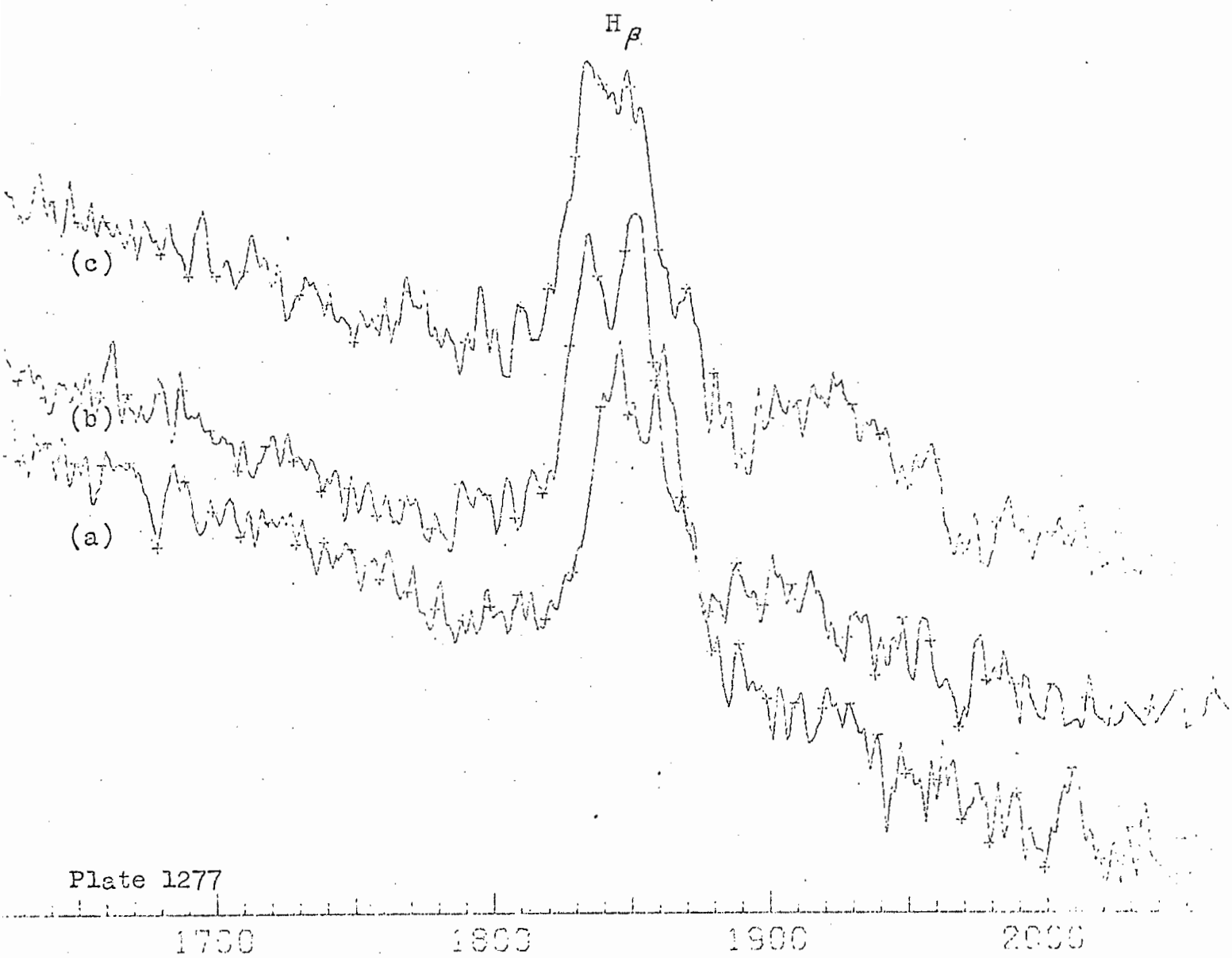
H_β
(c)
(b)
(a)
Plate 1277
1750
1800
1900
2000

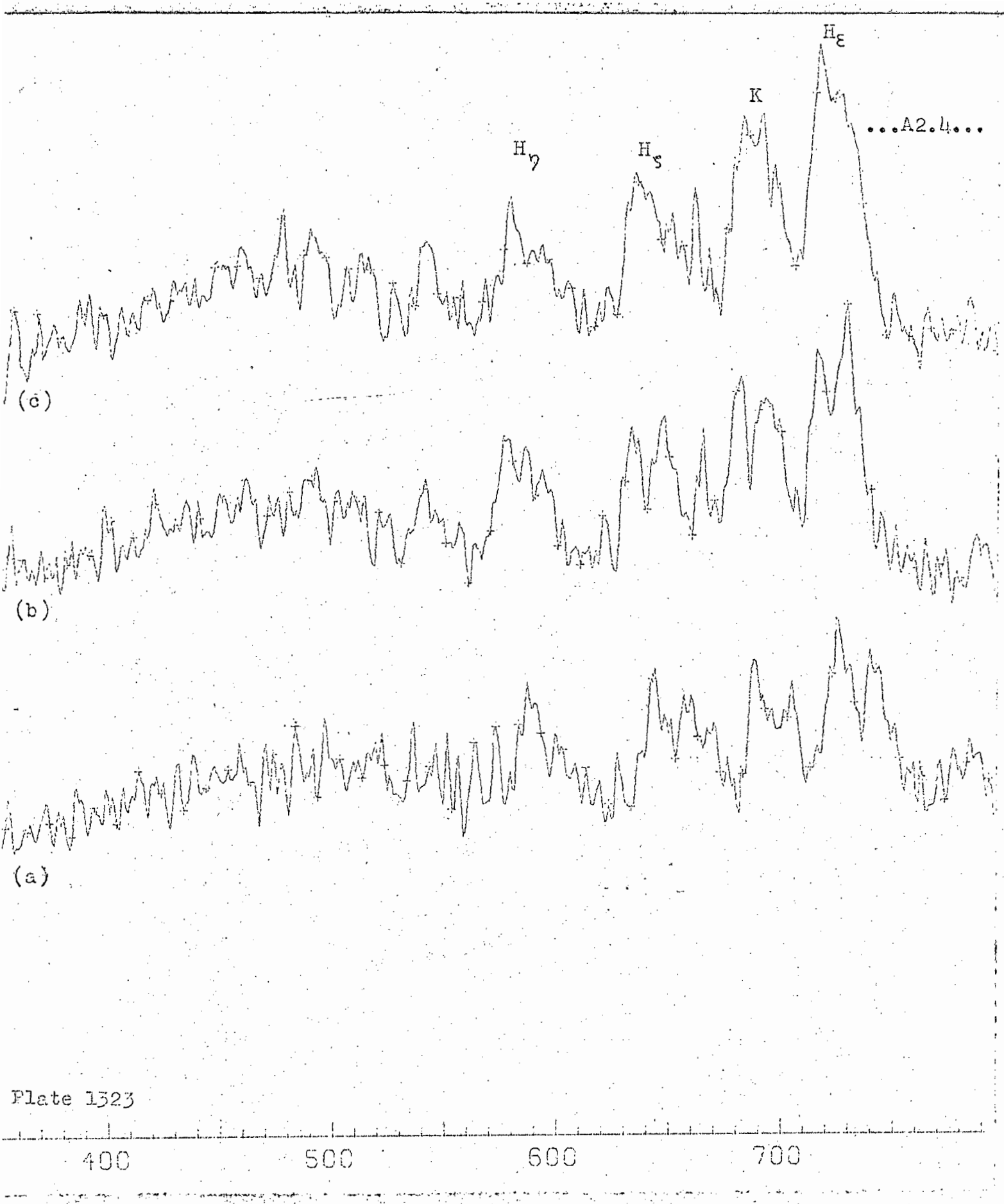

Plate 1323

400 500 600 700

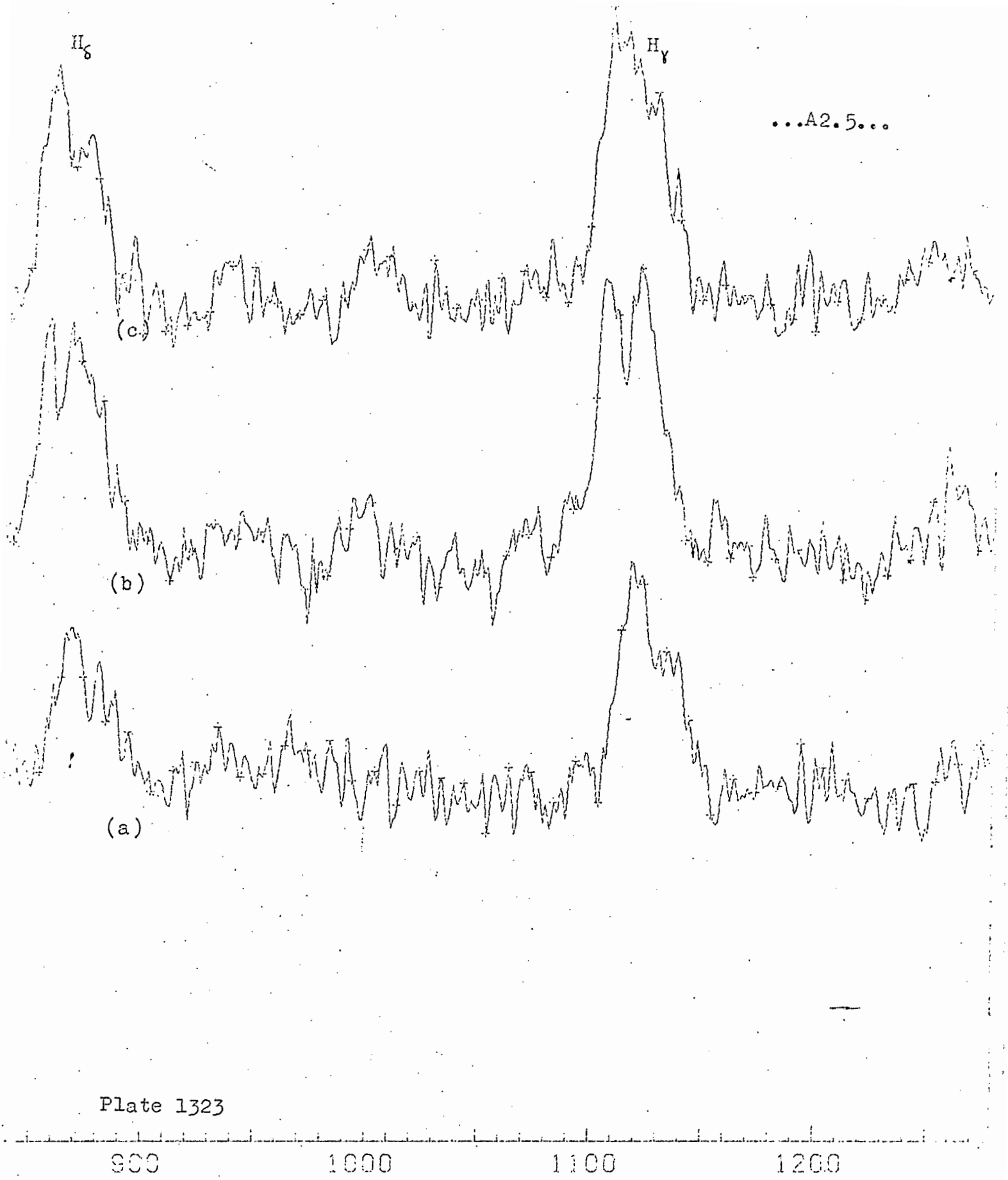

Plate 1323

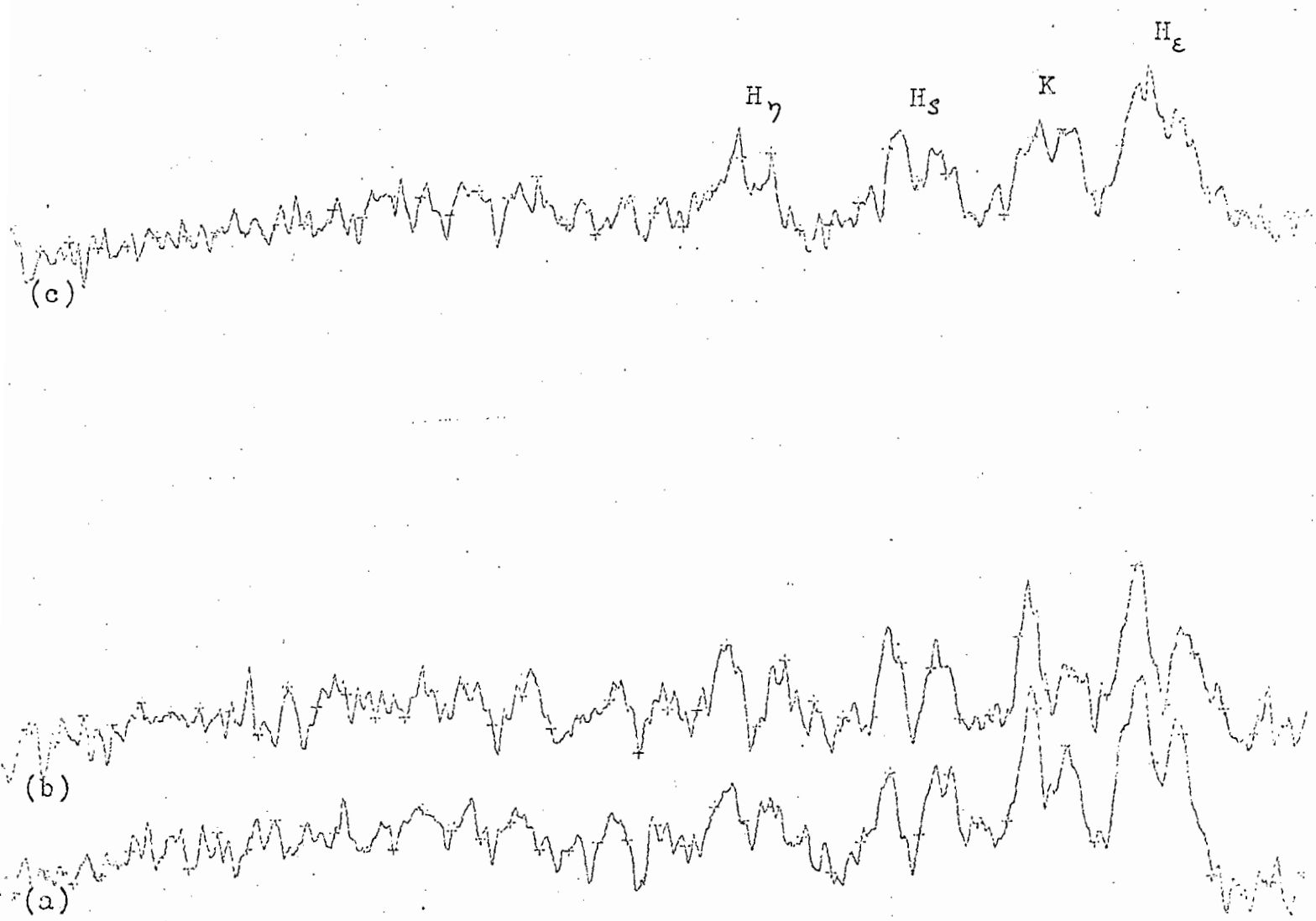

Plate 132b

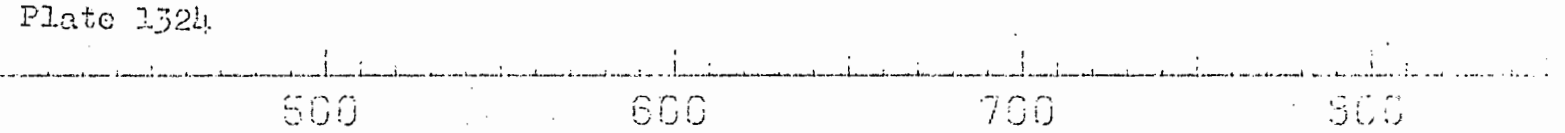

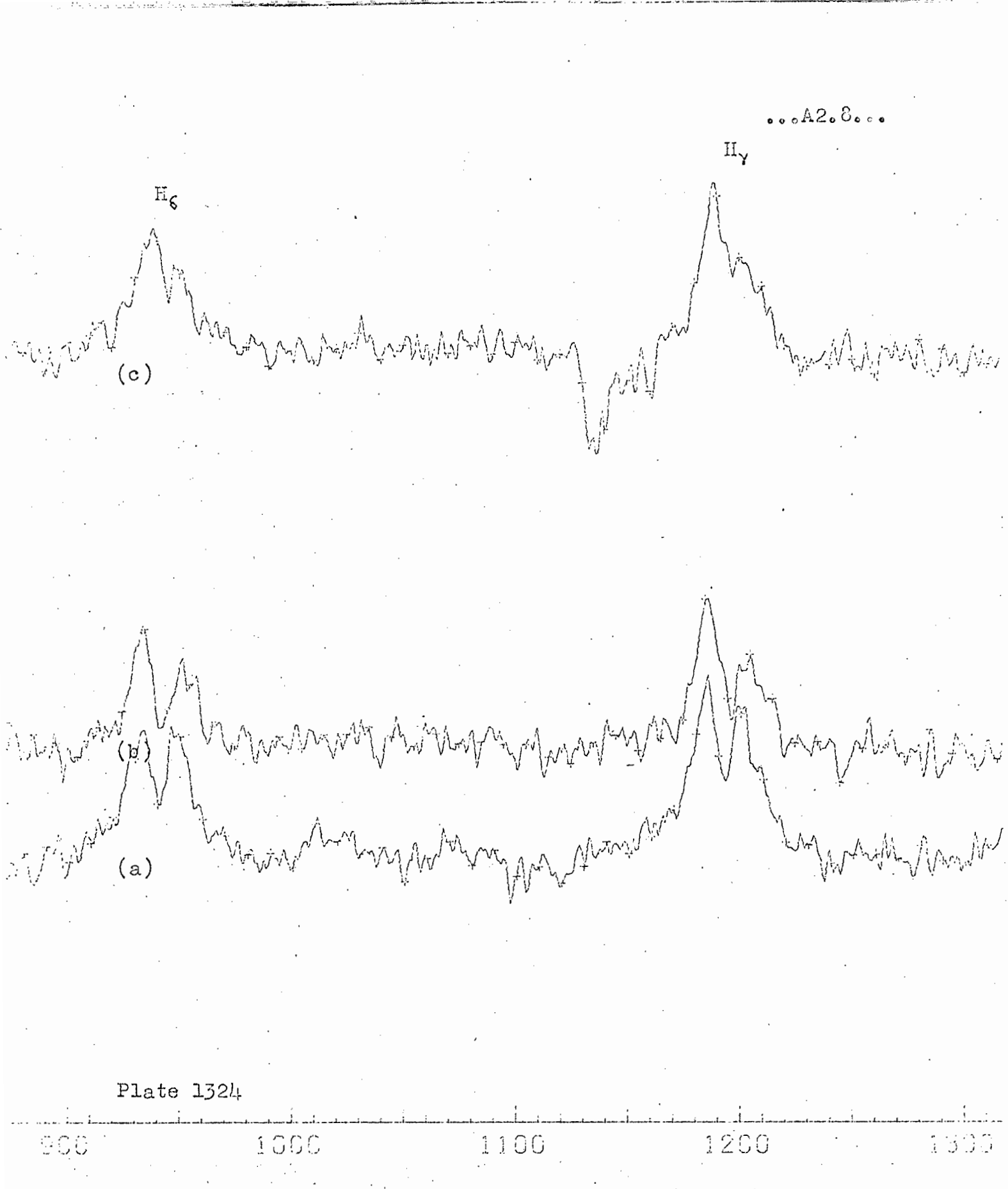

Plate 1324

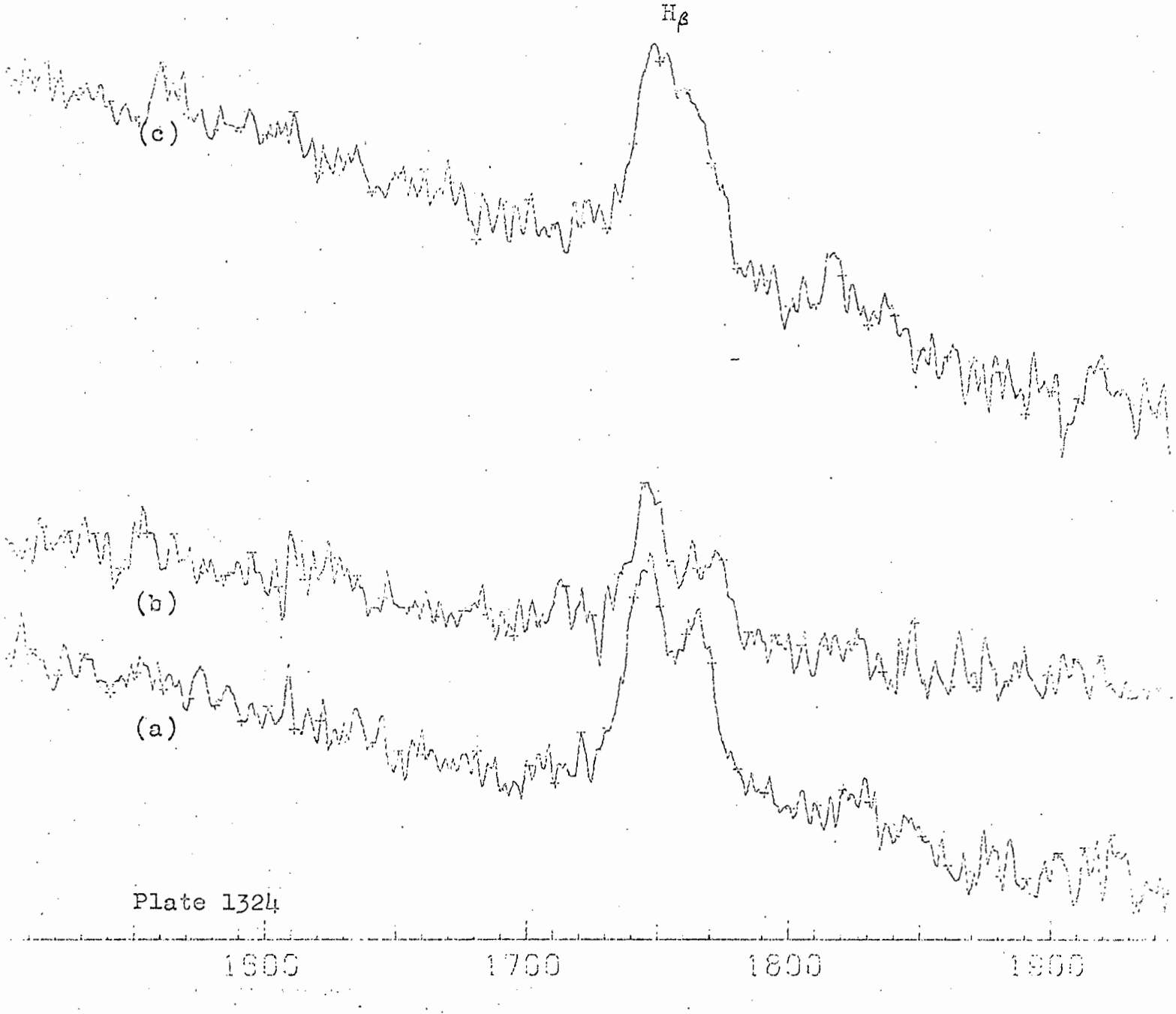
H_β
(c)
(b)
(a)
Plate 1324
1600
1700
1800
1900

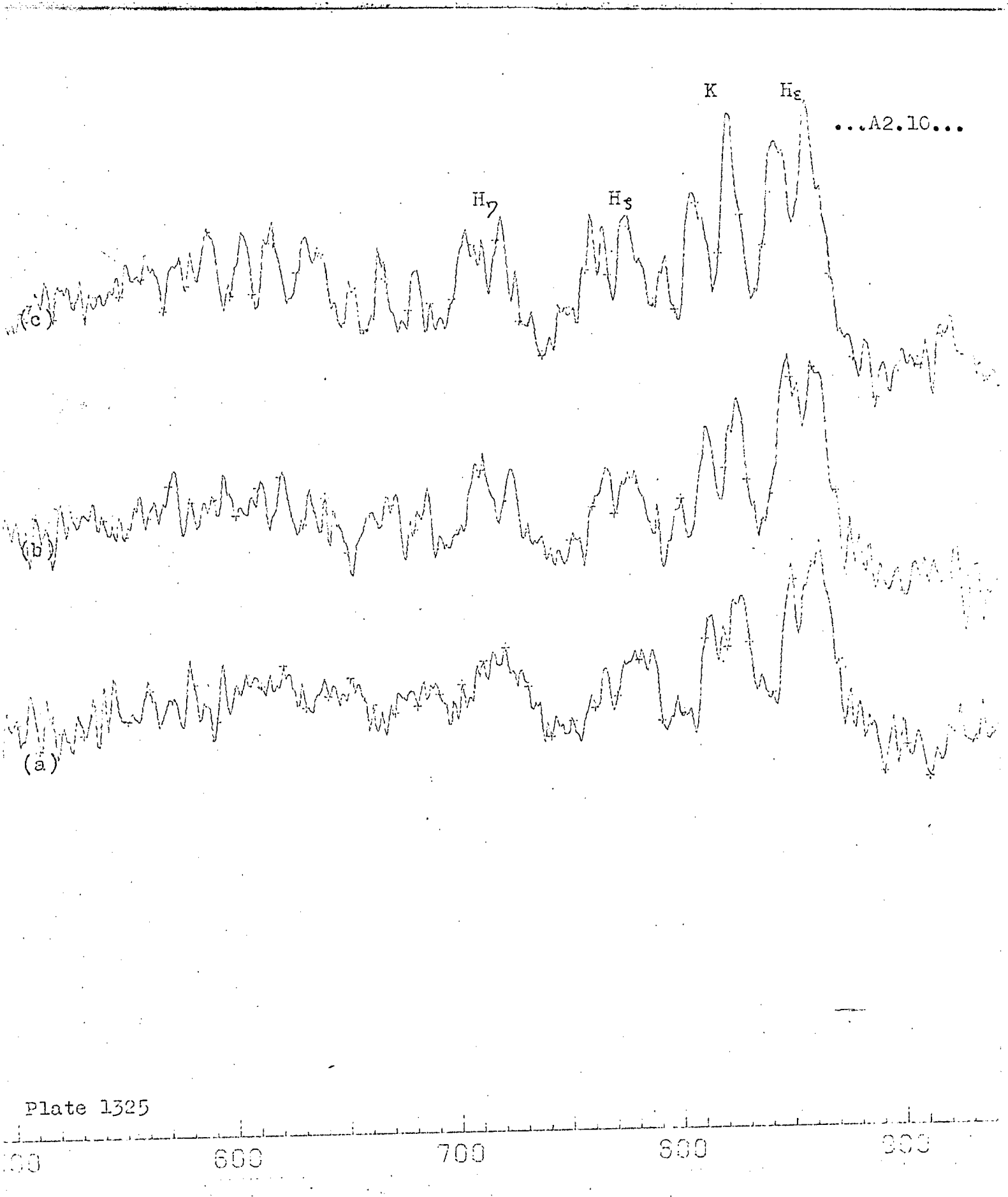

Plate 1325

500 600 700 800 900

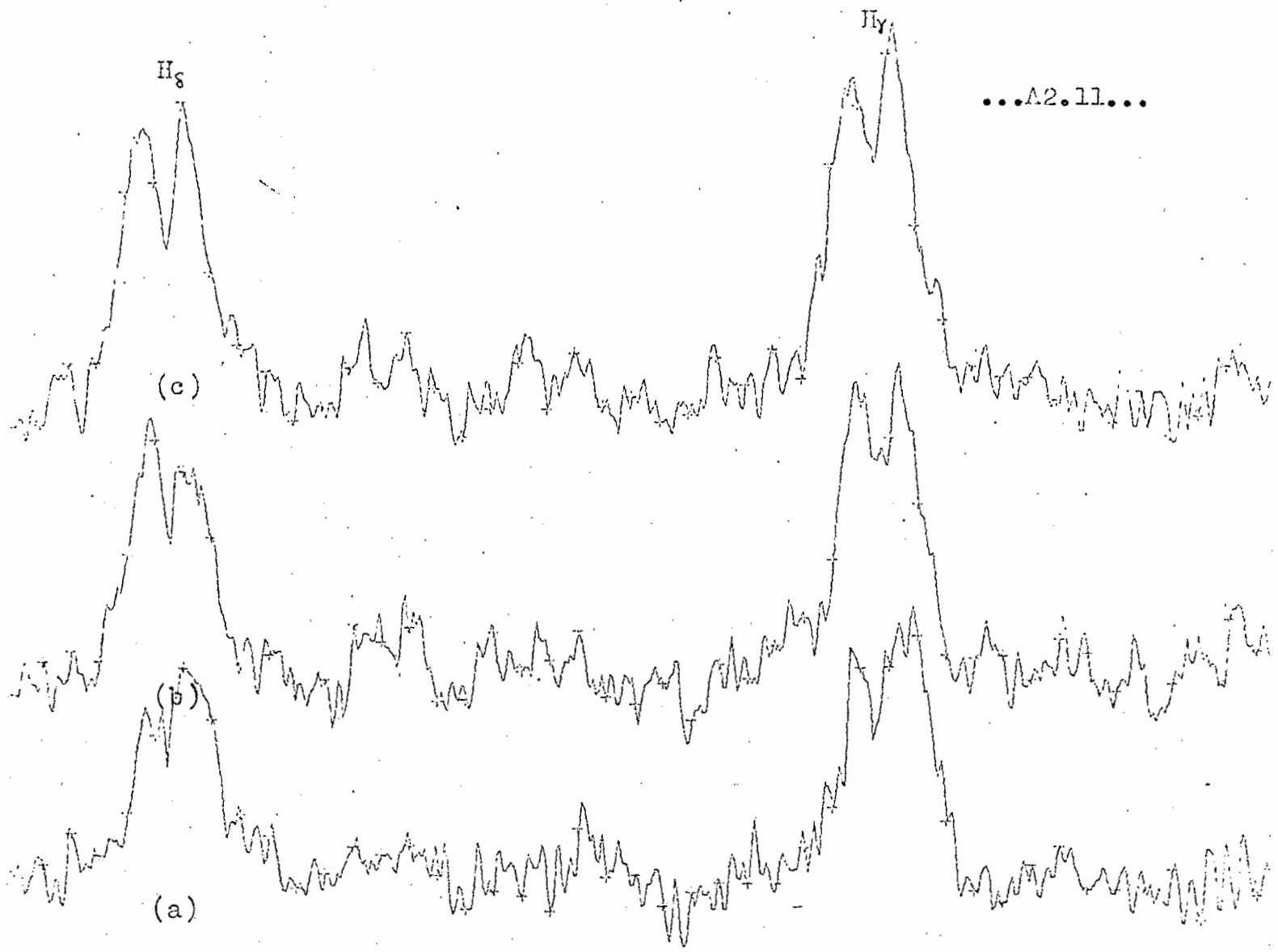

Plate 1325

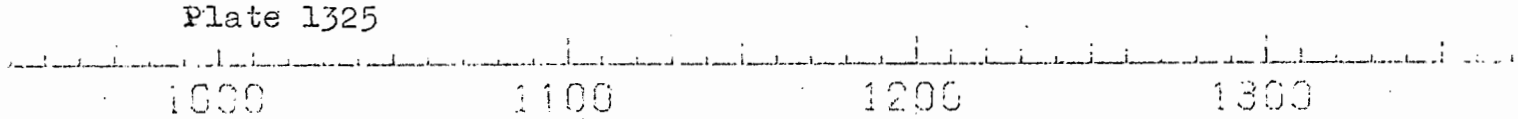

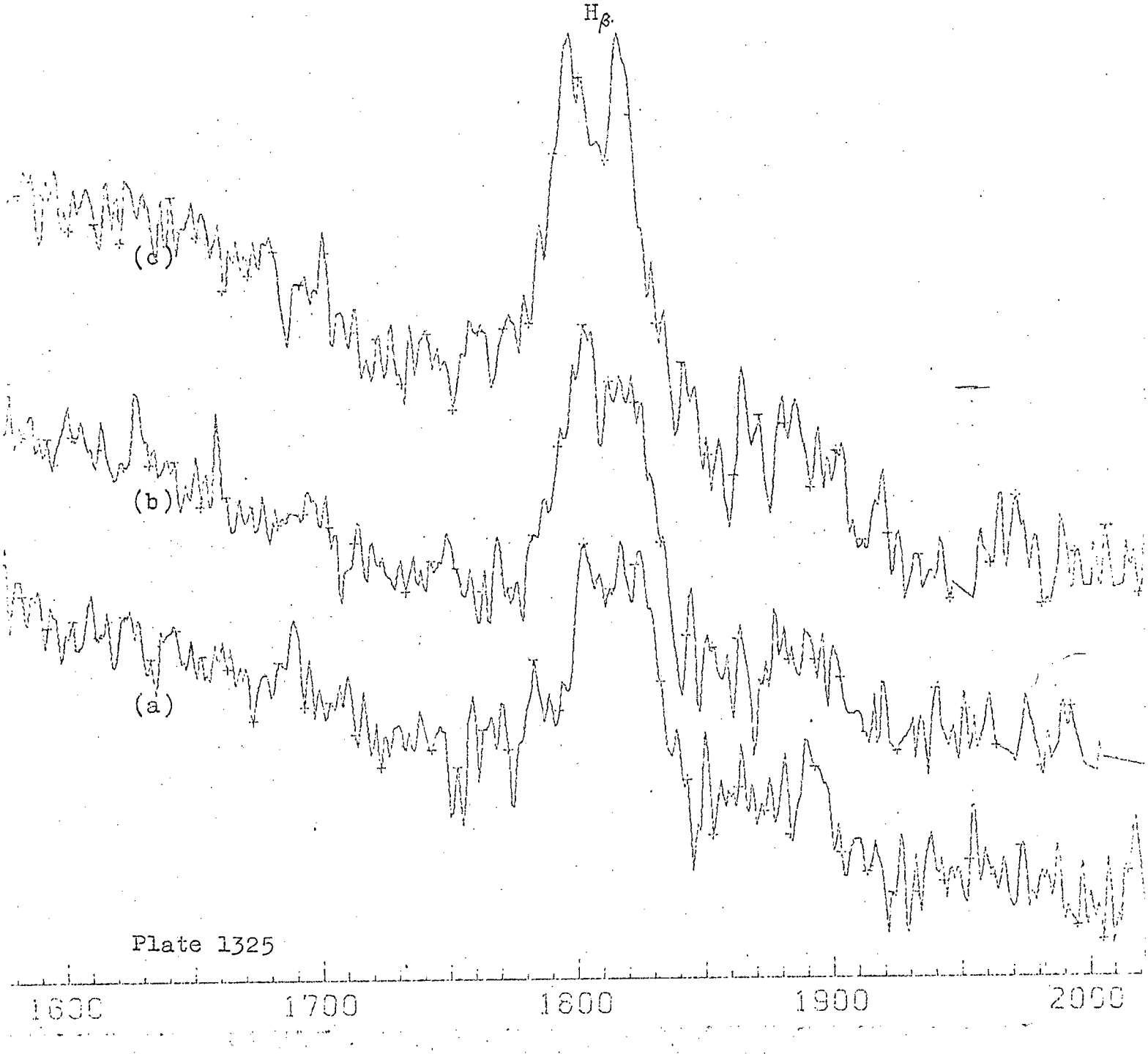

Plate 1325

1600 1700 1800 1900 2000

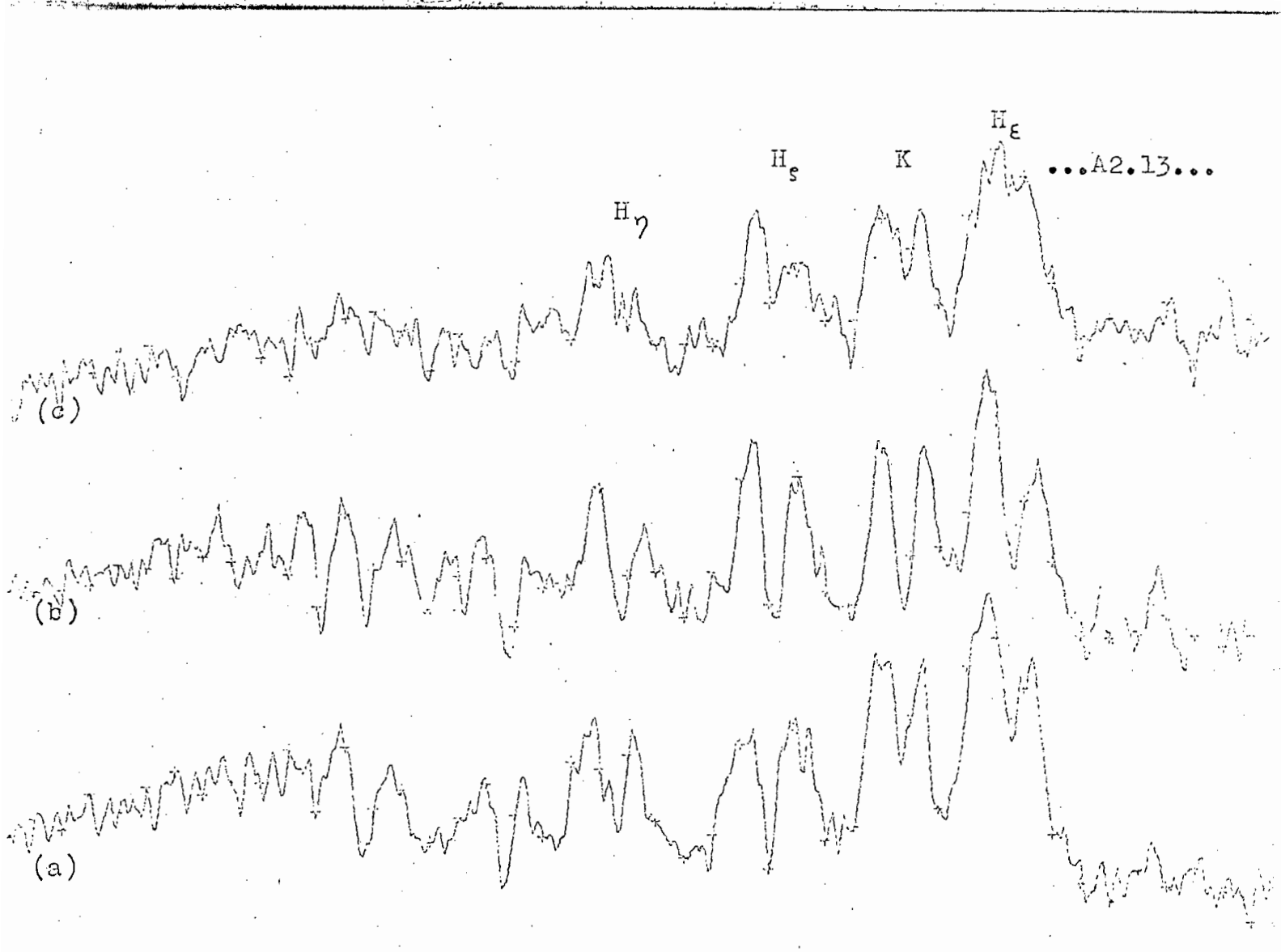

Plate 1326

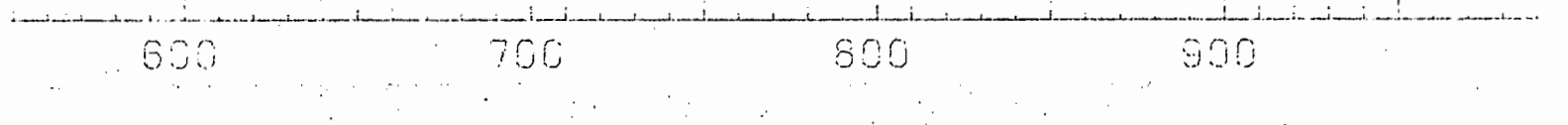

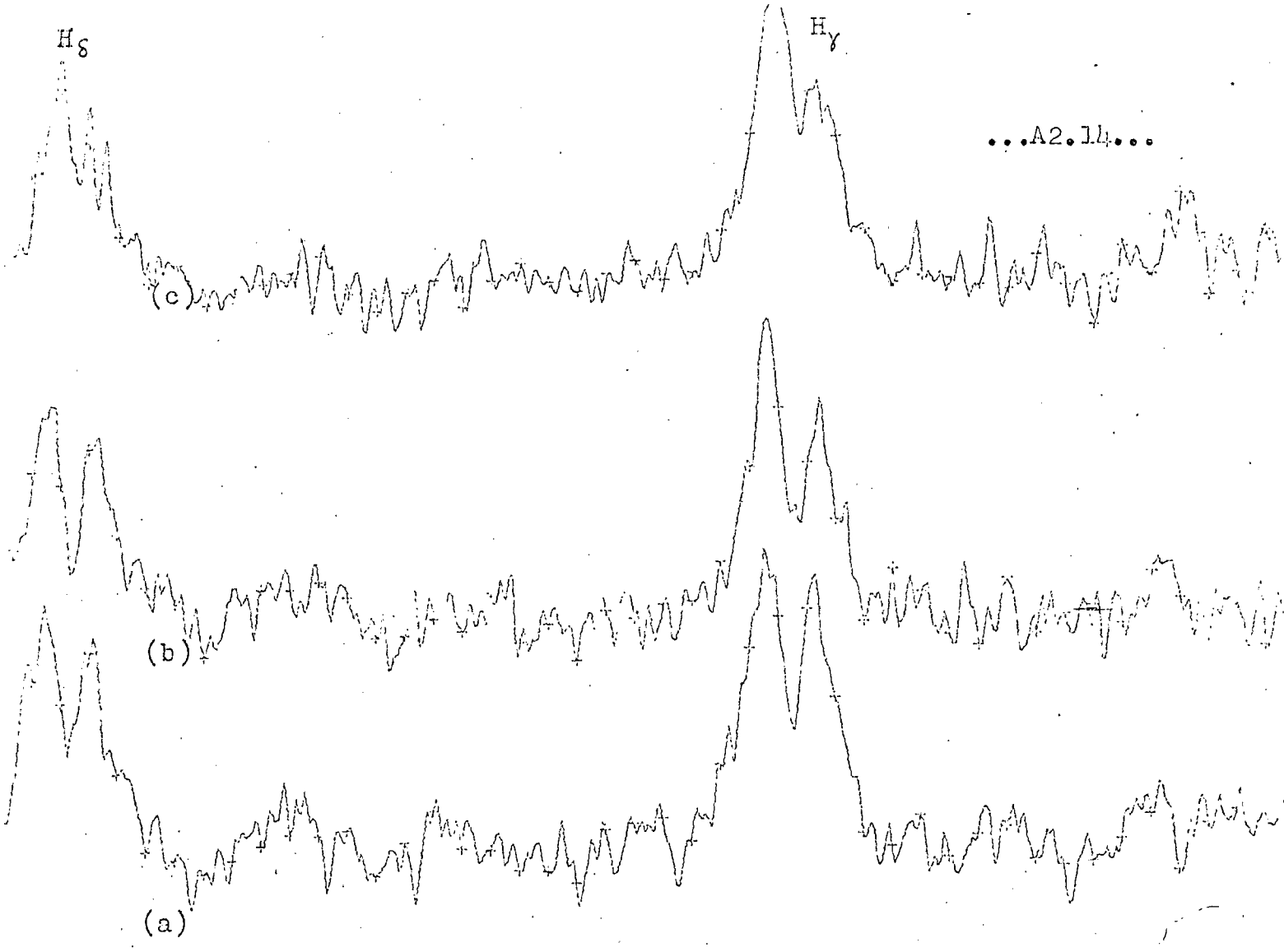

Plate 1326

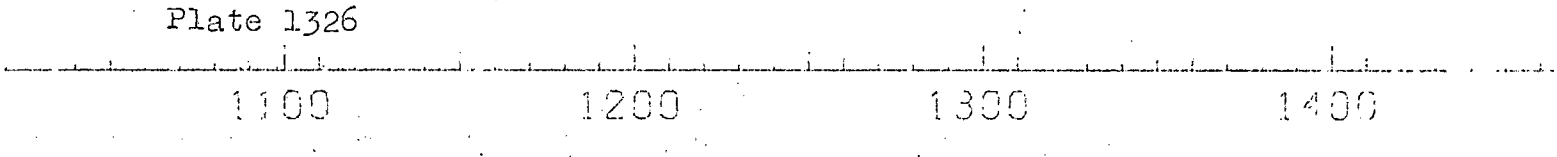

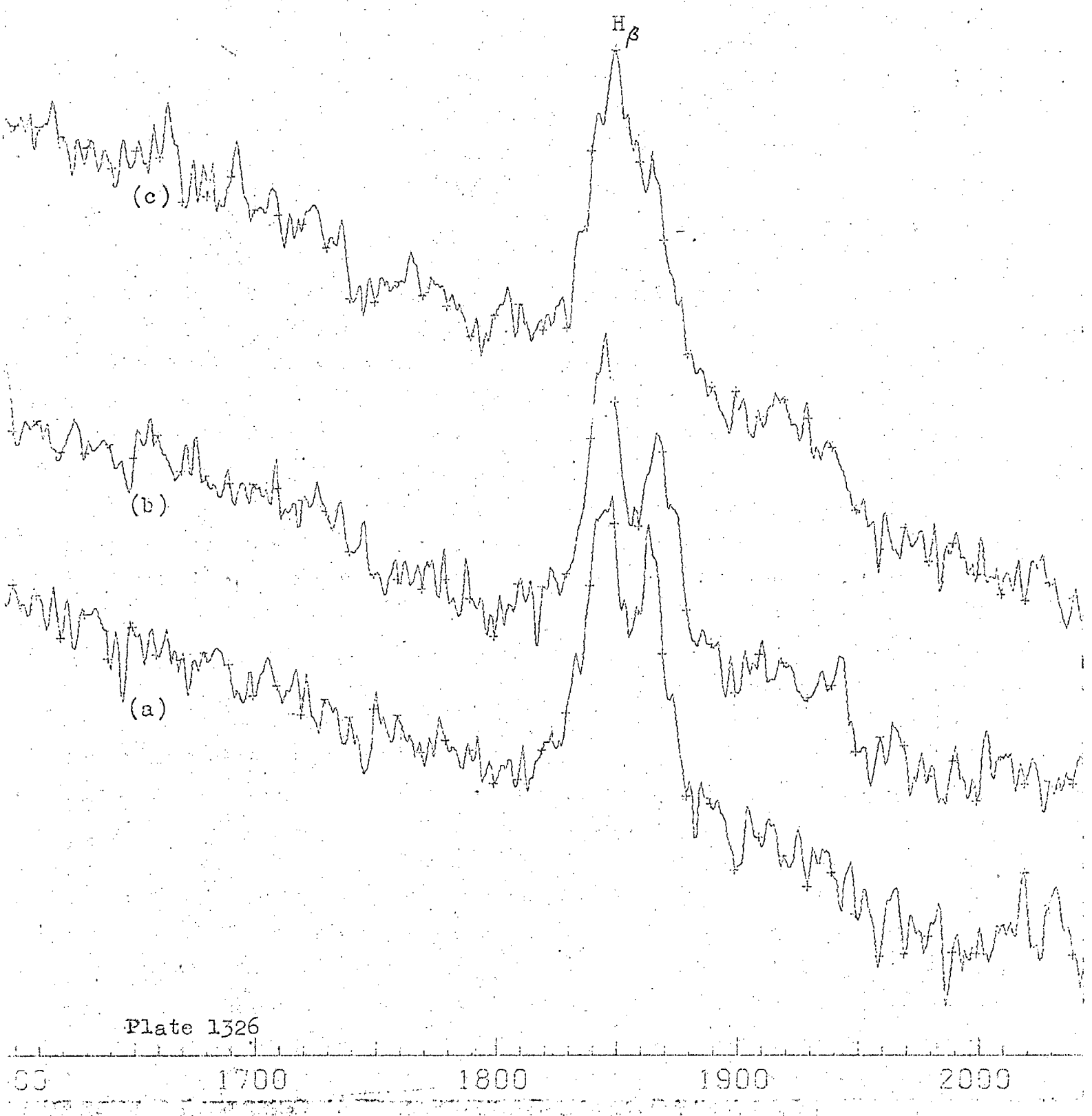

Plate 1326

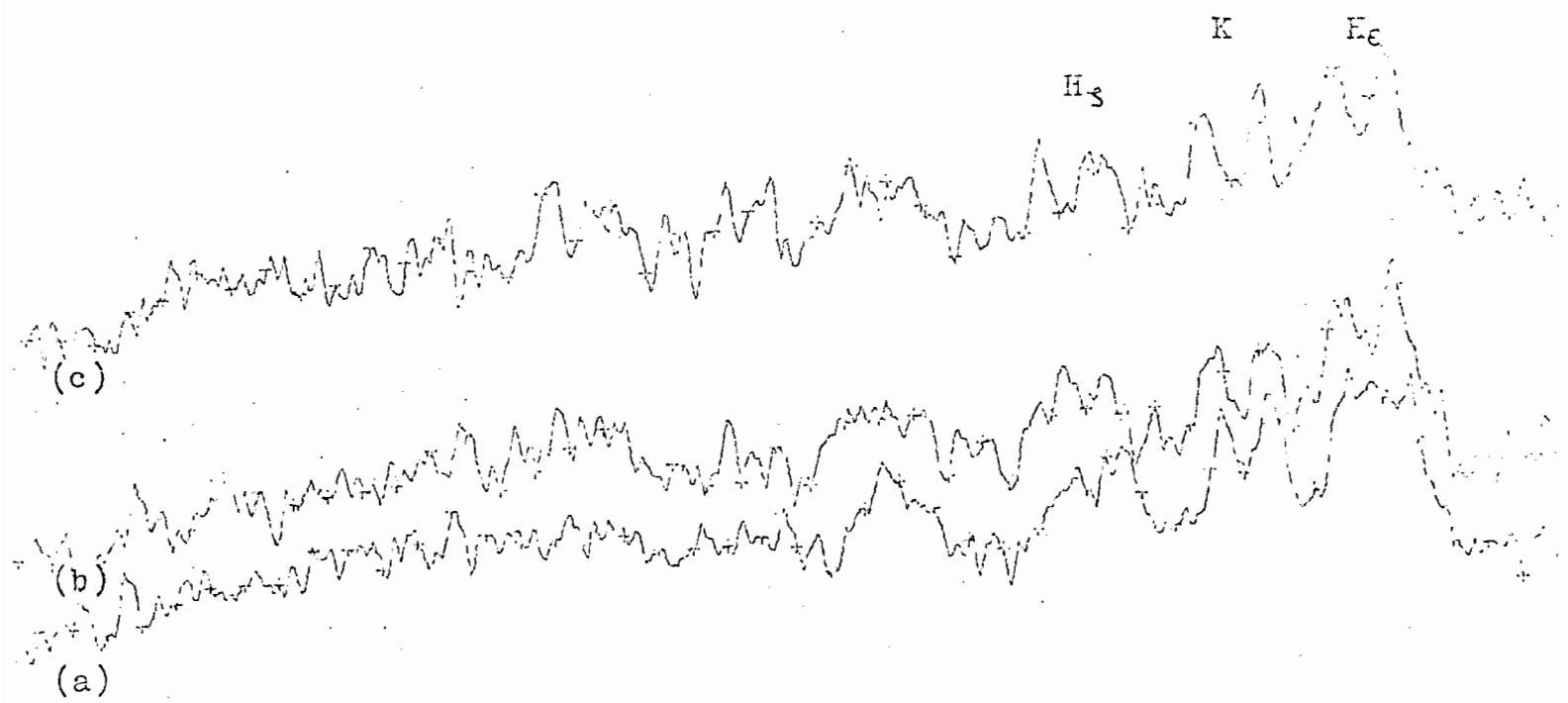

Plate 1327

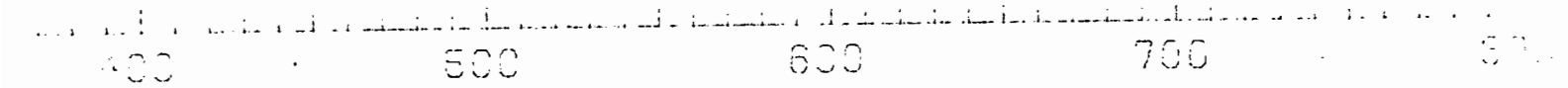

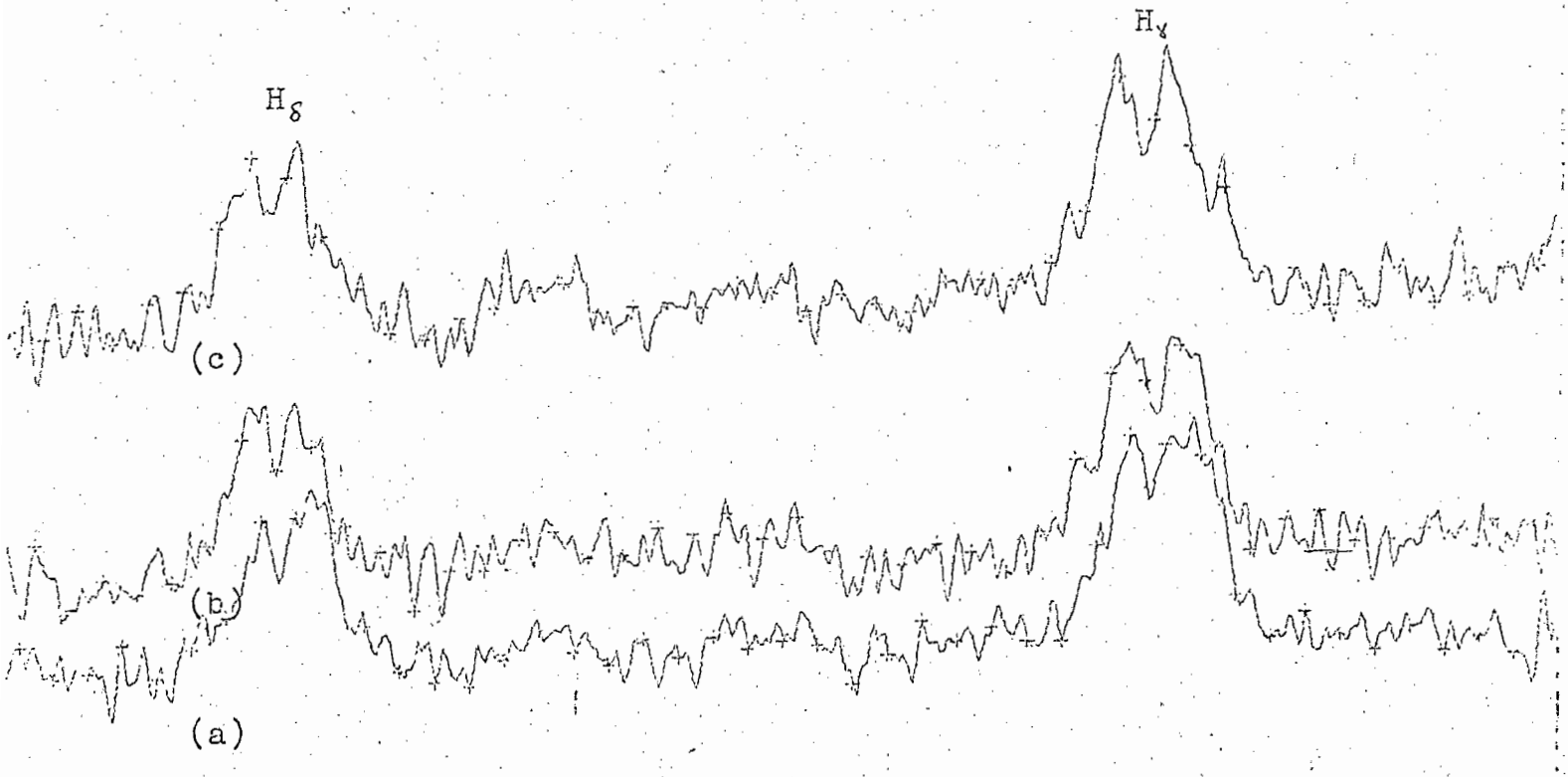

Plate 1327

900 1000 1100 1200

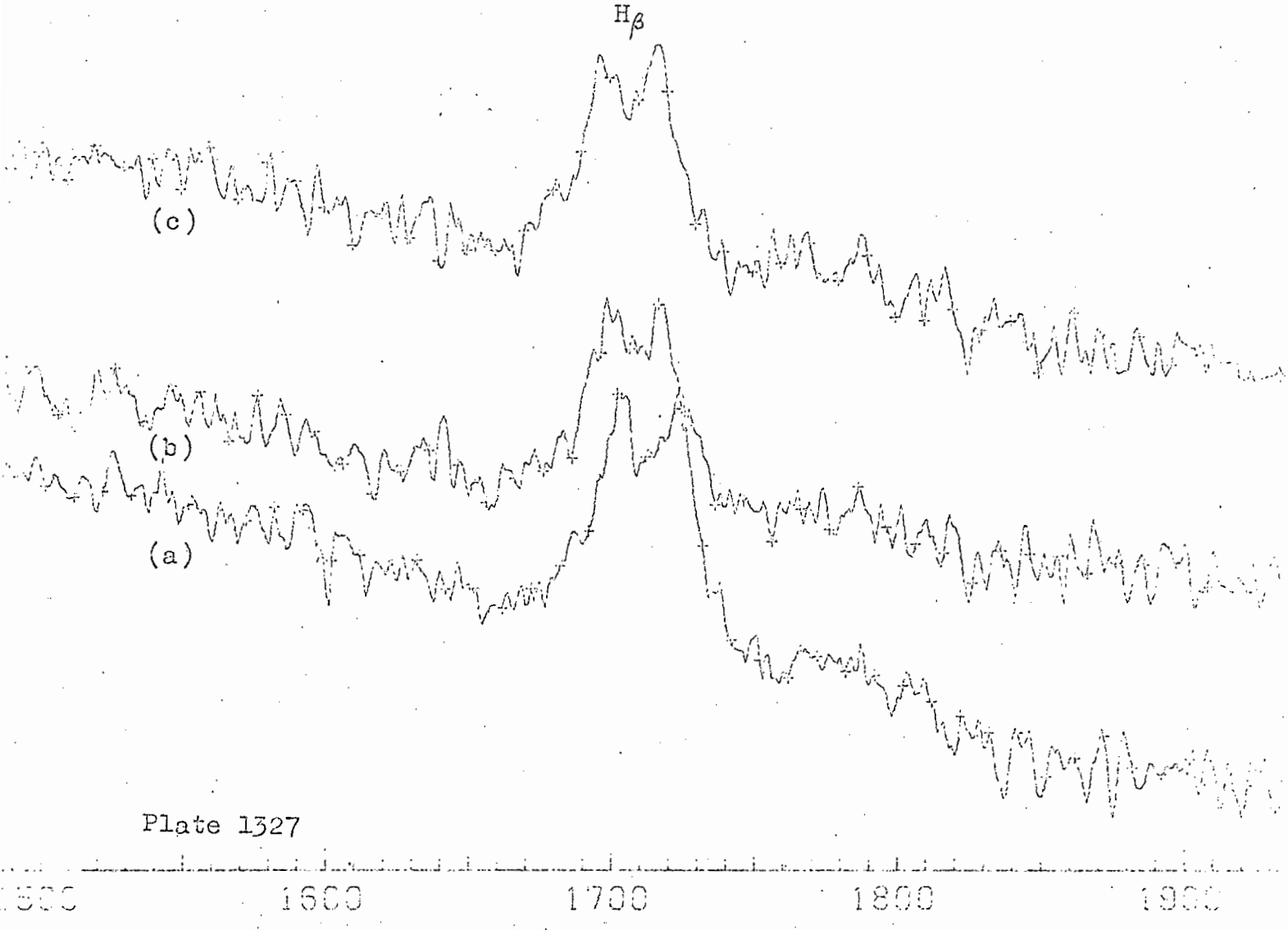

Plate 1327

1500 1600 1700 1800 1900

APPENDIX 3

Computer Programs.

The following three programs, written in Fortran V, were executed on the UNIVAC 1106 at the University of Cape Town.

1. Program ECLPAR

```
C*** THIS PROGRAM CALCULATES THE PARAMETERS OF THE ECLIPSE OF THE HOT SPOT
      IMPLICIT DOUBLE PRECISION(D)
      DIMENSION W(15),P(15),H(15)
      DATA PI/3.1415926536/
  100 FORMAT('1',' PARAMETERS FOR THE ECLIPSE OF THE HOT SPOT WITH : ALI
     *=',F4.1,'  AND R2=',F4.2,10X,'Q= ',F4.2,// ,7X,'  *42*     *43*
     **44*     *45*     *46*     *47*     *48*     *49*     *50*     *51*     *5
     *2*     *53*     *54*     *55*     *56*')
  101 FORMAT('0','*0',F3.2,'*',F7.6,14F8.6,' W')
  102 FORMAT(' ','      *',F7.6,14F8.6,' P')
  103 FORMAT(' ','      *',F7.6,14F8.6,' H')
      BI = 62.0
      DO 2 I = 1,9
      BI = BI + 1.0
      R2 = 0.33
      AI=(BI*PI)/180.0
      DO 1 J=1,11
      R2 = R2 + 0.01
      R = 0.05
      Q = (R2 - 0.38) / 0.20
      Q = 10.0**Q
      WRITE(5,100) BI,R2,Q
      DO 11 K=1,14
      R = R + 0.01
      BA = 41.0
      DO 10 L=1,15
      BA = BA + 1.0
      A=(BA*PI)/180.
      DP=DPSI(R,A)
      P(L)=SNGL(DP)/(2*PI)
      DW=DWIDE(R2,R,A,AI)
      W(L)=SNGL(DW)/(2*PI)
      H(L)=P(L)+A/(2*PI)
   10 CONTINUE
      WMAX=AMAX1(W(1),W(2),W(3),W(4),W(5),W(6),W(7),W(8),W(9),W(10),W(11
     *),W(12),W(13),W(14),W(15))
      IF(WMAX.LT.0.0000001) GO TO 11
      WRITE(5,101) R,(W(L),L=1,15)
      WRITE(5,102) (P(L),L=1,15)
      WRITE(5,103) (H(L),L=1,15)
   11 CONTINUE
    1 CONTINUE
    2 CONTINUE
      END
```

```
      FUNCTION DWIDE(R2,R,A,AI)
      IMPLICIT DOUBLE PRECISION(D)
      DX=DPSI(R,A)
      DX=DCOS(DX)
      DY=DBLE(R*COS(A))
      DY=1.DD0-DY
      DZ=DBLE(R2)
      DZ=(DZ*DX)/DY
      DZ=1.DD0-DZ**2
      IF(DZ) 1,2,2
    1 DWIDE=0.000
      RETURN
    2 DA=DBLE(SIN(AI))
      DZ=SQRT(DZ)/DA
      IF(DZ.GE.1.D) GO TO 1
      DWIDE=DACOS(DZ)
      DWIDE = 2.DDD * DWIDE
      RETURN
      END

      FUNCTION DPSI(R,A)
      IMPLICIT DOUBLE PRECISION(D)
      DX=DBLE(R*SIN(A))
      DY=DBLE(R*COS(A))
      DY=1.DDD-DY
      DZ=DX/DY
      DPSI=DATAN(DZ)
      RETURN
      END
```

****

2. Program RMS

```
C*** THIS PROGRAM CALCULATES  THE ROOT MEAN SQUARE OF THE FLICKERING
      DIMENSION IY(12D),X(3DD),Y(3DD),Z(3DD),C(5,3DD),AA(5)
  1DD FORMAT(1DI7)
  1D1 FORMAT('1',' PHASE',5X,'AMPLITUDE',5X,'  RMS   ',5(3X,'C=',F8.D),/)
  1D2 FORMAT(' ',F6.3,F13.3,F12.8,1X,5F13.1)
  3DD FORMAT(F6.3,2F1D.D,5F1D.1)
      N=1
      INIT=6
    1 READ(8,1DD,END=2) (IY(K),K=1,6D)
      INIT=INIT + 1
      Z(N)=RMEANS(IY,6D,YM,81,INIT)
      Y(N)=YM
      NNN=2*N
      X(N)=PHASER(NNN)
      N=N+1
      GO TO 1
    2 CONTINUE
      A=7DDDDD.
      DO 4 I=1,5
      DO 3 J=1,N
      B=(Y(J)-A)/Z(J)
      C(I,J) = B
    3 CONTINUE
```

```
      AA(I)=A
      A=A-100000.
    4 CONTINUE
      M=1
      MM=52
   10 WRITE(5,101) AA
      WRITE(5,102) (X(K),Y(K),Z(K),(C(L,K),L=1,5),K=M,MM)
      IF(MM.GE.N) GO TO 11
      M=M+52
      MM=MM+52
      IF(MM.GE.N) MM=N
      GO TO 10
   11 CONTINUE
      PUNCH 300,   (X(K),Y(K),Z(K),(C(L,K),L=1,5),K=1,N)
      END
```

```
      FUNCTION RMEANS(X,N,A,S,INIT)
      IMPLICIT INTEGER (X)
      DIMENSION X(N),XX(120)
      SUM=0.0
      S=0.0
      IF(INIT.GT.1) GO TO 2
      DO 1 I=1,N
    1 XX(I)=X(I)
      RMEANS=0.0
      RETURN 4
    2 CONTINUE
      DO 3 I=1,N
    3 S=S + X(I) + XX(I)
      A=S / FLOAT(2*N)
      DO 4 I=1,N
      D1=(X(I)-A)**2
      D2=(XX(I)-A)**2
    4 SUM=SUM + D1 + D2
      DO 5 I=1,N
    5 XX(I)=X(I)
      RMEANS=SQRT(SUM/FLOAT(2*N))
      RETURN
      END
```

```
      FUNCTION PHASE8(X)
      DATA TZERO,TMIN / 0.62819,0.66620 /
      Y=FLOAT(X)
      T = TZERO + (Y / 60.0) / 24.0
      T = T - TMIN
      PHASE8 = T / 0.1769
      RETURN
      END
```

****

3. Program HOTSPOT

This simple analogue program generates a set of light curves for the eclipse of the hotspot by varying one of the parameters i, R_2, , or r . The spot is modelled as a flat emitting surface (i.e. its intensity $I = I_0 \cos(\ +\ )$.) composed of 120 elements each of dimension $\frac{1}{2}^{o}$ square, forming an elongated, tear-shaped spot. At each value of the position of each element is calculated and then projected onto the plane of the sky. The program then tests each to see whether it is obscured by the secondary. The brightness of the spot is taken, quite arbitrarily, to be eight units.

```
C*** THIS PROGRAM CALCULATES THE THEORETICAL LIGHT CURVE FOR AN ECLIPSE
C     OF A HOT SPOT
      DIMENSION X(5,300),Y(5,300),Z(5,300),XPLOT(268),YPLOT(268)
      DATA ALI,ALS,RDS,RD2,EPS / 67.0,45.0,0.120,0.39,0.50 /
      DO 1 K =1,5
      ALS = ALS + 1.0
      CALL MODEL (K,ALI,ALS,RDS,RD2,EPS,X,Y,Z)
    1 CONTINUE
      CALL BGNPLT
      DO 3 K = 1,5
      DO 2 N = 1,268
      XPLOT(N) = X(K,N)
      YPLOT(N) = Y(K,N)
    2 CONTINUE
      N = 268
      CALL PLOTIT(XPLOT,YPLOT,N)
    3 CONTINUE
      CALL ENDPLT
      END
```

```
      SUBROUTINE MODEL (K,ALI,ALS,RDS,RD2,EPS,H,UGEM,FRAC)
      DIMENSION H(5,300),FRAC(5,300),UGEM(5,300),X(150),Y(150)
      COMMON /SPOTS/X,Y,N,BETA,PSI,RAD,PI
  100 FORMAT('1',' U GEM LIGHT CURVE FOR INCLINATION =',F4.1,'; SPOT POS
     *ITION (',F4.2,',',F4.1,') AND SECONDARY RADIUS = ',F4.2)
  101 FORMAT('0',5(2X,'PHASE',2X,'LIGHT',2X,'FRACT '))
  102 FORMAT(' ',5(3F7.1,' '))
  103 FORMAT(' ',I4,3F10.5,2I10,2F10.5,3F10.7)
  104 FORMAT('1')
      DATA PI / 3.14159 /
      RAD = PI / 180.0
      PSI0 = ATAN((RDS*SIN(ALS*RAD))/(1.0 - RDS*COS(ALS*RAD)))/(2.0*PI)
C
C****
C
      DO 1000 I = 1,268
      N = 1
      H(K,I) = -ALS/360.0 + I/1080.0
      PSI = H(K,I)*2*PI
      X2 = SIN(PSI)
      Y2 =-COS(PSI)*COS(ALI*RAD)
      DO 1001 J=1,5
      BETA = EPS*(3-J)*RAD
      CALL SPOT(J,ALS,ALI,RDS,EPS)
 1001 CONTINUE
      IFRAC = 0
      N = N - 1
      DO 1002 J=1,N
      DISC = (X(J) - X2)**2 + (Y(J) - Y2)**2
      IF(SQRT(DISC).LE.RD2) IFRAC = IFRAC + 1
 1002 CONTINUE
      FRAC(K,I) = FLOAT(IFRAC)/FLOAT(N)
      FRAC(K,I) = 1.0 - FRAC(K,I)
      A = PSI + ALS*RAD
      U1 = 8.0*COS(A)
      H(K,I) = H(K,I) - PSI0
      UGEM(K,I) = U1*FRAC(K,I) + 2.0
      WRITE(5,103) I,PSI,X2,Y2,IFRAC,N,U1,PSI0,X(55),Y(55),BETA
 1000 CONTINUE
      WRITE(5,100) ALI,RDS,ALS,RD2
      WRITE(5,101)
      DO 1 M1 = 1,54
      M2 = 54 + M1
      M3 =108 + M1
      M4 =162 + M1
      M5 =216 + M1
      IF(M1.LE.52) WRITE(5,102) H(K,M1),UGEM(K,M1),FRAC(K,M1),
     *                          H(K,M2),UGEM(K,M2),FRAC(K,M2),
     *                          H(K,M3),UGEM(K,M3),FRAC(K,M3),
     *                          H(K,M4),UGEM(K,M4),FRAC(K,M4),
     *                          H(K,M5),UGEM(K,M5),FRAC(K,M5)
      IF(M1.GE.53) WRITE(5,102) H(K,M1),UGEM(K,M1),FRAC(K,M1),
     *                          H(K,M2),UGEM(K,M2),FRAC(K,M2),
     *                          H(K,M3),UGEM(K,M3),FRAC(K,M3),
     *                          H(K,M4),UGEM(K,M4),FRAC(K,M4)
    1 CONTINUE
      WRITE(5,104)
      RETURN
      END
```

```
      SUBROUTINE SPOT(J,ALS,ALI,RDS,EPS)
C**** THIS SUBROUTINE CALCULATES THE POSITIONS OF THE ELEMENTS OF THE SPOT
C     AND THEN PROJECTS THESE ONTO THE PLANE OF THE SKY
      DIMENSION X(150),Y(150)
      COMMON /SPOTS/X,Y,N,BETA,PSI,RAD,PI
      GO TO (1,2,3,2,1), J
    1 N1 = 3
      N2 = 18
      GO TO 4
    2 N1 = 2
      N2 = 27
      GO TO 4
    3 N1 = 1
      N2 = 34
    4 CONTINUE
      DO 5 K = N1,N2
      A = ((ALS - 11.0*EPS) + K*EPS)*RAD
      XS = RDS*COS(A)
      YS = RDS*SIN(A)
      ZS = RDS*TAN(BETA)
      X(N) = SIN(PSI)*XS + COS(PSI)*YS
      Y(N) = -COS(PSI)*COS(ALI*RAD)*XS + SIN(PSI)*COS(ALI*RAD)*YS +
     * SIN(ALI*RAD)*ZS
      N = N + 1
    5 CONTINUE
      RETURN
      END


      SUBROUTINE BGNPLT
      DIMENSION IBUF(2000)
      CALL PLOTS(IBUF,2000,3)
      CALL PLOT(4.0,4.0,-3)
      CALL AXIS(0.0,0.0,'LIGHT',5,10.0,90.0,0.0,1.0)
      CALL AXIS(0.0,0.0,'PHOTOMETRIC PHASE',-17,20.0,0.0,-0.15,0.0125)
      CALL SYMBOL(9.0,9.0,0.21,'U GEM MODEL',0.0,11)
      RETURN
      ENTRY PLOTIT(X,Y,N)
      M = N + 2
      DIMENSION X(M),Y(M)
      Y(M) = 1.0
      Y(M-1) = 0.0
      X(M) = 0.0125
      X(M-1) = -0.15
      CALL LINE(X,Y,N,1,0,0)
      RETURN
      ENTRY ENDPLT
      CALL PLOT(24.0,0.0,-3)
      CALL SYMBOL(0.0,0.0,0.35,'HRWOOD',90.0,6)
      CALL PLOT(2.0,-4.0,999)
      RETURN
      END
```

****

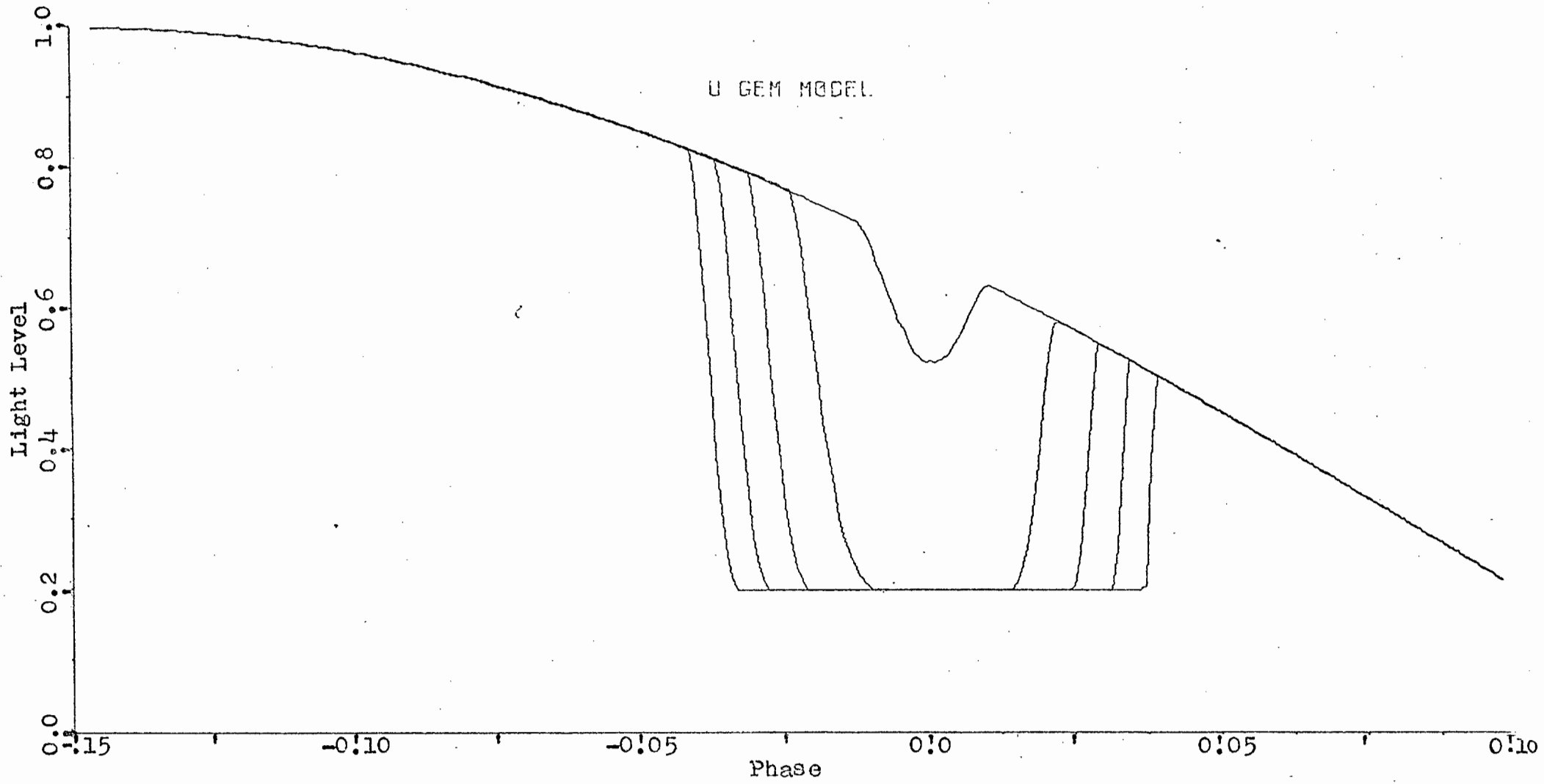

1. Showing the change of eclipse as the angle of inclination is increased in steps of 1°.

$R_2 = 0.39$, $\alpha = 48^{\circ}$, $r = 0.12$, $65 \leqslant i \leqslant 69^{\circ}$

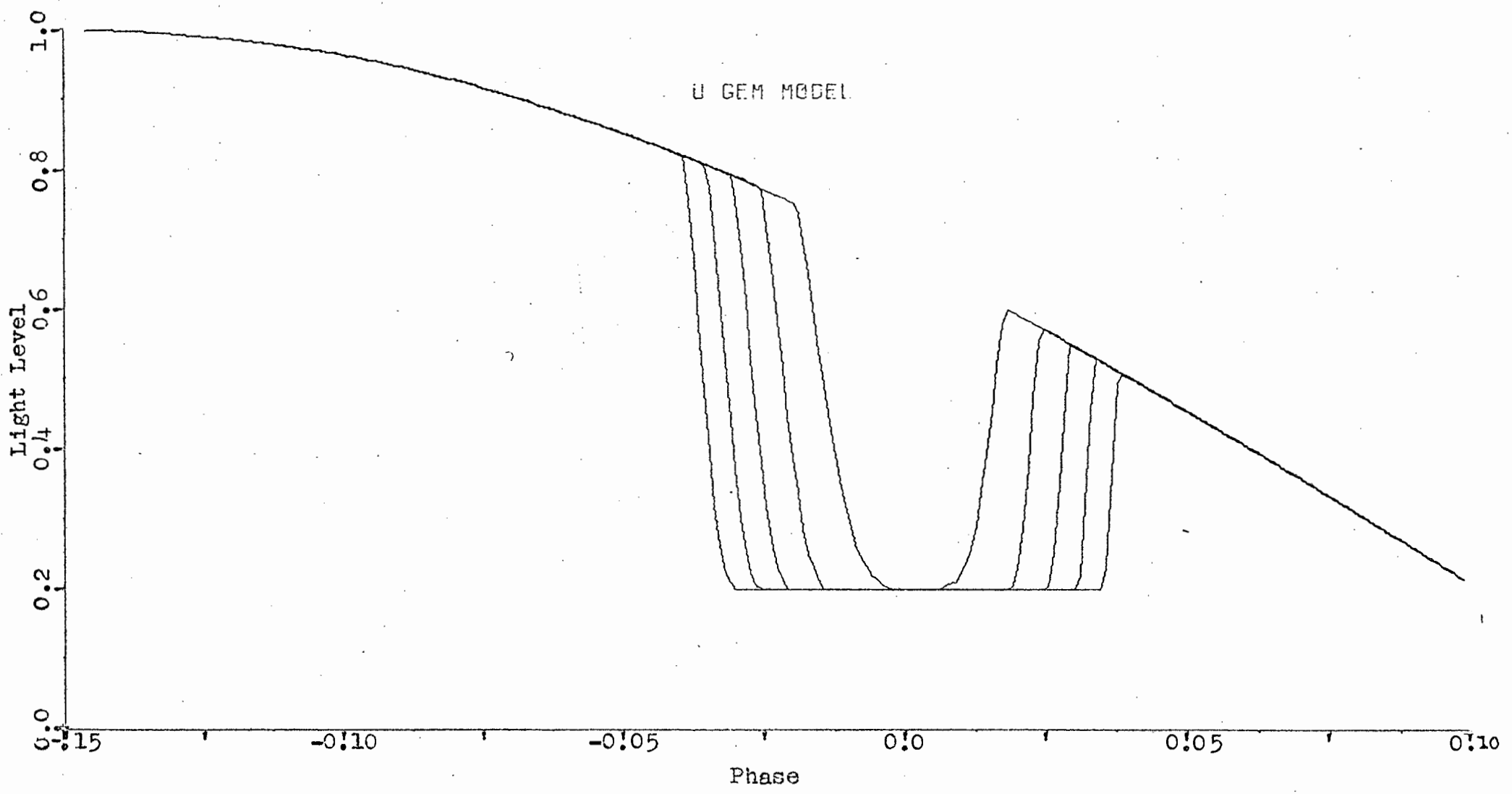

2. Showing the change of eclipse as the secondary radius is increased in steps of 0.01 .

$i = 67^{\circ}$, $\alpha = 48^{\circ}$, $r = 0.12$, $0.37 \leqslant R_2 \leqslant 0.41$

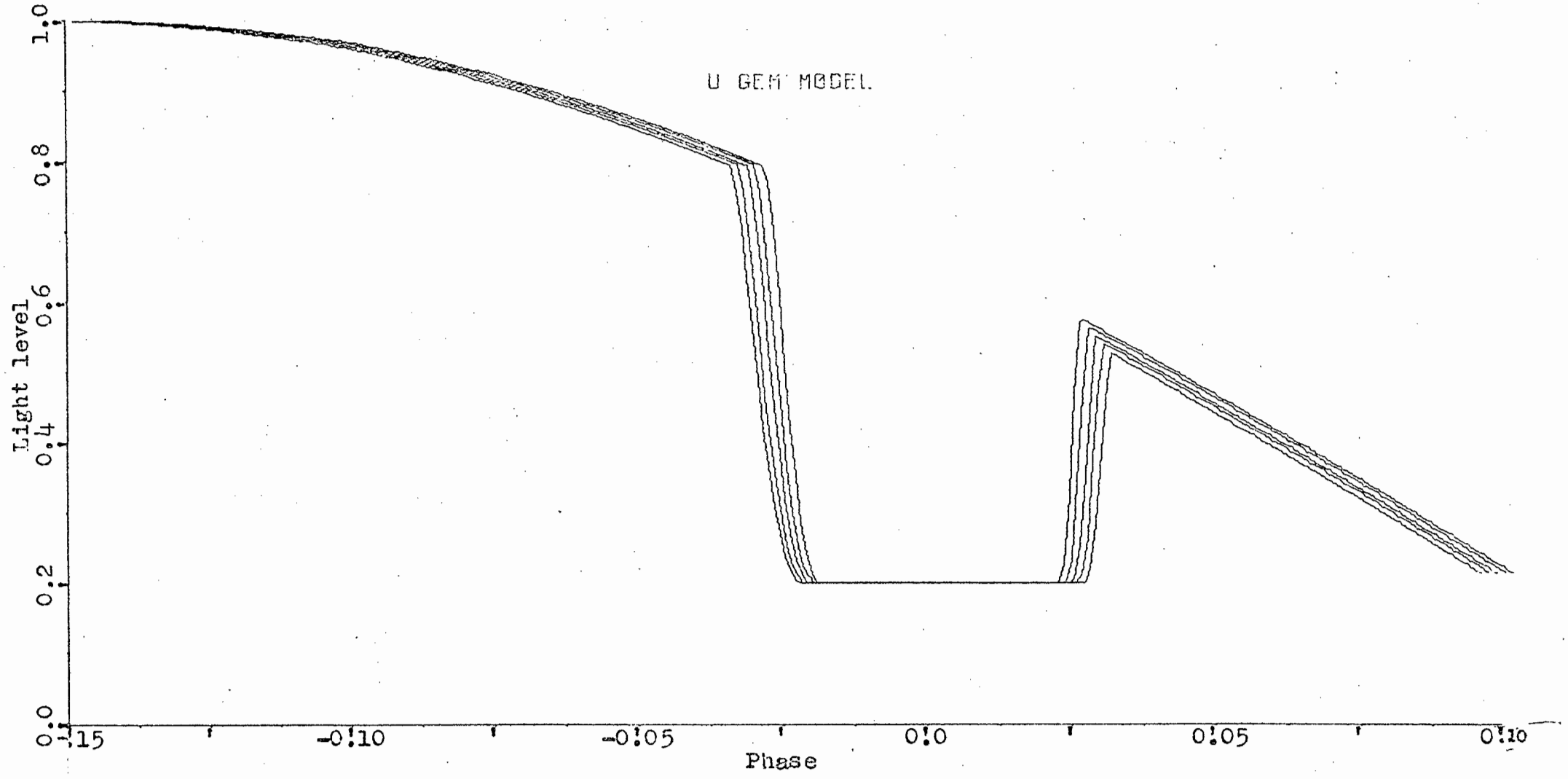

3. Showing the change of eclipse as the radius vector of the spot is increased in steps of 0.01 .

$i = 67^{\circ}$, $R_2 = 0.39$, $\alpha = 48^{\circ}$, $0.09 \leqslant r \leqslant 0.14$

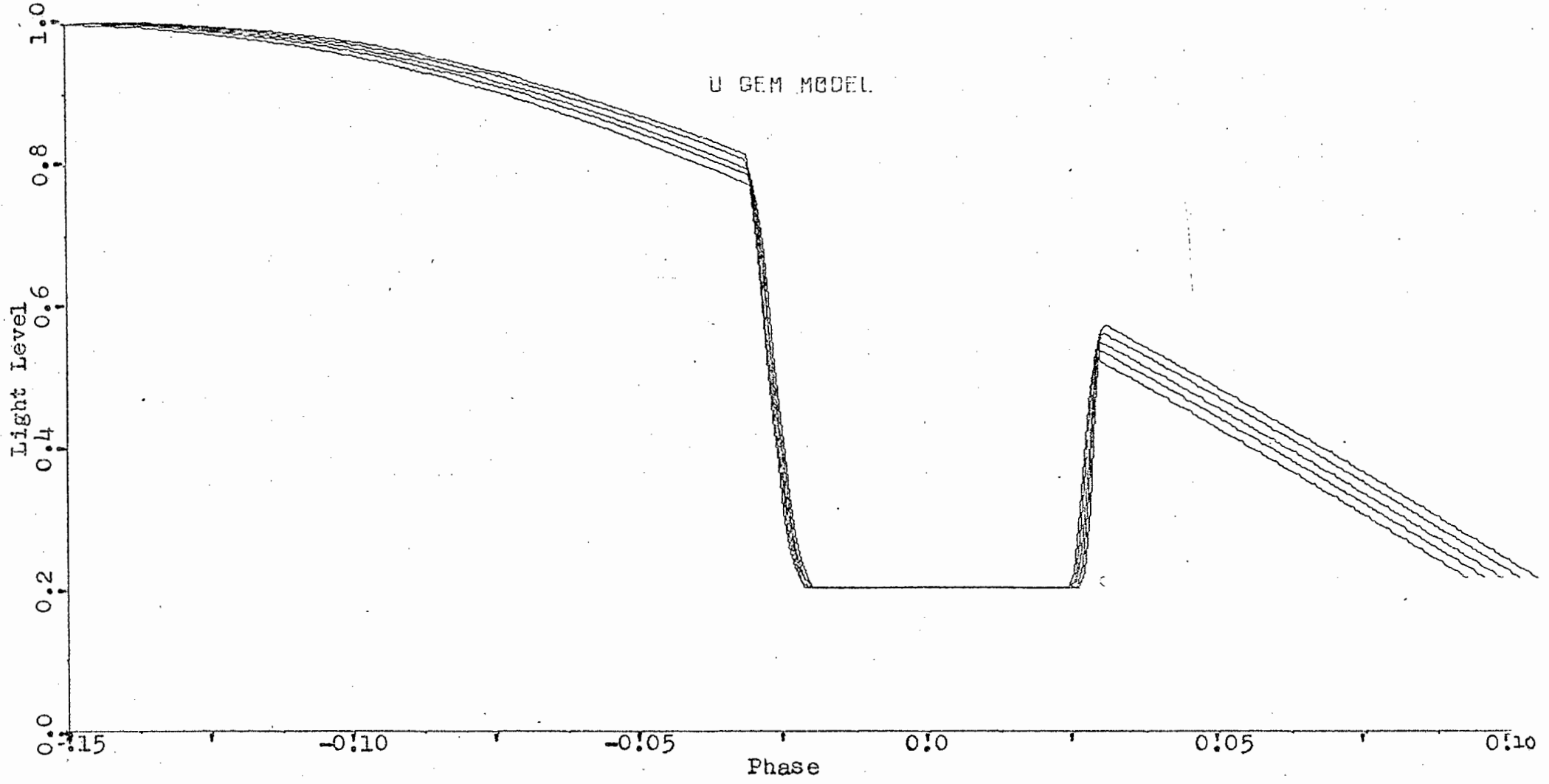

4. Showing the change of eclipse as the angle of the spot is increased in steps of 1°.

$i = 67^{\circ}$, $R_2 = 0.39$, $r = 0.12$, $46^{\circ} \leqslant \alpha \leqslant 50^{\circ}$